

QATAR UNIVERSITY

COLLEGE OF PHARMACY

THE EFFECT OF NATURAL AND SYNTHETIC COMPOUNDS ON COLORECTAL

CANCER: IN VITRO AND IN VIVO STUDIES

BY

Arij Fouzat Hassan

A Thesis Submitted to

the College of Pharmacy

in Partial Fulfillment of the Requirements for the Degree of

Masters of Science in Pharmacy

June 2022

© 2022. Arij Fouzat Hassan. All Rights Reserved.

COMMITTEE PAGE

The members of the Committee approve the Thesis of  
Arij Fouzat Hassan defended on 11/05/2022.

---

Prof. Ashraf A. Khalil  
Thesis Supervisor

---

Prof. Ala-Eddin Al Moustafa  
Thesis Co-Supervisor

---

Dr. Layla Kamareddine  
Thesis Co-Supervisor

---

Prof. Hesham Korashy  
Internal Examiner

---

Prof. Mohey Elmazar  
External Examiner

Approved:

---

Feras Alali, Dean, College of Pharmacy

## ABSTRACT

HASSAN, ARIJ, F., Masters: June : [2022:], Pharmaceutical Sciences

Title: The Effect of Natural and Synthetic Compounds on Colorectal Cancer: In vitro and In vivo Studies

Supervisor of Thesis: Asharf, A., Khalil.

Colorectal cancer (CRC) is one of the deadliest malignancies in the world. Despite improved treatment, CRC incidence and mortality rates have been increasing lately. Current conventional therapies are associated with severe side effects that affect patients' quality of life. Drug resistance, severe pain, hair loss, and blood abnormalities are the most common side effects. Therefore, novel, and safe alternatives are required to control metastasis and prevent CRC with minimum or no side effects. Recently, natural products became an attractive target as a safe resource for anticancer agents. Flavonoids are a group of biologically active compounds naturally found in a wide range of human dietary. Additionally, flavonoids from natural and synthetic sources, showed significant therapeutic effects against CRC. *Elaeagnus Angustifolia* (EA) is a natural resource for flavonoids traditionally used to treat different illnesses. Another resource for flavonoids is synthetic chalcone analogs. Previous work from our team explored the effect of EA and chalcone compounds against various types of cancer. In this study, we sought to particularly illustrate the impact of the EA flower's aqueous extract and the nitrogen-based-synthetically designed chalcone analogs (DK13 and DK14) and their underlying mechanisms of action on CRC using *in vitro* (the human CRC cell lines [*HCT-116* and *LoVo*]) and *in vivo* (the *Drosophila melanogaster Ras* mutant fly lines) model systems.

Our results showed that EA extract inhibits cell proliferation and alters cell cycle progression of both CRC cell lines as compared to the control group. Moreover, EA

extract significantly reduces colony formation and cell invasive ability of HCT-116 and LoVo cell lines; a phenotype accompanied by a significant upregulation of E-cadherin and a downregulation of vimentin and  $\beta$ -catenin, which are important epithelial-mesenchymal transition (EMT) biomarkers. Also, and as detected in our *in vivo* model, *EA*-treated *Ras85D* mutant fly lines exhibited a significantly increased survival rate as compared to their control. Furthermore, molecular pathway analysis *in vitro* revealed a significant suppression in total and phosphorylated EGFR and AKT expression in *EA*-treated cells as compared to controls, suggesting the EGFR-RAS and PI3K-AKT pathways as key molecular pathway targeted by *EA* to control ongoing oncogenic events. Along this, our data related to DK13 and DK14 also revealed that these compounds inhibit cell proliferation and deregulate cell-cycle progression in both cell lines. Additionally, DK13 and DK14 significantly reduce cell invasion and colony formation of both cell lines compared to the action of conventional anticancer 5'-fluorouracil (5-FU) and DMSO-treated control. This was translated into a significant increase in the survival rates of *D. melanogaster Ras85D* mutant fly lines as compared to their controls. Moreover, the molecular pathway analysis of chalcone- treated cells revealed an inhibitory effect of DK13 and DK14 on the expression patterns of both AKT and mTOR, highlighting RAS/MAPK and PI3K/AKT/mTOR pathways as key molecular pathway targeted by DK13 and DK14 to control ongoing oncogenic events.

Collectively, our study findings demonstrate an apparent anticancer effect of *EA* extract and chalcone compounds on CRC, presenting *EA*, Dk13, and Dk14 as promising chemotherapeutic agents.

**Keywords:** Colorectal cancer, *Elaeagnus Angustifolia*, Nitrogen-based chalcones, *D. melanogaster*, Epithelial-mesenchymal transition (EMT), EGFR/RAS, RAS/MAPK, PI3K/AKT/mTOR, Wnt/ $\beta$ -catenin.

## DEDICATION

*This research is dedicated to my family for their unconditional love and care.*

## ACKNOWLEDGMENTS

" First, I would like to express my profound, sincere thanks to my supervisor, who always believed in me, Prof. Ashraf Khalil, for his academic and moral support. And for Prof. Ala-Eddin Al Moustafa, who has always motivated me to complete this thesis. I would also like to thank Dr. Layla Kamareddine for all the experience I gained. Thanks to my friend Mrs. Ola Hussein for her help and advice since the first day I started my degree. Thanks to Dr. Ishita Gupta and Mrs. Hadeel Kheraldine for all their support thru all the ups and downs. A special thanks to the college of pharmacy and its faculty for their tremendous efforts. Finally, thanks to Qatar university for all the opportunities I have had since I was an undergraduate student.

# TABLE OF CONTENTS

DEDICATION.....	v
ACKNOWLEDGMENTS .....	vi
LIST OF TABLES.....	xi
LIST OF FIGURES .....	xii
CHAPTER 1: INTRODUCTION .....	1
1.1    Colorectal cancer (CRC).....	2
1.1.1    Burden of CRC .....	2
1.1.2    Etiology of CRC .....	5
1.1.3    Types of CRC .....	9
1.1.4    Risk factors of CRC .....	10
1.1.4.1    Environmental factors.....	10
1.1.4.2    Genetic factors .....	11
1.1.5    Prognostic and prediction of CRC .....	14
1.1.6    Diagnosis and management of CRC .....	15
1.1.7    Treatment of CRC.....	18
1.2    Complementary and alternative medicine (CAM).....	19
1.2.1    Flavonoids.....	20
1.2.1.1    Elaeagnus Angustifolia (EA).....	23
1.2.1.2    Chalcones.....	25
1.2.2    Promising CRC molecular targets for natural and synthetic flavonoids	27
1.2.2.1    Wnt/ $\beta$ -Catenin Signaling .....	28
1.2.2.2    PI3K/AKT/mTOR pathway.....	30
1.2.2.3    EMT pathway .....	32
1.3 <i>Drosophila melanogaster</i> as a model for CRC studies.....	33

1.4	Thesis Objectives .....	36
CHAPTER 2: MATERIALS AND METHODS .....		37
2.1	Plant material collection and extraction .....	37
2.2	Synthesis of nitrogen-based chalcone analogs (DK13 and DK14).....	37
2.3	<i>Drosophila</i> stocks husbandry and maintenance .....	39
2.4	Cell culture .....	39
2.5	Cell viability assay (Alamarblue™ assay) .....	40
2.6	Cell morphology analysis.....	41
2.7	Flow cytometric analysis of cell cycle .....	41
2.8	Cell invasion assay .....	42
2.9	Soft agar colony formation assay .....	42
2.10	RNA extraction and quantitative real-time PCR (qRT-PCR).....	43
2.11	Western blot analysis .....	45
2.12	Survival assay.....	48
2.13	Statistical analysis .....	48
CHAPTER 3: RESULTS.....		49
3.1	Effect of <i>EA</i> aqueous extract on CRC cell lines.....	49
3.1.1	Cell viability assay (Alamarblue™ assay).....	49
3.1.2	Cell morphology analysis .....	52
3.1.3	Flow cytometric analysis of cell cycle.....	54
3.1.4	Cell invasion assay.....	57



3.1.5	Soft agar colony formation assay.....	60
3.1.6	Outcome of <i>EA</i> extract on AKT/EGFR and EMT biomarkers in CRC cell lines	63
3.2	Effect of DK13 and D14 on CRC cell lines.....	66
3.2.1	Cell viability assay (AlamarBlue™ assay).....	66
3.2.2	Cell morphology analysis.....	69
3.2.3	Flow cytometric analysis of cell cycle.....	71
3.2.4	Cell invasion assay.....	74
3.2.5	Soft agar colony formation assay.....	77
3.2.6	Outcome of DK13 and DK14 on EMT biomarkers and AKT/mTOR in CRC cell lines.....	79
4.1	<i>Drosophila melanogaster</i> as a model for CRC studies.....	82
4.1.1	<i>Ras</i> expression in <i>D. melanogaster</i> fly lines with <i>ras</i> mutation.....	82
4.1.2	ERK1/2 and AKT expression in <i>D. melanogaster</i> fly lines with <i>ras</i> mutation	82
4.1.3	Effect of <i>EA</i> extract on the survival rates of fly lines with <i>Ras</i> mutation as compared to wild type flies.....	84
4.1.4	Outcome of DK13 and DK14 on the survival rates of fly lines with <i>ras</i> mutation as compared to wild –type flies.....	86
CHAPTER 4: DISCUSSION.....		88
4.1	Effect of <i>EA</i> aqueous extract on CRC.....	89
4.2	Effect of nitrogen-based chalcone analogs (DK13 and DK14) on CRC.....	93

CHAPTER 5: CONCLUSIONS AND FUTURE DIRECTIONS .....	96
5.1 Limitations .....	98
REFERENCES .....	99

## LIST OF TABLES

Table 1. Staging system of colorectal cancer according to UICC. ....	17
Table 2. Examples of natural flavonoids explored on different CRC cell lines .....	27
Table 3. Examples of synthesized chalcone analogs explored on different CRC cell lines .....	27
Table 4. Reverse transcription and cDNA synthesis reaction constituents.....	44
Table 5. RT-qPCR reaction constituents.....	44
Table 6. List of used primers in RT-qPCR .....	44
Table 7. Antibodies used in western blot analysis of proteins extracted from CRC cell lines. ....	46
Table 8. List of the used antibodies in Western blotting analysis of <i>D. melanogaster</i> fly lines. ....	47
Table 9: IC <sub>50</sub> of <i>EA</i> aqueous extract in CRC cell lines after 48 hours of treatment. ...	51
Table 10. IC <sub>50</sub> of DK13 and DK14 in CRC cell lines after 48 hours of treatment. ....	68

## LIST OF FIGURES

Figure 1. Distribution of incidence and mortality for the top three Most Common Cancers in females in 2020. ....	3
Figure 2. Distribution of incidence and mortality for the top three Most Common Cancers in males in 2020. ....	4
Figure 3. Anatomy of the large intestine in the digestive system of human body.....	6
Figure 4: Development of CRC .....	8
Figure 5. Structure of flavan .....	21
Figure 6. General biosynthesis of flavonoids .....	21
Figure 7. Flavonoid classes.....	22
Figure 8. Fresh <i>EA</i> flower.....	24
Figure 9. General structure of chalcones .....	26
Figure 10. General Claisen–Schmidt scheme to synthesize chalcone analogs.....	26
Figure 11. Overview of Wnt/ $\beta$ -catenin signaling .....	29
Figure 12. Overview of Wnt/ $\beta$ -catenin signaling in cancer.....	30
Figure 13. Overview of PI3K/AKT/mTOR signaling in cancer.....	31
Figure 14. Comparison between human and <i>Drosophila</i> gut .....	35
Figure 15. Chemical structure of DK13.....	38
Figure 16. Chemical structure of DK14.....	38
Figure 17. Outcome of <i>EA</i> aqueous extract on the viability of CRC cell lines .....	50
Figure 18. Outcome of <i>EA</i> aqueous extract on the viability of NCE-1 E6/E7 .....	51
Figure 19. Outcome of <i>EA</i> aqueous extract on the morphology of CRC cell lines .....	53
Figure 20. Outcome of <i>EA</i> aqueous extract on cell cycle of HCT-116 cells.....	55
Figure 21. Outcome of <i>EA</i> aqueous extract on cell cycle of LoVo cells.....	56
Figure 22. Outcome of <i>EA</i> extract on cell invasion of HCT-116 cells .....	58

Figure 23. Outcome of <i>EA</i> extract on cell invasion of LoVo cells .....	59
Figure 24. Outcome of <i>EA</i> extract on colony formation of HCT-116 cells.....	61
Figure 25. Outcome of <i>EA</i> extract on colony formation of LoVo cells.....	62
Figure 26. Expression patterns of EMT biomarkers and their molecular pathways provoked by <i>EA</i> extract in HCT-116 cells.....	64
Figure 27. Expression patterns of EMT biomarkers and their molecular pathways provoked by <i>EA</i> extract in LoVo cells .....	65
Figure 28. Outcome of DK13 and DK14 on the viability of CRC cell lines.....	67
Figure 29. Outcome of DK13 and DK14 on the morphology of CRC cell lines.....	70
Figure 30. Outcome of DK13 and DK14 on cell cycle of HCT-116 cells.....	72
Figure 31. Outcome of DK13 and DK14 on cell cycle of LoVo cells.....	73
Figure 32. Outcome of DK13 and DK14 on cell invasion of HCT-116 cells .....	75
Figure 33. Outcome of DK13 and DK14 on cell invasion of LoVo cells .....	76
Figure 34. Outcome of DK13 and DK14 on colony formation of HCT-116 cells .....	77
Figure 35. Outcome of DK13 and DK14 on colony formation of LoVo cells .....	78
Figure 36. Expression patterns of EMT biomarkers and their molecular pathways induced by DK13 and DK14 in HCT-116 cells.....	80
Figure 37. Expression patterns of EMT biomarkers and their molecular pathways induced by DK13 and DK14 in LoVo cells.....	81
Figure 38: Relative quantification of <i>ras1</i> mRNA expression levels in the whole body of <i>Ras85D</i> as compared to <i>Yw</i> controls. ....	83
Figure 39: Relative quantification of ERK1/2 and Akt expression patterns in <i>Ras85D</i> as compared to <i>Yw</i> controls.....	83
Figure 40. Outcome of <i>EA</i> extract on the survival rates of <i>Yw</i> .....	84
Figure 41. Outcome of <i>EA</i> extract on the survival rates of <i>Ras85D</i> .....	85

Figure 42. Outcome of DK13 and DK14 on the survival rates of *Yw* flies and *Ras85D*  
fly line .....87

Figure 43: Summary of the main study findings .....97

## **CHAPTER 1: INTRODUCTION**

Cancer is a major concern for public health around the world, with an increasing burden on health systems each year. It is predicted that cancer cases may reach 420 million by 2025 (1). Typically, cells divide and grow in a controlled and systemic process to form new cells needed by the human body. Further, the body generally eliminates damaged, old, or useless cells. However, this is not the case in cancer, in which the cells divide uncontrollably and reach different regions of the human body. Cancer is raised through the transformation of normal cells into tumors that occur in multiple stages. This transformation is a result of complicated genetic or environmental factors. Cancer is a complex disease caused by numerous factors at cellular and genetic levels and can affect any cells, tissues, and organs with particular hallmarks. These hallmarks include uncontrollable cell division, independent microenvironment for cellular growth, angiogenesis, and the ability to metastasize to different parts of human body. The abnormal proliferation of cells leads to tumor formation. Tumors are lumps of tissues that can be benign or malignant. The main difference is that benign tumors do not invade nearby tissues. On the other hand, malignant tumors can invade distant parts of the human body. If cancer metastasis spreads without efficient treatments, it will lead to death eventually (2). Although tremendous efforts are made to manage the cancer burden, the cancer mortality rate is expected to increase by 60% in the upcoming years (3).

## 1.1 Colorectal cancer (CRC)

### 1.1.1 Burden of CRC

CRC or also called bowel cancer, is a disease that occurs in the colon (large intestine), rectum, or anus due to abnormal growth of cells. It is considered the second deadliest cancer after breast and second for malignancy in females (Figure 1) (4). In males CRC is the third deadliest cancer and malignancy in males (Figure 2). According to cancer statistics in 2022 by the American Cancer society, CRC is the third most diagnosed cancer, and the third deadliest cancer in both genders in the USA (5). Globally, CRC is responsible for 10% of cancer incidence and more than 9% of cancer deaths in 2020 (6). Further, CRC incidence may reach 2.5 million cases in 2035 (7). In addition, 13% of the malignant tumors in the GI tract are due to CRC (8). The incidence of CRC in males is more than in females, with 576,000 and 521,000 cases in 2018, respectively. In 2020, 50 new CRC cases were diagnosed per day (9). The CRC burden is expected to increase to more than 2 million cases and 1 million deaths globally (10).

Moreover, the risk of CRC is high in developed countries and Hungary is the country with the highest CRC incidence in males and Norway for females (11). In Arab countries, CRC incidence is the highest in the KSA, UAE, and Qatar (12). On the other hand, all African regions have the lowest rates of CRC incidence for both genders (11). In Qatar, CRC is diagnosed in 11.71% and 8.63 % of males and females, respectively which makes the second most common cancer. Further, 68% of CRC cases are diagnosed in advanced stages in Qatar (13).

Regarding the age of CRC patients, they are mostly above 50 years old, 80% of them is due to colon cancer and 75% due to rectal cancer (14). In addition, CRC incidence in age younger than 50 years old has increased over the last decades, called



Early onset of CRC (EOCRC). EOCRC is the occurrence of CRC in people below 50 years old due to hereditary cancer syndromes and familial CRC (15).

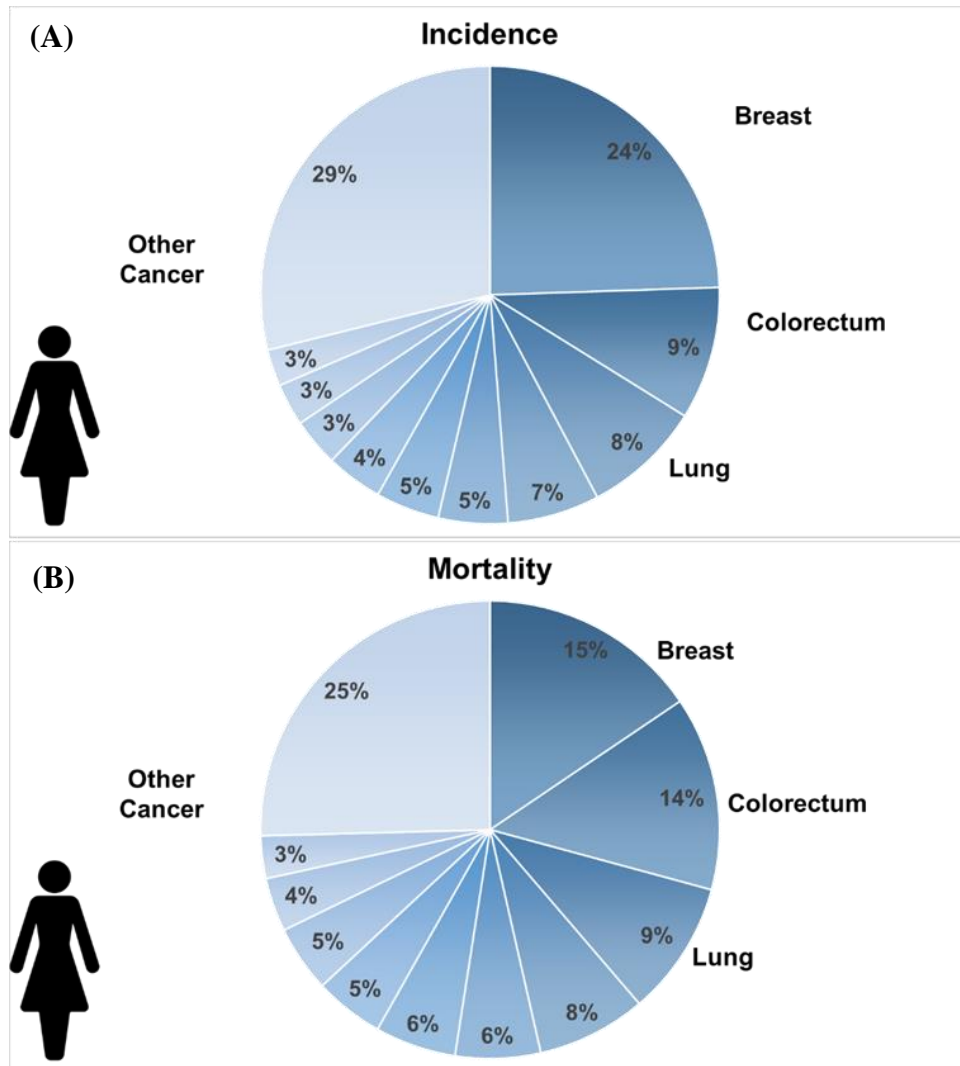


Figure 1. Distribution of incidence and mortality for the top three Most Common Cancers in females in 2020. The area of the pie charts reflect the total number of (A) cases and (B) deaths of the most common cancers in femlaes world wide according to the estimation of global cancer incidence, mortality and prevalence (GLOBOCAN) 36 cancers in 185 countries. Picture is adapted from Sung, H et al. (2020).

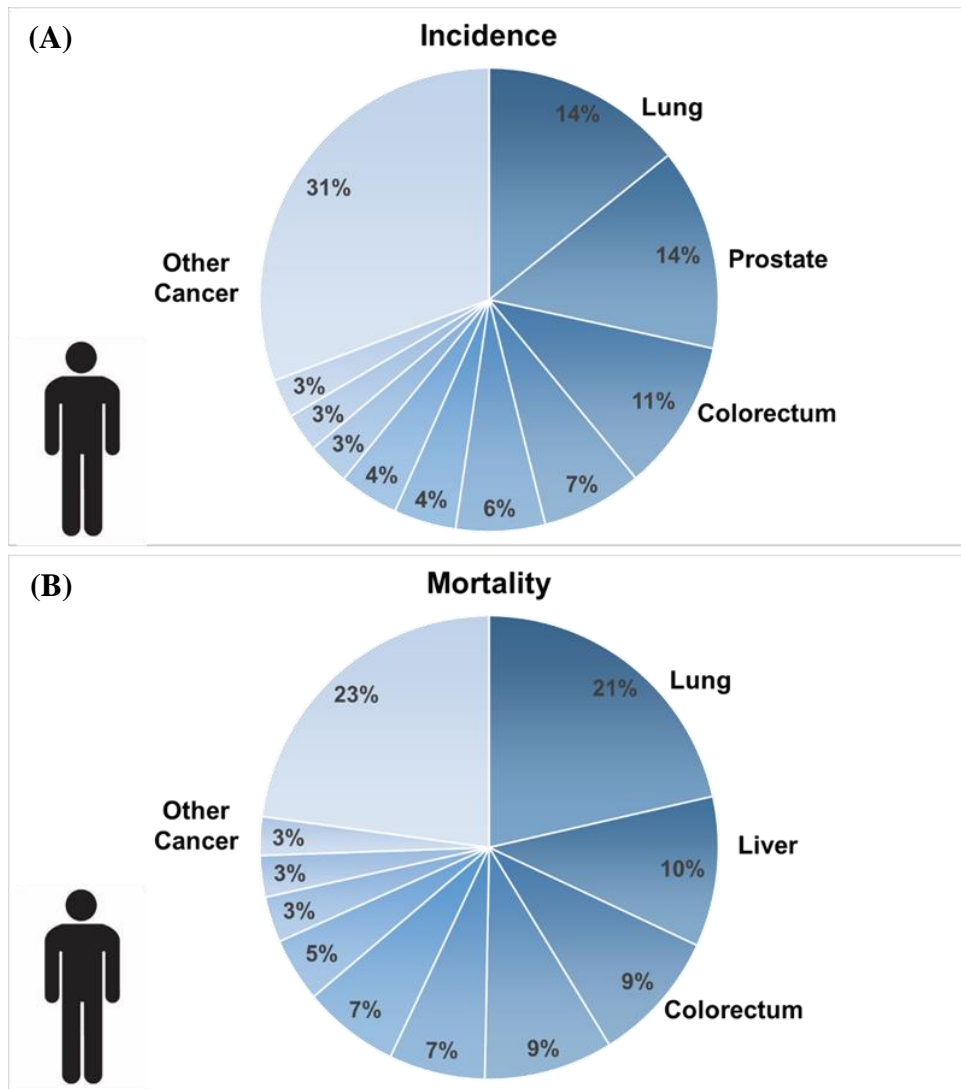


Figure 2. Distribution of incidence and mortality for the top three Most Common Cancers in males in 2020. The area of the pie charts reflect the total number of (A) cases and (B) deaths of the most common cancers in femlaes world wide according to the estimation of global cancer incidence, mortality and prevalence (GLOBOCAN) 36 cancers in 185 countries. Picture is adapted from Sung, H et al. (2020).

### 1.1.2 Etiology of CRC

Colon is a region in the large intestine at the end of the GI tract that performs vital roles in digesting food and absorbing nutrients and water. The GI tract or digestive system consists of upper and lower GI. The upper GI comprises the mouth, pharynx, esophagus, and stomach. Lower GI consists of the small and large intestines (16). The small intestine is 7 meters long from the pylorus to the ileocecal valve. This valve presents between small and large intestines to block the returning of intestinal contents from the large to small intestine. Small intestine comprises of duodenum, jejunum, and ileum (17). Large intestine is 1.5 meters long, and it exists as a frame surrounding the small intestine, at the end of the GI tract, and it begins from the ileocecal valve to the anus. Absorption of water and indigested food is the responsibility of the large intestine to relieve the body from any waste matter. From left to right, the large intestine is made up of the cecum with the appendix, ascending colon, transverse colon, descending colon, sigmoid colon, rectum, and anal canal (Figure. 3). The cecum is the beginning portion of the large intestine existing as a large pouch connected to the ileum. It is responsible for the reabsorption of fluids, and it temporarily stores the chyme. Part of the cecum is a blind lymphoid pouch called an appendix that maintains the flora in the gut. Colon is a term used to describe the regions between the cecum and rectum: ascending colon, transverse colon, descending colon, and sigmoid colon (18). Colon has three vital functions: absorption of water, electrolytes, and vitamins, forming feces to eliminate waste out of the body, and microbial digestion (19). The colon starts when the cecum receives food materials known as chyme from the small intestine into the large intestine. Then, when cecum is full of chyme, this induces the movement of colon muscles to start functioning. As chyme slowly moves through ascending colon, transverse colon, descending colon, and sigmoid colon, some materials cannot be digested by the human body. Thus, the gut microbiota is essential to digest these

indigestible materials. Ascending colon and transverse colon are responsible for absorbing water and nutrients from indigestible chyme to form stool by solidification. Then, feces are stored by descending colon and removed into the rectum. The sigmoid colon facilitates the movement of stool into the rectum by increasing the pressure inside the colon. Finally, the rectum holds the feces until defecation to eliminate all wastes (20). The colon is considered simple in structure compared to other organs; however, it is susceptible to different diseases such as cancer.

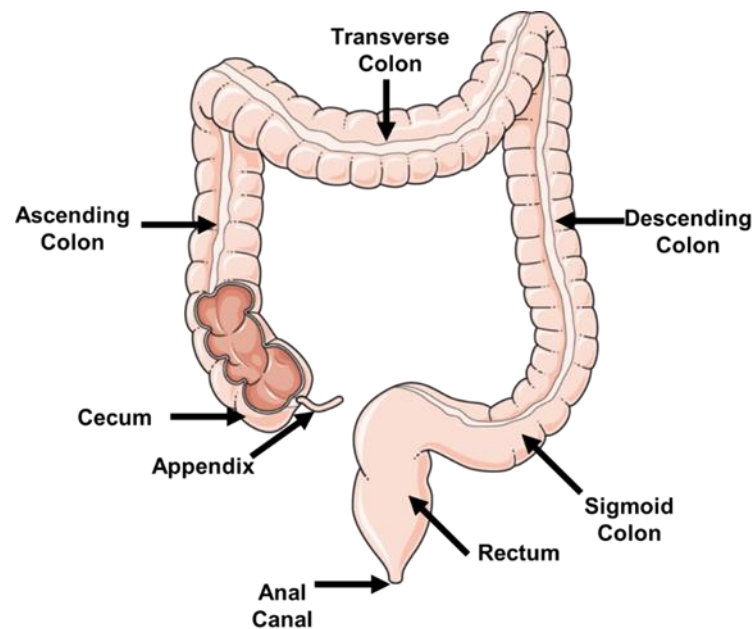


Figure 3. Anatomy of the large intestine in the digestive system of human body. Colon is the region between the cecum and rectum: ascending colon, transverse colon, descending colon, and sigmoid colon. Illustration of different organs in the upper and lower GI tract of human body.

Most CRC tumors are developed from the colonic epithelium layer in three phases initiation, promotion, and progression. According to recent studies, colorectal tumorigenesis is initiated due to stable mutations in the DNA sequence of tumor suppressor genes and oncogenes. These DNA alternations lead to abnormal neoplastic clones, eventually leading to cancer development (21). The sequence of CRC development starts as follows: normal mucosa- small adenoma, large adenoma, and cancer (Figure. 4). CRC beings from focal changes with the growth of benign pre-cancerous polyps. These polyps are accumulations of cells in the intestinal mucosa. Over cellular increase in these polyps, genetic alternations make these polyps able to invade other layers of the colon, which is a hallmark of cancer. With time, these polyps become more aggressive to invade local lymph nodes until they metastasize to other tissues (22). The growth of these malignant polyps is slow that may take several decades without apparent symptoms. CRC symptoms start when the tumor reaches several centimeters that inhibit the normal defecation. Mainly, CRC develops from dysplastic adenomatous polyps that involve alternations in multiple genes responsible for suppressing tumors and repairing DNA. All these are combined with significant oncogenes activation (23).

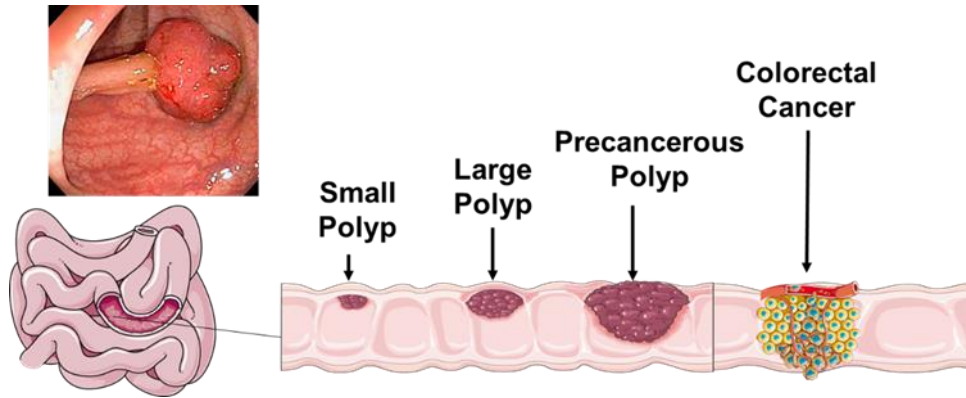


Figure 4: Development of CRC. Progression of CRC starts from small polyp. Then, due to accumulation of genetic and epigenetic alternations, polyp transform into precancerous polyp and into cancer eventually.

### 1.1.3 Types of CRC

CRC starts in the inner layer of the colon and gradually travels to the outer layer. When cancer begins in the colon is called colon cancer, and when it starts in the rectum is called rectal cancer. Mostly it is called colorectal cancer due to shared features between the colon and rectal cancer. CRC occurs in a complicated multistep process that begins with benign tissue to a malignant tumor. According to the World Health Organization (WHO), CRC is classified into histological subtypes adenocarcinomas (AC), mucinous adenocarcinomas (MAC), and signet-ring cell carcinomas (SC), and other types that rarely occurred (24). AC affects glands of epithelial cells, and the colon has a vast network of glands to facilitate the absorption of water and nutrients. Thus, AC is the most common type of CRC; it accounts for 90% of CRC cases. The development of AC, MAC, and SC is associated with the excess production of mucin. However, AC might develop due to the lack of mucus, which damages the lining layer of the colon and eventually leads to genetic disturbance and abnormal cell proliferation (25). MAC is found in more than 10% of CRC patients and usually occurs in the proximal colon with a specific characteristic that 50% of tumor volume is mucinous. The incidence rate of mucinous adenocarcinoma is much higher than non-mucinous adenocarcinoma. It has a poor prognosis, and it is chemo-resistant compared to non-mucinous adenocarcinoma (26). Many theories believe that mucus overproduction helps tumors metastasize to neighboring tissues aggressively (27). MAC shared several clinical features with SC, such as both subtypes occur in young patients with high invasive to the lymph nodes. Pathologically, SC has a particular characterization: the presence of intracytoplasmic mucin in single or tumor cells that displace the nuclei, and these cells are called signet-ring cells (28). CRC has other rare types like neuroendocrine carcinoma (NEC), accounting for less than 1% of all CRC cases. Although it is rare, NEC is considered an aggressive type of CRC with a high tendency

for metastasis. Additionally, it is diagnosed only at advanced stages with less than 20% of 3-year overall survival (29). Squamous, adeno-squamous, spindle cell, and undifferentiated carcinomas are other histological subtypes of CRC that rarely occur (30).

#### 1.1.4 Risk factors of CRC

At present, we live in an era with high standards of living. However, this comes with consequences that have negative impacts on human health and diseases. CRC was not diagnosed several decades ago, and now it is the cause of more than 50% of deaths related to cancer in the world (31). Multiple reasons explain the increase in incidence and mortality of CRC. For instance, poor dietary habits, aging, smoking, and alcohol addiction, along with a destructive lifestyle. In addition, several genetic, bacterial/viral infections and environmental factors contribute to CRC.

##### 1.1.4.1 Environmental factors

Individual lifestyles are strongly associated with CRC development, such as obesity and smoking. Recent studies in the U.S claimed that over 50% of CRC incidences could be prevented by modifying lifestyle habits. The most common risk factor of CRC is obesity. Several epidemiological studies confirmed the association between overweight and CRC as 5% of CRC cases in the U.S are due to obesity (32). The association between obesity and CRC is highly related to gut microbiota that induces epigenetic alternations. These epigenetic alternations occurred due to a diet rich in fat that affects transcriptional responses, eventually causing CRC initiation and progression (33). A gut flora *F. nucleatum* bacteria is the most common type of bacteria associated with CRC. A crossover study found that *F. nucleatum* levels were higher in people with a high-fat diet than those who switched to a low-fat diet and were high in fiber (34). Further, overconsumption of red and processed meat and being low in



calcium and vitamins are risk factors for CRC. Insufficient physical activity is also a risk factor related to gut microbiota. Animal studies showed that exercising affects the short-chain fatty acids in the gut microbiota. Additionally, the gut of obese rates found to restore bacterial variety upon exercising (35, 36).

Moreover, addiction to alcohol and smoking are considered severe risk factors of CRC. The association of alcohol consumption with CRC depends on the dose; however, many data showed that even a small amount might cause CRC (37). Drinking 150 mL/week of alcohol increases the risk of CRC incidence significantly compared with nondrinkers (38). According to a meta-analysis, 10 per 100x10<sup>3</sup> of CRC cases and deaths is associated with smoking cigarettes (39). Although drinking alcohol and smoking cigarettes are confirmed to aid CRC development, the molecular pathological pathways are not well explained yet (40). Other risk factors, including age, gender, and race, can contribute to CRC. over 50 years old age group is found to be more susceptible to CRC, and people after 60 years old were found to be three times more likely to arise CRC. Gender is also a risk factor for CRC, as males are more likely to develop CRC than females with 30% and 40 % higher risk of incidence and mortality, respectively (10).

#### 1.1.4.2 Genetic factors

Genetically, CRC has three categorizations sporadic, inherited, and familial. Sporadic CRC accounts for 70% of CRC cases and usually develops in the distal colon without inherited causes (41). The development of sporadic CRC is associated with mutations in oncogenes and tumor suppressor genes. CRC is developed due to more than 80 mutations, and at least 15 of these mutations are the leading cause of tumorigenesis (42). A theory called adenoma-carcinoma sequence is assumed for the occurrence of sporadic CRC, in which mutation in adenomatous polyposis coli (APC)

gene will initiate several modifications in multiple genes like Kirsten RAS (KRAS) and TP53. According to this theory, sporadic CRC pathogenesis requires at least seven genes (43, 44). The second type of CRC is inherited CRC, which includes colonic polyps that may manifest into disease or may not. And these colonic polyps include two syndromes, hereditary nonpolyposis CRC (HNPCC) (Lynch syndrome I) and the cancer family syndrome (Lynch syndrome II). Finally, familial CRC is a not well understood yet; however, it accounts for 25% of the cases. In families affected with cancer, the development of CRC is frequent and considered as sporadic CRC but the not inconsistent pattern as the inherited CRC (45).

CRC is a very complex disease with multiple pathways at the molecular level accompanied by mutator mechanisms and classic suppressors (46). It involves mutations in the APC protein and heterozygosity and chromosomal instability (CIN). The other molecular mechanism of CRC involves APC and KRAS mutations, which are more heterogeneous than the common pathway (47). Mutations at baseline are not enough to cause the required modifications for CRC development. Mutations per base pair of a nucleotide is estimated to be  $10^{-9}$  per cellular generation. Therefore, CRC acquires intrinsic genomic instability to increase the new mutations rate (48). CRC is recognized to have three genetic instability pathways which are Chromosomal Instability (CIN), Microsatellite Instability (MSI), and CpG Island Methylator Phenotype pathways (CIMP) (49). The most common and characterized pathway of CRC is CIN, also called the adenoma-carcinoma sequence. CIN accounts for 70% of sporadic CRC with a predictable genetic progression and histological alternations. This genetic progression includes three significant changes, which are suppression of tumor suppressor gene such as *APC* in region 5q21 of chromosome, loss of *p53* in region 17p13 of chromosome, and activation of proto-oncogenes such as *RAS*. In addition,

tumorigenesis involves several proteins and regulator checkpoints for a different mitotic spindle that affect the stability of the mitotic chromosome (50). CIN pathway is characterized by several mutations in the structural chromosomes that lead to loss of heterozygosity (LOH) at the loci of tumor suppressor gene, aneuploid karyotype, and chromosomal rearrangements (51). The worst outcomes of CRC are caused by the CIN pathway more than the MSI and CIMP pathways (52).

The second pathway of CRC is MSI, which accounts for 15% of all CRC cases, and it is considered the molecular characterization of deficient mismatch repair (MMR) system. Due to germline mutations in MMR genes, MSI occurred when it developed with inherited CRC (53, 54). Epigenetic silencing of MLH1 leads to MSI in tumors of sporadic CRC that arise because of CpG islands' methylation. Yet, MSI has better prognosis than microsatellite-stable tumors with no clear explanation (55, 56).

The third phenotype of genomic instability in CRC is CIMP. Several genes will be altered in their promoter methylation by CIMP. CIMP is one of the most recognized epigenetics forms in CRC in CpG islands. CpG islands are regions of DNA rich with CpGs stretching between 500 to 1000 base pairs with more than 0.6 ratios of CG: GC found at promoters (57). Stable promoter CpG islands methylation is required for normal cells and an essential mechanism for regulating gene expression. Therefore, alternations in this methylation mechanism led to gene silencing involved in DNA repair and tumor suppression, leading to cancer (58). Although CIMP is not well defined yet, it has been found that CRC caused by this genomic instability has the worse prognosis with KRAS or BRAF mutations related to the poor outcome (59).

### 1.1.5 Prognostic and prediction of CRC

CRC prognosis includes many factors like the type of cancer at the histological level, location and size of the tumor, and the metastasis to other organs. Most CRC cases are asymptomatic before they transform into malignant tumors. A proliferation antigen called Ki-67 that disturbs cell cycle at G0 phase is considered a prediction of CRC. Determining the level of Ki-67 is associated with the growth fraction of the tumor (60). Another marker for CRC is Proliferating cell nuclear antigen (PCNA), which is considered a vital prognosis factor of CRC. PCNA is expressed highly in proliferating cells, and the over-proliferation of cells is a hallmark of cancer. Therefore, increasing the expression of PCNA indicates a higher cancer malignancy (61)

Moreover, epidermal growth factor receptor (EGFR) plays an essential role in regulating proliferation and invasion and cell development (62). EGFR pathway is mediated by multiple downstream pathways like RAS-RAF-mitogen activated protein kinase (MAPK) and phosphatidylinositol 3-kinase (PI3K)-AKT-mTOR pathways (63). EGFR and KRAS are both considered essential biomarkers in patients with advanced CRC. KRAS mutations are found in more than 40% of advanced CRC patients (56). In addition, serum markers like Carcinoembryonic antigen (CEA) are important for CRC. It is an immunoglobulin gene and functions as an intercellular adhesion molecule, promoting cell aggregation in CRC. CEA helps CRC tumors metastasis to the lung and liver and is considered an adverse prognostic indicator (64).

Several oncogenes and tumor suppressor genes are important in CRC prognosis. *P53* is a tumor suppressor gene mutated in 70% of CRC cases and contributed to the worst outcomes. Clinically, *p53* mutations are found in primary tumors (65). The process starts with genetic instability that induces KRAS activation, which suppresses *p53* and *APC* from playing their role as tumor suppression genes. This process leads to

the transformation from adenoma to CRC adenocarcinoma, which is mainly resistant to chemotherapies (66). More than 40% of malignant CRC tumors have *RAS* mutations, characterized by the worst prognosis (67). *RAS* family has three genes *KRAS*, *NRAS*, and *HRAS*. *RAS* genes initiate signal transduction by binding to growth factor receptors on the cell membrane to perform important functions like cell survival (68). MAPK and PI3K are the two main pathways involving *RAS* proteins. In CRC, 45% and 8% of the malignancies are due to *KRAS* and *HRAS* mutations, respectively (69).

#### 1.1.6 Diagnosis and management of CRC

CRC is asymptomatic at early stages, and if symptoms exist, they would be similar to other lower abdomen diseases. Thus, CRC diagnosis is challenging, and it is a long and complex process with multiple events, including the patient, physician, and the health system. CRC is diagnosed because of severe symptoms in the patient or due to screening. Symptoms of CRC include pain in the lower abdomen, fatigue, blood in stools, and others like weight loss and shortness of breath. Colonoscopy is the preferred first investigation method in the case of symptomatic CRC. Other methods for primary assessment are there for population screening and then followed by colonoscopy in mild cases (70). The accuracy of colonoscopy is high and can access the tumor location specifically. It allows biopsy sampling, which provides an opportunity to diagnose the molecular profiling of the sample for confirmation histologically. Additionally, colonoscopy is the only investigation method that offers a diagnostic and therapeutic effect, and it reduces CRC death by 53% (71). The second diagnosis method for CRC is capsule endoscopy. It is a wireless capsule swallowed by the patient, and it detects more than 70% of CRC cases. Further, capsule endoscopy allows the investigation of the whole GI tract (72, 73). Finally, computed tomography (CT) is a CRC diagnosis by taking several images for the colon using X-rays. Then, specific software combines

these images to show any tumors or abnormal growth in the colon (74).

Another method to diagnose CRC is by fecal occult blood test (hemoccult). Usually, CRC leads to bleeding in the large intestine and causes anemia. Therefore, quantifying the number of red blood cells can indicate bleeding triggered by CRC (75). Further, biomarker testing is effective in CRC diagnosis by determining important biomarkers found in the blood or tumor tissue of the patient. There are several important biomarkers in CRC such as KRAS, NRAS, BRAF, EGFR, HER2, PIK3CA, and PD-L1. The determination of these biomarkers specifies the treatment plan for each patient (76). According to Union for International Cancer Control (UICC), CRC has five stages described by the TNM system. TNM refers to T for tumor size, N stage for lymph nodes involvement, and M indicates the distant metastases of cancer (77) (Table. 1).

Table 1. Staging system of colorectal cancer according to UICC.

UICC Stage	TNM	N stage	M stage	Events
0	TIS	N0	M0	Growing polyps are in the lining layer of the colon and considered as non-cancerous growing
I	T1, T2	N0	M0	Dukes' A colon cancer, in which cancer spreads to the middle layer of the colon.
IIA	T3	N0	M0	Dukes' B colon cancer. Stage IIA in which cancer spreads to the outer layers of the colon, stage IIB cancer spreads out of the colon and stage IIC cancer spreads to the neighboring tissue, but it did not reach the lymph nodes.
IIB	T4	N0	M0	
IIIA	T1, T2	NI	M0	Dukes' C colon cancer. Stage IIIA cancer spreads to one or three lymph nodes, stage IIIB cancer spreads to four or more lymph nodes and stage IIIC cancer reaches the adjacent tissues.
IIIB	T3, T4	NI	M0	
IIIC	TI-4	N2	M0	
IV	TI-4	NI-2	MI	Dukes' D colon cancer. Cancer reaches one or more of the organs such as lung or liver. It may reach distant regions of the peritoneum

T: Tumor, N: Lymph node, M: Metastasis

### 1.1.7 Treatment of CRC

CRC treatment is mainly dependent on the stage of cancer. Surgery is the first choice for treating CRC at stage 0 as the polyp grows only in the lining layer of the colon. Thus, the polyp is eliminated by local excision, or if the size of the cancer is big, then a part of the colon is removed (colectomy). Surgery is also an option at stage I if there are no cancer cells left after local excision. In some cases, multiple surgeries are required at stage I to remove the polyps. At stage II, cancer reaches some tissues, thus removing a section of the colon or a partial colectomy. Adjuvant chemotherapy is needed after the surgery at stage II. Stage III also required partial colectomy along with affected lymph nodes. Standard chemotherapies at stage III are FOLFOX such as 5-FU, leucovorin, and oxaliplatin or CapeOx such as capecitabine and oxaliplatin. Some stage III cases are advanced and cannot be treated with surgery (78). Therefore, neoadjuvant chemotherapy with radiation or chemoradiation is needed to shrink cancer and remove it with surgery later. The last stage is stage IV, in which cancer spreads to distant regions like the liver, brain, lung, and distant lymph nodes. At this stage, surgery is not functional; however, it can be helpful to remove cancer from the affected organs. At this stage combination of chemotherapies is needed to control cancer (7, 79).

Despite the strenuous efforts to control and treat CRC at all stages, the five-year survival rate of CRC dropped from 64% to 12% (80). Furthermore, several studies have recently reported that tumors develop resistance against these drugs over the treatment course, apart from the severe side effects generated by these treatment regimens (81). Additionally, CRC highly impacts the patient and their family's life directly because of symptoms like severe pain, loss of appetite, and blood or indirectly by the treatment regimens. All these challenges of CRC and its conventional treatments necessitate developing alternative, reliable, and targeted therapies against CRC. These alternative



therapies should provide a means to prevent the progression of CRC, control metastasis, and treat the disease with minimal to no side effects.

### 1.2 Complementary and alternative medicine (CAM)

CAM is a term that refers to a wide range of preventions and treatments based on folklores and traditional techniques other than systemic medicines. CAM mainly consists of mind and body therapies like meditation and yoga or biologically based natural resources to extract vitamins and dietary supplements. According to the WHO, 80% of people use CAM techniques to treat different illnesses worldwide (82). For instance, the prevalence of CAM is notably high in France and Germany compared to other European countries, and more than 70% of Canadians use at least one technique of CAM. In Asia, 60% of Chinese people and more than 20% of doctors in Japan are using CAM (83-85).

Moreover, CAM has been used to treat different chronic diseases like cancer. Biologically based CAM or also called phytotherapy considered the most common technique used by cancer patients. It includes plants extract or a combination of different plants to treat a specific disease. Several studies have shown that phytotherapy enhances the capability of the human body to protect and heal itself (86). Therefore, it has been a trusted resource for valuable anticancer agents for several decades. According to the National Cancer Institute (NCI), 3,000 plant species out of 35,000 were potential in treating cancer (87). In the middle east region, more than 700 plant species are considered for cancer treatment (88). Furthermore, several medicinal plants showed significant anti-CRC activities based on *in vitro* and *in vivo* studies (89, 90). In addition, many promising anticancer compounds were synthesized according to the molecular structure found in different phytochemical families such as flavonoids.

### 1.2.1 Flavonoids

Flavonoids are an enormous phytochemical group found in most plants, flowers, fruits, and vegetables. They are secondary metabolites in plants in the family of polyphenolic compounds with a wide range of different structures. Naturally, flavonoids are responsible for other plants' characterizations, such as the attractive colors and leaves, the fragrance of flowers, and sweet flavor. Additionally, they exhibit a protective effect in plants against ultraviolet radiations, invaders, and pathogens (91). The general chemical structure of flavonoids consists of the essential core flavan C6-C3-C6, two phenyl rings connected by a ring containing Oxygen or called heterocyclic ring (Figure. 5). There are two biosynthesis pathways for natural flavonoids in plants, the phenylpropanoid, which generates the C6-C3 skeleton, and the polyketide pathway that produces units of polymeric C2 (92). Several co-enzymes like p-coumaroyl CoA and malonyl CoA and chalcone synthase enzyme are used in multiple steps to make different forms of flavonoids (Figure. 6) (93).

Furthermore, flavonoids are subdivided into groups based on several factors like the saturation degree of the central heterocyclic ring. Other factors like substituents on the A and B rings and molecular size can affect flavonoids classification. The main subgroups of flavonoids are chalcones, flavones, flavonols, flavonones, flavononols, flavan-3-ols, anthocyanins, and isoflavones (Figure. 7) (92).

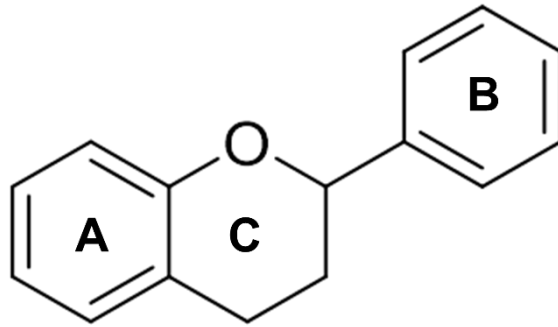


Figure 5. Structure of flavan, basic core of flavonoids C6-C3-C6. A and B are two phenyl rings connected by C the heterocyclic ring.

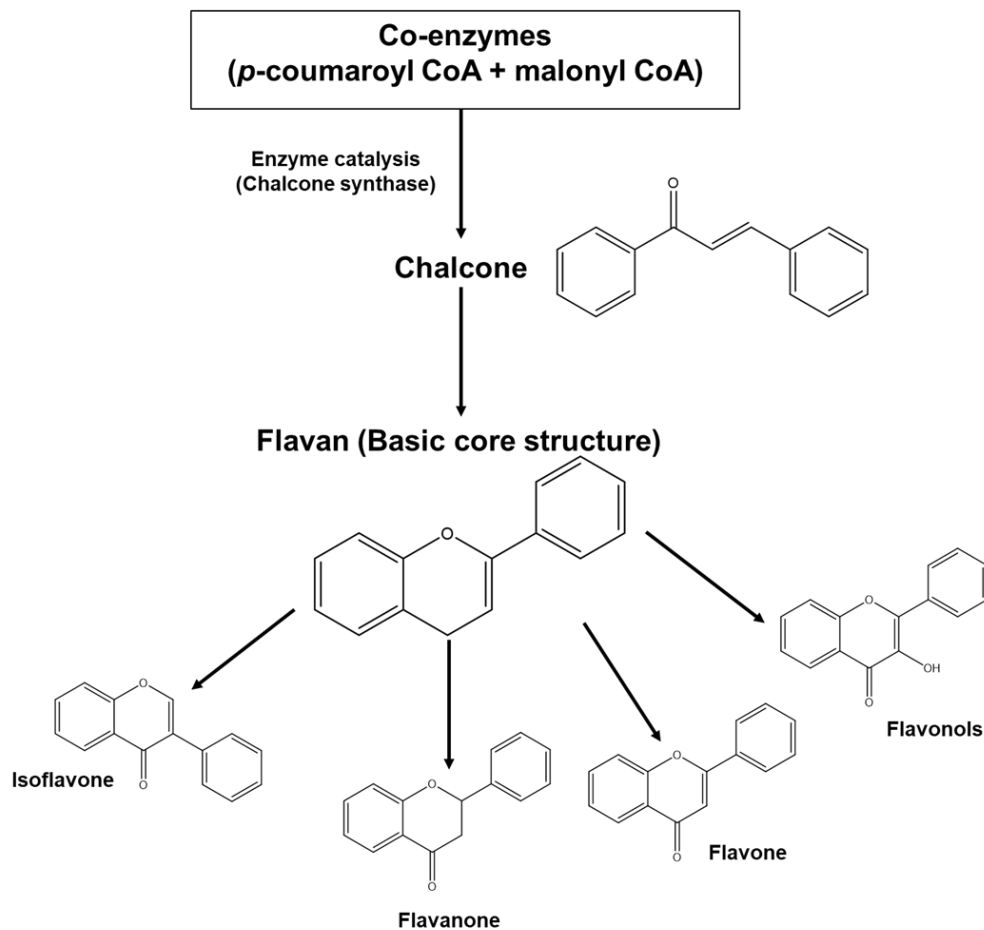


Figure 6. General biosynthesis of flavonoids. Flavonoids are polyphenols and secondary metabolites corresponding in plants and have wide range of variety in terms of structure and function. Flavonoids mostly found as aglycones or glycosides in many edible plants. Biosynthesis of flavonoids is occur by phenylpropanoid metabolic pathway in which coumaroyl-CoA is produced. Then, the backbone of flavonoids, chalcones are synthesized. Pictutre adabtred from Dias, MC et al (2021).

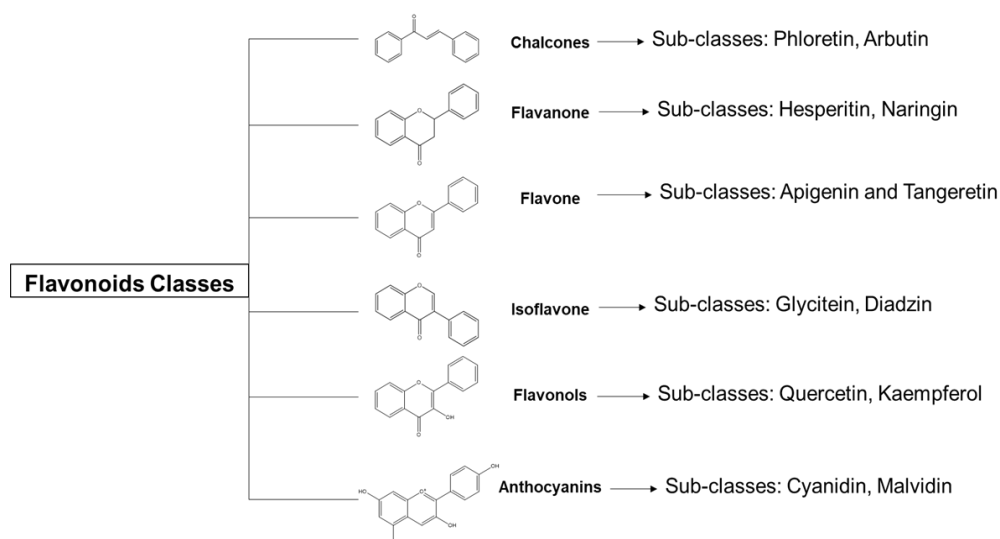


Figure 7. Flavonoid classes, and examples of subclasses. Chemical structure of flavonoids consists of 15 carbons constituted by a common skeleton of nucleus flava (C6–C3–C6). Picture adapted from Liu, W et al (2021).

Nowadays, flavonoids have become the focus of research from natural and synthetic resources due to their significant health benefits. In addition, flavonoids become essential in human daily dietary intake of food like fruits and vegetables. Although it is not easy to accurately determine the amount of flavonoids intake by humans due to their complexity and diversity, A study estimated that about 158 to 203 mg/day is the total amount of food flavonoids consumed by human (94, 95).

Several studies showed the significant effect of flavonoids as anticancer agents (96). Phytotherapy can treat cancer by three means: suppressing agents that inhibit procarcinogens from transforming into cancer, blocking agents that block carcinogenic compounds from reaching vital sites and initiate cancer, or altering agents that help metabolize carcinogenic components to inhibit their biological activity (97). Flavonoids can function in all of these methods (98). Since flavonoids exist in a vast range of edible natural products and are consumed by humans daily, they considerably

affect colon and bowel diseases. An updated meta-analysis of epidemiological studies reported that a flavonoids-rich diet might decrease the risk of human CRC (99, 100). Therefore, flavonoids from natural and synthetic resources are considered for future potential treatments for CRC. Thus, *Elaeagnus Angustifolia* and chalcones can both be considered as promising natural and synthetic flavonoids as potential therapeutic agents for CRC treatment.

#### 1.2.1.1 *Elaeagnus Angustifolia* (EA)

*Elaeagnus Angustifolia* (EA), or Russian olive, is a large shrub with flexible branches as a perennial tree with 5 to 12 meters in height. It belongs to Family *Elaeagnaceae* that includes about 80 species in the world. EA is a deciduous plant with alternate leaves. Flowers of EA are characterized by their pleasant fragrance with an oval shape, and they are sweet, fleshy, and edible. Geographically, EA is widely spread in Asia and Europe. Further, it has high adaptability to different environments in many countries, from the Mediterranean to northern Russia. Traditionally, EA has been used for centuries for its valuable extract. As a result, it has a wide diversity of folklore medicine in different nations. Recently, several studies focused on EA extract's biological and pharmacological activities from its various parts like flowers and fruits (101, 102).

Phytochemical studies revealed that EA contains a wide variety of effective compounds like flavonoids, phenolic acids, carotenoids, terpenoids, lignanoids, organic acids, coumarins, alkaloids, steroids, and vitamin C. EA biological activities were evaluated and found to have multiple activities like muscle relaxation, antinociceptive, antimicrobial, anti-inflammatory and later proved to have chemoprevention activity (103). Chemoprevention is a strategy to suppress, reverse, or prevent cancer using natural or synthetic agents, whether it is an extract or chemical to reduce the adverse

side effects of conventional chemotherapies. Accordingly, *EA* flowers have been used traditionally as a drink to treat diseases such as asthma, diarrhea, and osteoporosis. Based on phytochemical studies flowers and leaves, *EA* has a significant abundance of flavonoids that are suggested to be responsible for its therapeutic effect (104, 105).



Figure 8. Fresh *EA* flower.

### 1.2.1.2 Chalcones

Chalcones are a class of flavonoids found naturally in many medicinal plants in flowers, fruits, and vegetables. They are made of unsaturated ketone, including a reactive keto-ethylenic group that unique pigmentation for chalcones compounds. Chalcones have other chemical names like benzalacetophenone and benzylidene acetophenone, and they are the biosynthetic precursor for many cyclic derivatives. Further, chalcones structure contains conjugated double bonds with two aromatic rings (106). They considered the main precursors for biosynthesis of different classes of flavonoids. Chalcones are not like the rest of flavonoids classes and are called open-chain flavonoids due to the presence of an open ring structure (Figure. 9). The advantage of the chalcones' system is that it assists in skeletal modification and is used as a unique scaffold in medicinal chemistry to synthesize novel compounds. Chemically, chalcones analogs can be synthesized by several condensation reactions. Claisen–Schmidt reaction is the most common and straightforward reaction used in chalcone synthesis. It's the condensation of substituted acetophenone and selected benzaldehyde analogs under base catalyzed conditions at room temperature for specified period of time (Figure. 10) (107).

For decades, chalcones were found to have a wide range of pharmacological activities as anticancer and chemoprevention. They exhibit different activities against cancer, such as inhibiting the metabolism of procarcinogen, inducing enzymes responsible for carcinogen-detoxifying, and inhibiting tumor growth at early stages. (108).

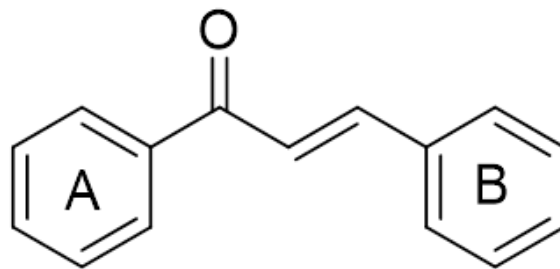


Figure 9. General structure of chalcones. A and B are two rings conjugated with a carbonyl group.

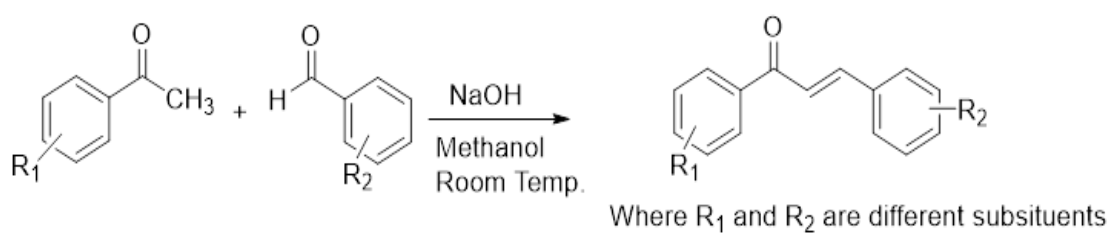


Figure 10. General Claisen-Schmidt scheme to synthesize chalcone analogs.



### 1.2.2 Promising CRC molecular targets for natural and synthetic flavonoids

CRC is a heterogeneous disease that involves multiple genetic and epigenetic alternations. Thus, different molecular pathways are involved in CRC development and are aimed for treatment as shown in Tables 2 and 3. Nowadays, significant efforts have been made to understand how extracted flavonoids from natural and synthetic resources affect fundamental cellular functions in CRC at the molecular level. These studies focused on the signaling pathways that these natural products might function in healthy and cancer conditions. Flavonoids affect different pathways, including Wnt/ $\beta$ -Catenin Signaling, PI3K/AKT/mTOR pathway, apoptosis, and epithelial-mesenchymal transition (EMT) (109).

Table 2. Examples of natural flavonoids explored on different CRC cell lines

CRC cell lines	Flavonoid	Signaling and target pathways	References
HT-29	Quercetin	Wnt/ $\beta$ -Catenin Signaling, cell cycle	(110)
HCT-116	Rutin	Apoptosis	(111)
DLD-1	Naringenin	Apoptosis	(112, 113)
HT-29	Silibinin	EMT and Wnt/ $\beta$ -Catenin Signaling	(114)
W480, HT-29, and Caco-2	Chrysin	Apoptosis	(115)

Table 3. Examples of synthesized chalcone analogs explored on different CRC cell lines

CRC cell lines	Chalcone analogs	Signaling and target pathways	References
HCT116	Benzylidenetetralones, cyclic chalcone	Cell cycle and apoptosis	(116)
HCT-116 and LoVo	Polymethoxylated Chalcones	EMT	(117)
LoVo, COLO 205	4-Boc-piperidone chalcones	Apoptosis	(118)

### 1.2.2.1 Wnt/ $\beta$ -Catenin Signaling

The Wnt signal transduction pathway is considered one of the most studied in recent research in the hope of finding the mechanisms controlling normal development. Wnt signaling pathways consist of many signal transduction pathways that function thru proteins and receptors on the cell's surface (119). Wnt name refers to two parts, Wnt refers to the *wingless* gene in *Drosophila* flies and the second part is the name of the vertebrate homolog of this gene, which is *integrated* or *int-1* (120). Wnt signaling pathways function through glycol-lipo proteins under the Wnt family; these proteins play crucial roles during embryonic development. Therefore, mutations in Wnt pathways are associated with severe defects in human birth and chronic diseases like cancer (121). Wnt signal stimulates multiple signal transduction cascades in the cell, such as Wnt/ $\beta$ -Catenin dependent and independent pathways (122).

In healthy cases, Wnt/ $\beta$ -Catenin pathways are off as  $\beta$ -catenin protein is degraded constantly by Axin complex that includes Axin protein, APC, casein kinase 1 (CK1), and glycogen synthase kinase 3 (GSK3) (123)The amino-terminal region of the  $\beta$ -catenin protein is phosphorylated, which makes it recognizable for the  $\beta$ -Ttcp, an ubiquitin ligase subunit. Subsequently,  $\beta$ -catenin is degraded and prevented from reaching the nucleus (124) (Figure. 11). In cancer cases, the Wnt/ $\beta$ -Catenin signaling pathway is responsible for cell proliferation and has a crucial pathological function in tumorigenesis. In addition, it modulates several genes that regulate cell cycle genes and oncogenes (125) (Figure. 12).

Further, Wnt/ $\beta$ -Catenin signaling pathway induces chemoresistance in CRC patients. Several studies illustrated that induction of Wnt/ $\beta$ -catenin signaling and accumulation of  $\beta$ -catenin enhance therapeutic resistance to 5-FU (126). Thus, CRC sensitivity to the drug can be adjusted by Wnt/ $\beta$  -catenin signaling pathway (127).

Furthermore, anticancer activity of flavonoids is associated with Wnt/ $\beta$ -catenin signaling pathway modulation. Flavonoids regulate the Wnt/ $\beta$ -catenin signaling pathway thru the interaction with ligand-receptor or by component methylation in the genes expressing pathway. Subsequently, flavonoids inhibit the reach of  $\beta$ -catenin to the nucleus (128).

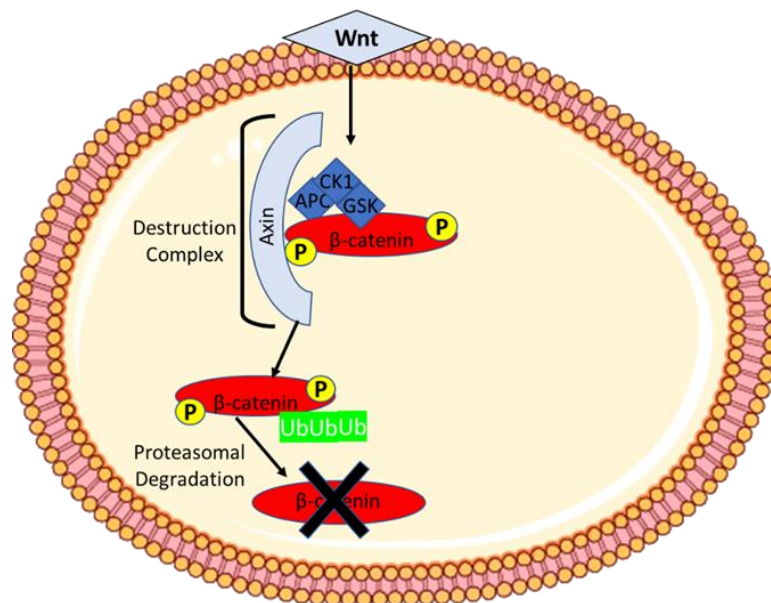


Figure 11. Overview of Wnt/ $\beta$ -catenin signaling. In Wnt-off state, Axin complex is the core component to activate  $\beta$ -catenin phosphorylation for degradation by  $\beta$ -Trop. GSK and CK1 promote Axin and APC phosphorylation to support their binding to  $\beta$ -catenin and destabilize the complex. The destruction of the complex lead to subsequent degradation of  $\beta$ -catenin. Picture adabted from Ozhan, G et al. (2015).

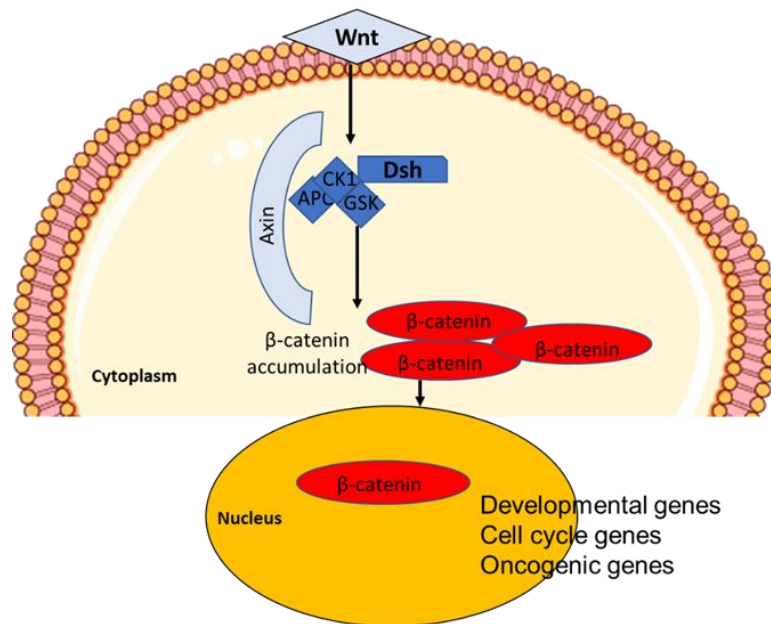


Figure 12. Overview of Wnt/ $\beta$ -catenin signaling in cancer. Accumulation of nucleic  $\beta$ -catenin with promotion of oncogenes contribute to CRC development and tumor progression. In Wnt-on state, translocation of  $\beta$ -catenin occurs to the nucleus as a result of destruction complex disturbance by LRP5/6, FRAT1, which enhances  $\beta$ -catenin phosphorylation. Picture adapted from Ozhan, G et al. (2015).

#### 1.2.2.2 PI3K/AKT/mTOR pathway

Phosphatidylinositol 3-kinase (PI3K)/protein kinase B (AKT)/ mammalian target of rapamycin (mTOR) pathway is an intracellular survival pathway that is essential for normal cellular development and cell cycle regulation (129). However, mutations in this pathway induce multiple processes related to human cancer (130). For example, in CRC, PI3K/AKT/mTOR pathway was involved in drug resistance, angiogenesis, EMT, and cancer progression. In addition, PI3K is a group of intracellular lipid kinases involved in regulating cellular proliferation. Thus, mutations in these proteins contribute to over-proliferation of cells by Phosphatase and Tensin Homolog (PTEN), which is controlled PI3K/AKT signaling cascade negatively (131). Along with overexpression of dephosphorylates PIP3 to PIP2 that present in more than 60% of

CRC patients (132). AKT/AKT1 is responsible for apoptotic and cellular survival pathways. In cancer, it induces the proliferation of cancer cells by blocking apoptosis. Moreover, overexpression of AKT induces resistance to mitogen-activated protein kinase (MEK) inhibitor treatment in RAS and BRAF-mutated CRC (133). Further, mTOR is an essential protein in multiple biological processes like immunity, autophagy, and cell survival. In CRC, mTOR signaling is upregulated, promoting tumorigenesis and its progression by different pathways. These pathways include angiogenesis, cancer cell migration, and inhibition of autophagy (134). Accordingly, PI3K/AKT/mTOR is a promising pathway for CRC therapy. Several studies showed that natural compounds are treating CRC through effectively downregulating this pathway. Recently, flavonoids were shown to potent affect cancer by affecting PI3K/AKT/mTOR (135).

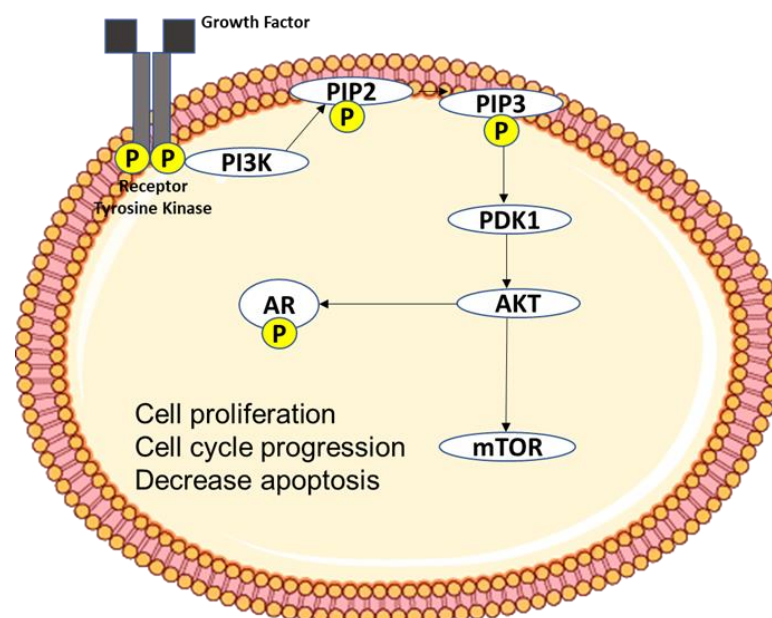


Figure 13. Overview of PI3K/AKT/mTOR signaling in cancer. Vital downstream effectors like mTOR are regulated by AKT by phosphorylation cascade reaction. These reactions occur by lipid and protein phosphatases modulation. Hyperactivation of AKT leads to uncontrrollable growth of cells. Picture adapted from Miricescu, D et al. (2021).

### 1.2.2.3 EMT pathway

Epithelial cells are responsible for maintaining cellular polarity and connections by tight junctions. Conversely, mesenchymal cells are separated due to the presence of ECM and the absence of apical-basolateral contradiction. EMT is a molecular pathway in which epithelial cells are polarized and interact with the basal surface of the basement membrane (136). Then, cells acquire mesenchymal cell phenotype via several biochemical alternations. Subsequently, cells become invasive with migratory capacity, increasing apoptosis resistance and producing extracellular matrix (ECM) components (137). EMT pathway is classified into three classifications. The first type is essential in embryogenesis, and the second type is necessary for adults in tissue repair and regeneration. Additionally, it is crucial in valves and septa formation during heart development through endothelial-mesenchymal transition (EndMT). The last type is responsible for cancer development (138). Several studies showed the implication of the EMT pathway in cancer development in primary tumors, which leads to its progression and metastasis (139).

During EMT, cells lose their adherent junctions due to the loss of critical epithelial-specific markers like E-cadherin and gain of mesenchymal markers like vimentin (140). These events gain several cancer properties, such as invasive and apoptosis resistance (141). In CRC, the loss of E-cadherin and gain of vimentin expression indicate the worse prognosis in CRC patients. In addition to lymph nodes metastasis and invasive tumorigenesis (142). Accordingly, the EMT pathway is the focus of research targeting cancer prevention. Flavonoids, due to their anticancer efficacy considered as potential agents against CRC by targeting the EMT pathway. Studies showed that a combination of natural flavonoids and 5-FU generates potential effects against cell proliferation in CRC by targeting EGFR (143).

### 1.3 *Drosophila melanogaster* as a model for CRC studies

Current *in vivo* models such as mice and rats have many constraints, including difficulty in handling, complications in obtaining ethical compliance, and cost-pertinent matters. As such, the search for alternative model systems to overcome the limitations of using these traditional models is ongoing. Among different non-conventional model organisms, the use of the *Drosophila melanogaster* fruit fly as a model of choice is emerging. *Drosophila* currently serves as one of the most employed organisms for investigating many common cellular and developmental processes in high eukaryotes, including humans, and for studying a wide range of human disorders and diseases. The choice of *Drosophila* relates to several aspects including its small size, fast generation time (around seven to twelve days), as well as it being harmless, fecund, and non-demanding in terms of laboratory needs and maintenance as compared to other model organisms (144, 145).

Genetically, *Drosophila* is characterized by a simple genetic makeup ;yet, with an ortholog congruency with humans, where 75% disease-causing genes homology with humans are also found in flies, supporting the use of *D. melanogaster's* as a foundation for further translational studies in humans (146). Moreover, the GAL4/UAS system in *D. melanogaster* allows targeted gene expression in a tissue-specific manner. This powerful technique in *Drosophila* allows *in-vivo* gene function studies with an ability of temporal and spatial control of the studied gene of interest (147).

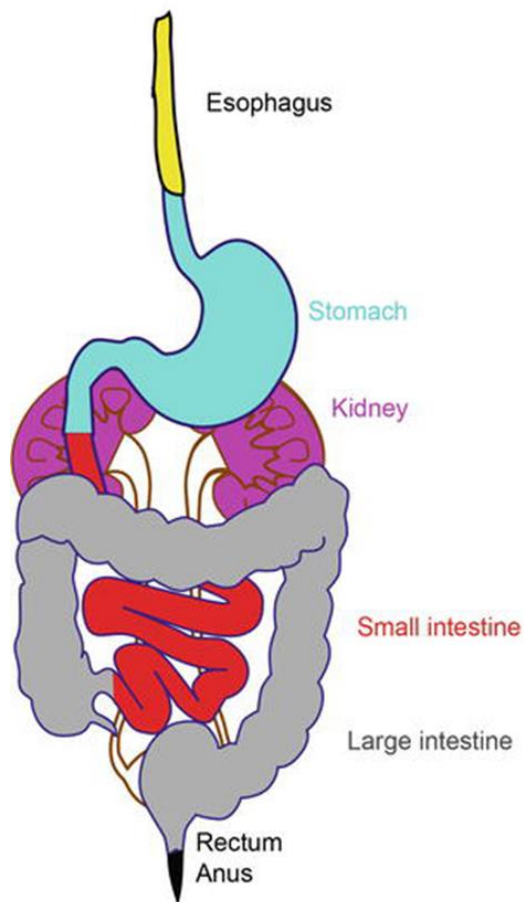
Furthermore, this evolutionary conservation between a fruity fly and a mammal is not only evident at the molecular level, as analogous organs with functional similarities also exists between both living being. The gut system, for example, of fruit flies, and although simpler, is very similar to that of humans. In brief, the gut of a *D.*

*melanogaster* encloses a foregut responsible for transferring consumed food to the crop for storage and digestion. This highly relates to the process in humans where food passes from the esophagus to the stomach. Then, nutrients get absorbed in the anterior midgut in flies, similar to the process occurring in the small intestine in humans. Likewise, and as is the defined role of the large intestine in absorbing water and electrolytes in humans, the fly hindgut is engaged in the same operation, where food passes through the middle midgut towards the posterior midgut, arriving to the hindgut and rectum for water and electrolytes exchange. The final region of the fly gut encompasses the anus, where wastes excretion happens. This is similar to the process occurring in the rectum and anus in the human gut. In addition, flies possess Malpighian tubules connected to the midgut-hindgut junction, and are responsible for water and solutes absorption, a function similar to the renal structure in humans (Figure. 14) (148).

The midgut epithelium of *D. Melanogaster* has one layer, and its renewal is dependent on intestinal stem cells (ISCs) proliferation, a process regulated by many signaling pathways. Interestingly, deletion in *D. Melanogaster* adenomatous polyposis coli (*APC*) genes promotes ISCs over-proliferation characterized by multilayered epithelium formation. This presents the *D. melanogaster* midgut as a consummate model for studying adenoma development (149). Advantageously, *D. melanogaster* lines with mutations in genes reported to be implicated in human CRC such as Kirsten Rat Sarcoma (*KRAS*), adenomatous polyposis coli (*APC*), basket (*BSK*), and E2F Transcription Factor 1 (*E2IF*) are readily and commercially available.



## Human intestine



## Drosophila intestine

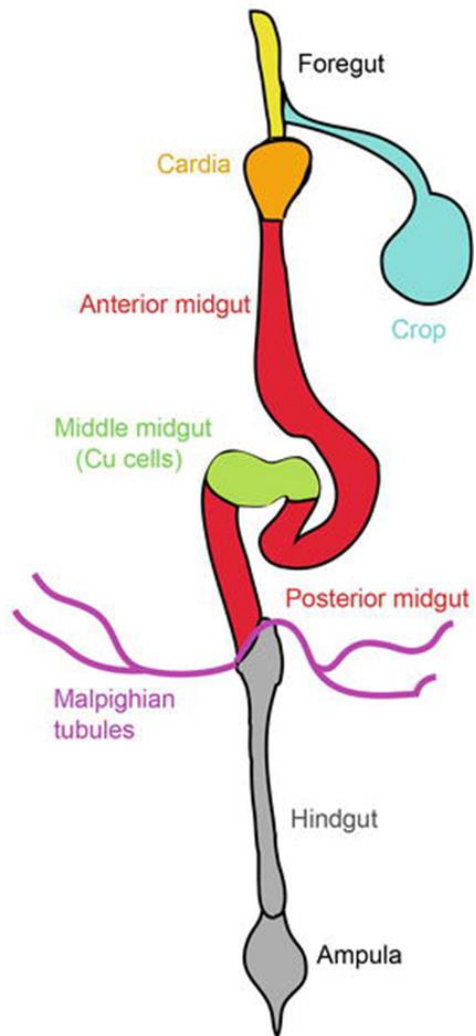


Figure 14. Representation of human and *Drosophila* gut. Colors indicate organs with similar functions. The organs and tissues in the gut of *Drosophila* flies are functionally similar to the human GI system. The foregut in *Drosophila* is similar to the esophagus in human, midgut and hindgut are similar to small and large intestines and crop is similar to the stomach in human. Picture is adapted from Sadaqat, Z et al. (2021).

#### 1.4 Thesis Objectives

CRC is considered among the most lethal malignancies globally after lung and breast cancer, with a notable increase in its incidence and mortality rates. Current chemotherapies are faced with several adverse side effects, mainly lack of selectivity. Thus, novel natural compounds are now presented as potential alternatives, not only for CRC treatment, but also for its prevention. Likewise, synthetically designed flavonoids are also suggested as plausible alternatives with potency against CRC. *EA*, for instance, is a medicinal plant well known for flavonoids abundance in its flowers and its therapeutic potential. Aqueous extract from *EA* flowers showed a significant effect against different types of cancers. Likewise, chalcones, a class of flavonoids, seems to possess promising anti-cancerous effect. However, the effect of *EA* and novel chalcone analogs (DK13 and DK14) against CRC has not been investigated yet. Hence, we hypothesized in this study an anti- CRC effect of these resources of flavonoids, an anticipation that will open up for the introduction of novel anti-CRC agents with high efficacy, selectivity, and safety, if borne out correctly.

**Objective 1:** To characterize the effect of *EA* extract and synthesized chalcones analogs (DK13 and DK14) *in-vitro* using the two CRC cell lines HCT-116 and LoVo and the NCE-1 E6/E7 normal immortalized colon cells.

**Objective 2:** To explore the underlying anti-cancerous mechanisms of action of *EA* and chalcones analogs (DK13 and DK14).

**Objective 3:** To determine the preventive and anti-cancerous effect of *EA* and chalcones analogs (DK13 and KD14) *in-vivo* using wild-type and cancer mutant fly lines of *D. melanogaster*.

## CHAPTER 2: MATERIALS AND METHODS

### 2.1 Extract preparation

Flowers of *Elaeagnus angustifolia* originated Montreal, Quebec, Canada, were collected from in June and extracted using water as previously described (150). In brief, fresh flowers were dried at room temperature and stored in dark. Then, 3000 mg of *EA* dry flowers were extracted in 100 mL of autoclaved distilled water for 15 minutes at 50°C, with continuous stirring by means of a magnet stirrer. To avoid any loss of water volume through evaporation, the beaker was sealed with aluminum foil. Following boiling, the extract solution was left to cool down for 30 minutes, filtered using a sterile filter with 0.45 µm pore size, and stored at 4°C. For *in-vitro* and *in-vivo* studies, dilutions of *EA* aqueous extract were prepared in cell culture media and Luria-Bertani media (LB) media, respectively. The extract was freshly prepared for each set of experiments and stored for a maximum of one-week.

### 2.2 Synthesis of nitrogen-based chalcone analogs (DK13 and DK14)

Our group recently synthesized and screened two nitrogen-based chalcone analogs (DK13 and DK14) (Figures 15 and 16), and patented DK14, as a lead chemotherapeutic compound for triple-negative breast cancer (TNBC). The two compounds were synthesized by Claisen-Schmidt condensation reaction as described by Elkhalfa et al. (2020) (151). Briefly, 4-[Bis-(2-chloroethyl) amino] benzaldehyde (1mmol, 1 eq.) was added to a solution of 4-(methylsulfonyl) acetophenone to synthesize DK13, 3-methoxy acetophenone was added to ethanol to synthesize DK14. The mixture was stirred until completely dissolved, cooled on ice, and then 3mmol of aqueous sodium hydroxide was added in a drop like mean. Reaction mixtures were stirred at room temperature until completion (24-48 hours). Reactions' progress was monitored by thin-layer chromatography (TLC) using pre-coated silica gel aluminum plates purchased from

Merck (USA). Upon reaction completion, the obtained precipitate was filtered, washed with cold ethanol and water, and dried under vacuum. Crude products were purified by flash chromatography using silica column as stationary phase and a mixture of ethyl acetate and hexane as mobile phase. All solvents and chemicals used for synthesis and purification were purchased from Sigma-Aldrich (USA).

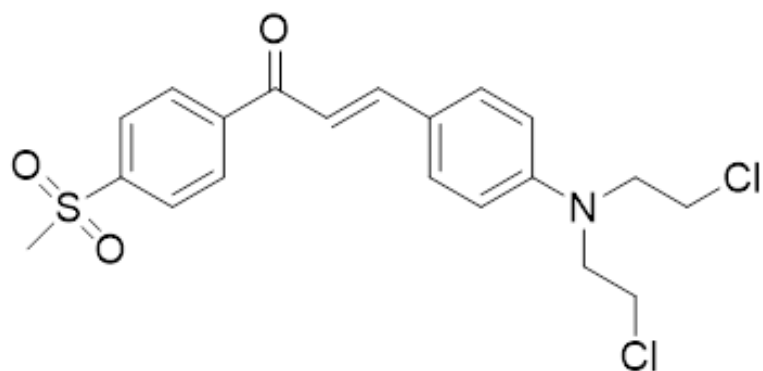


Figure 15. Chemical structure of DK13.

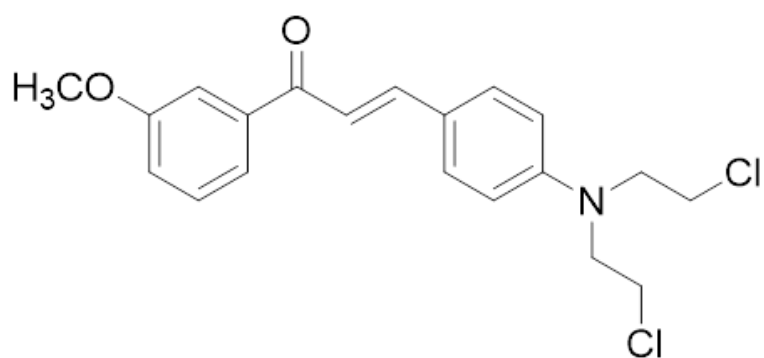


Figure 16. Chemical structure of DK14.

### 2.3 *Drosophila* stocks husbandry and maintenance

All fly lines were purchased from the Bloomington *Drosophila* Stock Center (<https://bdsc.indiana.edu/>) and reared in the *Drosophila* facility at Zone 4/H10. Flies' stocks were maintained on regular fly food containing corn syrup, cornmeal, soy flour, yeast agar and preserved with Napagin in ethanol in a controlled environment with 70% humidity at 25°C, 12-hour day/night cycle. For oral treatment with *EA*, flies were randomly distributed into three vials containing a cellulose acetate plug infiltrated with either 2.5 mL of LB alone (control) or with different dilutions of *EA* aqueous extract ranging from 25 to 500 µL/mL diluted in LB media. For oral treatment with DK13 and DK14, flies were randomly distributed into three vials containing a cellulose acetate plug infiltrated with either DMSO alone (control) or 10 µM of chalcone compounds (DK13 or DK14), or 5-FU, prepared in DMSO. For practical purposes and similar to many internationally adopted protocols, all experiments were conducted on female flies. All experimental procedures using *D. melanogaster* flies were performed according to the international standard guidelines and were approved by Qatar University's Institutional Biosafety Committee (QU-IBC-2020/070). Institutional Animal Care and Use Committee (IACUC) approval was not required as *D. melanogaster* is an invertebrate model organism.

### 2.4 Cell culture

Two CRC cell lines, HCT-116 and LoVo, were obtained from American Type Culture Collection (ATCC) (Rockville, MD, USA). To test the selectivity of *EA* aqueous extract, human normal colon cells immortalized by E6/E7 oncoproteins of HPV type 16 (NCE-1 E6/E7) were generated by the lab of Dr. Al Moustafa (152). All cell lines were cultured in a complete growth medium Dulbecco's modified Eagle medium (DMEM) supplemented with 10% fetal bovine serum (PAN-Biotech,

Aidenbach, Bavaria, Germany) and 1% penicillin/streptomycin (1X) antibiotics (Thermo Fisher Scientific, USA). Cells' maintenance was at 37°C, and 5% CO<sub>2</sub> in the air, in a humidified atmosphere in an incubator. All cells were routinely maintained by splitting them in T-75 and T-25 filtered tissue culture flasks per the experimental needs.

### 2.5 Cell viability assay (Alamarblue™ assay)

HCT-116, LoVo, and NCE-1 E6/E7 cells were seeded at density of 1x10<sup>4</sup> cells/well in 100 µL of DMEM media at 96-Well microplates and incubated for 24 hours. Then, old media was discarded, and fresh media was added as a negative control for cells treated with *EA* extract or DK13 and DK14. The *EA* extract was diluted in media with five different concentrations from 25 to 200 µL/mL for 48 hours. For chalcone compounds, CRC cells were treated with different concentrations of DK13 and DK14 from 2.5 to 60 µM or with vehicle (DMSO) of final concentration less than 0.1% for 48 hours. After treatment, 10 µL of alamarBlue™ (Invitrogen™, ThermoFisher Scientific, USA). AlamarBlue™ was added to each well and incubated for 3 hours. After incubation, fluorescence using a fluorescent plate reader (Infinite M200, Tecan, Austria) was determined at 560 nm and 590 nm. Viable cells were quantified according to the fluorescence of treated cells and relative to the untreated cells by using the following formula:

$$\text{Cell Viability (\%)} = \frac{\text{Fluorescence of Treated Cells}}{\text{Fluorescence of Untreated Cells}} \times 100$$

Next, with a scatter plot, we determined the half-maximal inhibitory concentration (IC<sub>50</sub>), the concentration that reduced 50% of cell viability compared to the control. IC<sub>50</sub> was calculated further to investigate *EA* extract, DK13, and DK14.

## 2.6 Cell morphology analysis

HCT-116, LoVo, and NCE-1 E6/E7 cells were seeded in a 6-well plate at a density of  $100 \times 10^3$  cells/well for 24 hours. The next day, old media was discarded from all wells and replaced with fresh media, and wells were treated with *EA* extract (100 and 200  $\mu\text{L}/\text{mL}$ ) and DK13, DK14, and 5-FU (10 $\mu\text{M}$ ) for 48 hours. Morphological changes of cells were examined with Leica SP8 UV/Visible inverted microscope (Leica Microsystems, Wetzlar, Germany) with 10X objective lens. Representative pictures were taken with Leica DFC550 digital camera (Leica Microsystems, Wetzlar, Germany) of 12.5 Megapixel resolution.

## 2.7 Flow cytometric analysis of cell cycle

HCT-116 and LoVo cells were seeded in 100 mm Petri dishes and incubated for 24 hours. The next day, all cells starved for 24 hours with serum-free media for synchronization at G0 phase. After starvation, cells were treated with *EA* extract (100 and 200  $\mu\text{L}/\text{mL}$ ) and DK13, DK14, and 5-FU (10 $\mu\text{M}$ ) for 48 hours. Then, all cells floated, and adherent were harvested by centrifugation, and the obtained pellet was washed twice with cold 1X Phosphate-buffered saline (PBS). After washing, cells were fixed with 70% ice-cold ethanol and kept at  $-20^\circ\text{C}$  overnight. For flow cytometric analysis, the DNA stained with 50  $\mu\text{g}/\text{mL}$  FXCycle PI/RNase staining solution® (Thermo Fisher Scientific, USA) was supplemented with 200 $\mu\text{g}/\text{mL}$  RNase, all cells incubated in the dark at room temperature in a shaking water bath for 50 minutes. Analysis of cell cycle was done using BD Accuri™ C6 Plus flow cytometry and data analyzed by FlowJo™ V10 software to quantify cells in G0/G1, S, G2/M phases according to the DNA content represented by histograms of PI signal intensity.

## 2.8 Cell invasion assay

To explore the effect of *EA* aqueous extract and chalcone compounds on the invasive characteristic of HCT-116 and LoVo cell lines, Matrigel-coated invasion chamber plates (CORNING, USA) were used. In the upper chambers of the plate, HCT-116 and LoVo cells with a density of  $50 \times 10^3$  cells/well were suspended in serum-free media containing *EA* extract (100 and 200  $\mu\text{L}/\text{mL}$ ) or DK13, DK14, and 5-FU (10 $\mu\text{M}$ ) to a final volume of 500  $\mu\text{L}/\text{well}$ . The lower chambers were loaded with a complete growth medium (DMEM with 10% FBS) as a chemoattractant to a final volume of 600  $\mu\text{L}/\text{well}$ . CRC cells were allowed to invade for 48 hours. After, non-invaded cells on the upper chamber were removed using sterilized cotton swabs wetted with 1X PBS. For the fixation of invaded cells, 3.7% formaldehyde was used for 10 minutes, then soaked in absolute methanol for permeabilization for 5 minutes. For staining, invaded cells were stained first with 0.5% crystal violet prepared in 2% ethanol for 30 minutes. Then cells were visualized under the microscope and took pictures with Leica MC170 HD camera. Then, for confirmation, invaded cells were stained with 4',6-Diamidino-2-Phenylindole (DAPI) for 5 minutes. Visualization and pictures were taken using EVOS fluorescence microscope. Finally, invaded cells were quantified by randomly counting at least four different fields/well.

## 2.9 Soft agar colony formation assay

To determine the ability of *EA* and chalcone compounds in preventing CRC cells (HCT-116 and LoVo) colony formation, we used the well-established soft agar colony formation assay. Noble agar (Sigma-Aldrich, USA) with 2% concentration was prepared in autoclaved water as a stock solution. DMEM medium with pre-solidified 0.4% agar plated in each well of 6-well plate, then cells were suspended in complete growth medium at a density of  $100 \times 10^3$ /well containing *EA* extract (100 and 200



μL/mL) or DK13, DK14 and 5-FU (10 μM) to a final volume of 1 mL/well and pre-solidified 0.3% agar plated on the top of the first layer. Colonies formation of both cell lines was examined every two days for three weeks. Representative pictures were taken with Leica MC170 HD camera for three weeks. For quantification, formed colonies were counted randomly in each group from four different fields/well.

## 2.10 RNA extraction and quantitative real-time PCR (qRT-PCR)

To confirm *ras1* mutation in cancer mutant fly line (*Ras85D*) used as compared to the *Yw* control group, total RNA was extracted from the whole body of one week old adult female flies by using NucleoSpin TriPrep, Mini kit for RNA purification (MACHEREY-NAGEL, Germany) according to the manufacturer's protocol. The concentration of the extracted RNA was measured using a nanodrop reader (ThermoFisher Scientific, USA) and RNA purity was evaluated by the 260/280nm ratio. An RNA sample with a ratio of ~2 was considered pure. To synthesize cDNA, RNA was then reverse transcribed using SuperScript™ III First-Strand Synthesis SuperMix (Thermo Fisher, USA) kit, according to the manufacturer's protocol (Table. 4) and the ProFlex™ 2 x 96-well PCR System (Applied Biosystems™, Thermo Fisher, USA) (30 minutes at 42°C, 85°C for 10 minutes). For qRT-PCR and using the iTaq™ Universal SYBR® Green Supermix kit (BIO-RAD, USA), a total volume of 10 μL per samples was prepared in 96 well microplate (Applied Biosystems™) (Table. 5) and RT-PCR was subsequently performed in QuantStudio® 5 Real-Time PCR System. The list of primer sequences used are shown in Table 6.

Table 4. Reverse transcription and cDNA synthesis reaction constituents

Reagent	Concentration	Volume
2X Reaction Mix	2.5 $\mu$ M	10 $\mu$ L
RT Enzyme Mix	0.4mM	2 $\mu$ L
<i>E. coli</i> RNase H	2U	1 $\mu$ L
Total RNA	Up to 1 $\mu$ g	X $\mu$ L
Nuclease Free Water	-	Up to a total reaction volume of 20 $\mu$ L

Table 5. RT-qPCR reaction constituents

Reagent	Concentration	Volume
SYBR® Green Supermix	2X	5 $\mu$ L
Forward primer	10 $\mu$ M	1 $\mu$ L
Reverse primer	10 $\mu$ M	1 $\mu$ L
cDNA template	1:10 diluted	1 $\mu$ L
Nuclease Free Water	-	Up to a total reaction volume of 10 $\mu$ L

Table 6. List of used primers in RT-qPCR

Target Gene	Forward (5' to 3')	Reverse (3' to 5')
<i>Ras1</i>	GCAACAAGTGCGACCTACAG TCG	CGGCTGACTTTATCTTTGCGTAT CTC
<i>Rp49</i>	TACAGGCCCAAGATCGTGAA G	GACGCACTCTGTTGTCGATAACC

## 2.11 Western blot analysis

CRC cells were seeded in 100 mm Petri dishes and incubated for 24 hours to attach. Next day, both cell lines were treated with *EA* extract (100 and 200  $\mu\text{L}/\text{mL}$ ) or DK13, DK14, and 5-FU (10  $\mu\text{M}$ ). First, floating, and adherent cells were washed with 5 mL ice-cold 1X PBS, all floating cells were harvested in a 15 mL tube. Then adherent cells were lysed using cold sodium dodecyl sulfate (SDS) lysis buffer (0.5M Tris pH 6.8, 0.2% SDS) with Halt™ Protease and Phosphatase Inhibitor Cocktail (Thermo Fisher Scientific, USA).

For proteins extraction from *Drosophila* whole body, 10 female flies per genotype were homogenized in cold sodium dodecyl sulfate (SDS) lysis buffer (0.5M Tris pH 6.8, 0.2% SDS) supplemented with Halt™ Protease and Phosphatase Inhibitor Cocktail (Thermo Fisher Scientific, USA).

Protein samples were then reduced and denatured in SDS-PAGE sample buffer (Thermo Fisher Scientific, USA) for 20 minutes 95°C. Extracted proteins were finally quantified by the Pierce BCA Protein Assay Kit (Thermo Scientific, USA) according to the manufacturer's protocol.

30  $\mu\text{g}$  of each sample was loaded on 10% polyacrylamide gels and SDS–polyacrylamide gel electrophoresis (SDS-PAGE)/ Mini-PROTEAN Electrophoresis System (BioRad, USA) was used to separate proteins based on their molecular weight. The resolution protein size was estimated relevant to the PageRuler™ Prestained Protein standard Ladder (10-250kDa) (Thermo Scientific, USA).

By means of wet transfer, proteins were transferred into a 0.45  $\mu\text{m}$  Polyvinylidene fluoride (PVDF) membrane. Membranes enclosing transferred proteins were then blocked with Bovine serum albumin (BSA) blocking buffer, and incubated with the primary antibodies (Table 7 and 8), overnight at 4°C. The next day, membranes were incubated with relevant secondary antibody for 2 hours. ECL Western blotting substrate

(Pierce Biotechnology, Rockford, IL, USA) was used to detect protein bands. Blots were imaged using Bio-Rad Chemidoc MP Imaging System and quantified by ImageJ software. Bands intensity reflecting relative protein expression was analyzed relative to GAPDH or alpha Tubulin.

Table 7. Antibodies used in western blot analysis of proteins extracted from CRC cell lines.

No.	Antibody	Source	MW (KDa)	Manufacturer	Dilution
1.	Anti-Mouse	Mouse	N/A	Cell Signaling CST: Ab #7076	1:1000
2.	Anti-Rabbit	Rabbit	N/A	Cell Signaling CST: Ab #7074	1:1000
3.	E-cadherin	Rabbit	135	Cell Signaling CST: mAb #3195	1:1000
4.	Vimentin	Mouse	57	Cell Signaling CST: mAb #46173	1:1000
5.	$\beta$ -Catenin	Rabbit	92	Cell Signaling CST: Ab #9562	1:500
6.	Phospho- $\beta$ -Catenin	Rabbit	92	Cell Signaling CST: Ab #4176	1:500
7.	AKT	Rabbit	60	Cell Signaling CST: Ab #9272	1:1000
8.	Phospho-AKT	Rabbit	60	Cell Signaling CST: mAb #4060	1:1000
9.	EGFR	Rabbit	134	Abcam: abID# ab52894	1:1000
10.	Phospho-EGFR	Rabbit	170	Santa Cruz, SC-57545	1:500
11.	m-TOR	Rabbit	289	Cell Signaling CST: mAb #2983	1:1000
12.	Phospho-m-TOR	Rabbit	289	Abcam: abID# ab 109268	1:1000

13.	GAPDH	Rabbit	37	Cell Signaling CST: Ab #7074	1:1000
-----	-------	--------	----	---------------------------------	--------

MW: Molecular weight, NA: Not Applicable

Table 8. List of the used antibodies in Western blotting analysis of *D. melanogaster* fly lines.

No.	Antibody	Source	MW (KDa)	Manufacturer	Dilution
1.	Anti-Mouse	Mouse	N/A	Cell Signaling CST: Ab #7076	1:1000
2.	Anti-Rabbit	Rabbit	N/A	Cell Signaling CST: Ab #7074	1:1000
3.	ERK1/2	Mouse	44	Abcam: abID# ab50011	1:500
4.	Phospho- <i>Drosophila</i> AKT	Rabbit	65	Cell Signaling CST: Ab #4054	1:100
5.	AKT	Rabbit	65	Cell Signaling CST: Ab #9272	1:100
6.	Alpha- Tubulin	Rabbit	50	Abcam: abID# ab52866	1:500

MW: Molecular weight, NA: Not Applicable

## 2.12 Survival assay

To explore the effect of *EA* extract and synthesized chalcones (DK13 and DK14) on the survival rates of the fly line with *ras* mutations *Ras85D* as compared to wild-type *Yw* flies, different dilutions of *EA* aqueous extract or chalcone compounds were used as described above. Dead flies were counted twice a day (12-hour interval between each count) until flies in all groups succumbed to death. Mean survival was calculated, and the results were compared to untreated control flies fed with LB only for *EA*-treated groups or with DMSO only for chalcone compounds-treated ones.

## 2.13 Statistical analysis

The IBM® SPSS® software version 28.0.0.0 (190), was used to analyze all data. All experiments were conducted at least three independent times, and the obtained data represents mean  $\pm$  standard error of the mean (SEM) of the three independent biological repeats.  $IC_{50}$  values were calculated using non-linear curve and exponential equation using Microsoft Excel. One-way analysis of variance (ANOVA) followed by Tukey's multiple measurement tests was used to compare three or more levels of the investigated factor. For survival analysis, at least 30 flies per biological replicate were used in treated and untreated groups. The Kaplan-Meier survival test was used to calculate percent survival, and statistical significance between compared groups was calculated using the log-rank test. Cox proportional hazards regression analysis was used to determine the hazard ratio (HR). Differences with *p-values*  $<0.05$  ( $\alpha$ -level =0.05) were considered statistically significant. For all the statistical analysis, \* indicates  $p<0.05$ , \*\* indicates  $p<0.01$ , and \*\*\* indicates  $p<0.001$ .

## CHAPTER 3: RESULTS

### 3.1 Effect of *EA* aqueous extract on CRC cell lines

#### 3.1.1 Cell viability assay (Alamarblue™ assay)

Cell viability assay is used to study the effect of our plant extract and chalcone compounds on the viability of normal and cancer cells. AlamarBlue™ Assay (resazurin) is a colorimetric assay that is used as an indicator to define the percentage of viable cells under certain conditions. The active ingredient of alamar blue is resazurin, which is not toxic and characterized by high permeability through the cell membranes, soluble in water with stability in culture media. Therefore, it is the best candidate for our aim in this experiment (153).

The effect of *EA* on HCT-116 and LoVo, was assessed after exposing both cell lines to different dilutions of *EA* extract for 48 hours. After analyzing the viability of CRC cells (HCT-116 and LoVo) relative to the untreated controls, we found that *EA* significantly inhibits the proliferation of HCT-116 and LoVo cells. The percentage of viable cells decreases with increasing the *EA* concentrations, as shown in Figures 17 A and B. *EA* extract reduces cells viability up to  $59.76 \pm 4.04$  and  $86.45 \pm 1.89$  in HCT-116 cell line and up to  $49.76 \pm 1.28$  and  $55.39 \pm 1.59$  in LoVo cell line at 150 and 200  $\mu\text{L}/\text{mL}$ , respectively. Then, the  $\text{IC}_{50}$  values of *EA* extract in HCT-116 and LoVo cell lines are calculated for further investigation. After treating the cells for 48 hours with five different dilutions of *EA* (0, 25, 50, 100, 150, and 200  $\mu\text{L}/\text{mL}$ ), the percentage of viable cells is obtained by alamar blue. A scatter plot is created as a function of concentrations. Then  $\text{IC}_{50}$  of *EA* extract in HCT-116 and LoVo cell lines is calculated as shown in Table. 9. Accordingly, two concentrations (100 and 200  $\mu\text{L}/\text{mL}$ ) of *EA* extract are used in all experiments. To assess the selectivity of cytotoxic effect of *EA* aqueous extract on cancerous cell lines, the effect of 100 and 200  $\mu\text{L}/\text{mL}$  concentrations were explored on the viability of NCE-1 E6/E7 cell line. *EA* aqueous extract does not

affect the viability of NCE-1 E6/E7, as the cell proliferation is not affected by any dilution used (Figure. 18).

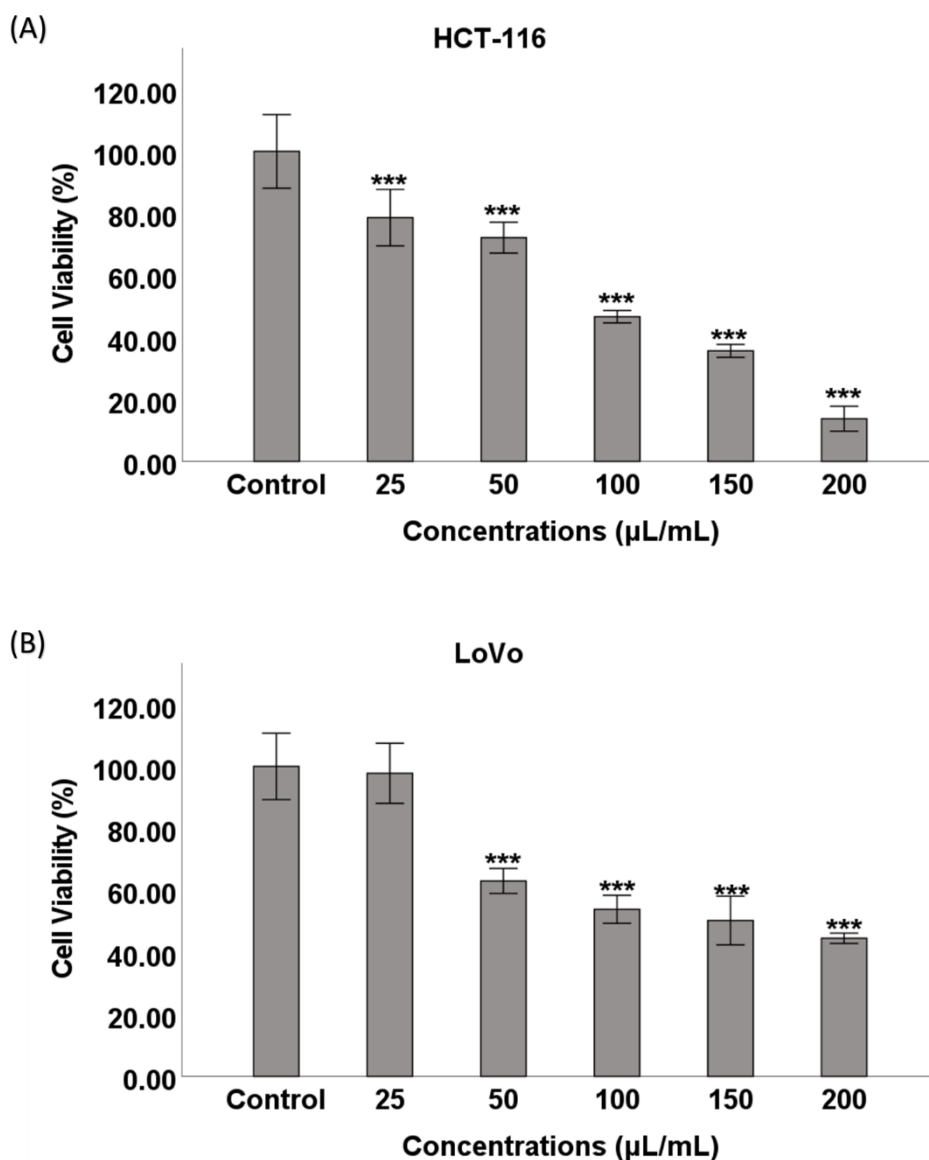


Figure 17. Outcome of different doses of *EA* aqueous extract on the viability of (A) HCT-116 and (B) LoVo. Both cell lines were treated with a range of five different concentrations of *EA* extract. Cell viability was quantified 48 hours post-treatment relative to the untreated control for each cell line (Mean  $\pm$  SEM; n=3). Statistical analysis was performed using one-way ANOVA, Tukey's post-hoc test was conducted to compare treatment groups. Asterisks indicate significant results compared to the untreated control at \*\*\*  $p < 0.001$ .



Table 9: IC<sub>50</sub> of *EA* aqueous extract in CRC cell lines after 48 hours of treatment.

CRC cell line	IC <sub>50</sub> of <i>EA</i>
HCT-116	91.04 $\mu\text{L}/\text{mL} \pm 4.2$
LoVo	155.67 $\mu\text{L}/\text{mL} \pm 3.6$

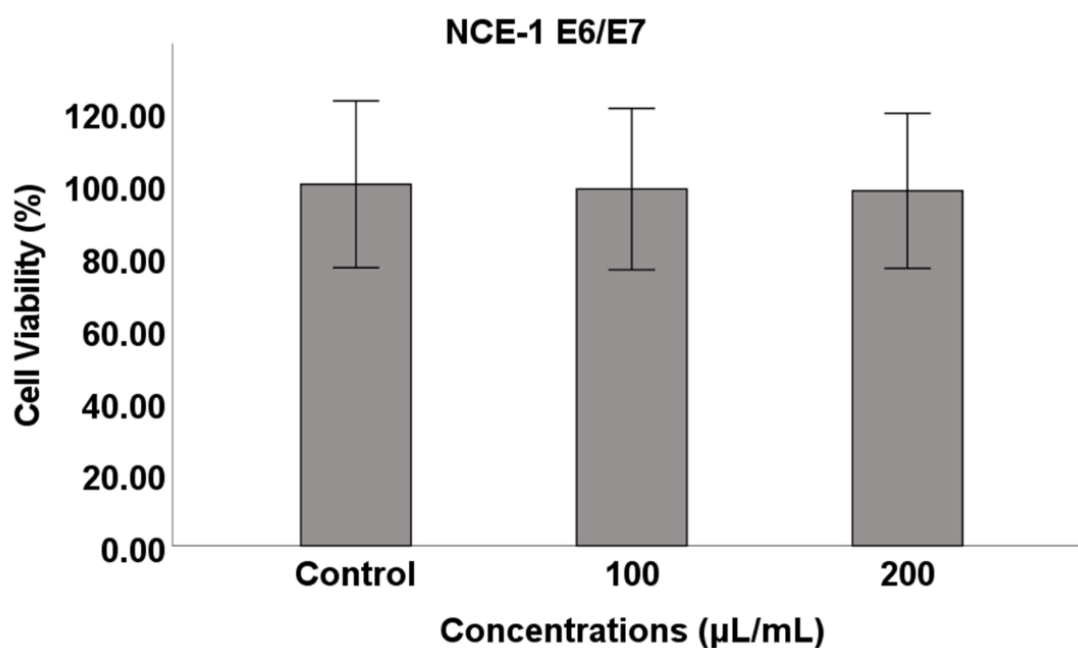


Figure 18. Outcome of *EA* aqueous extract on the viability of NCE-1 E6/E7 cell lines at 100 and 200  $\mu\text{L}/\text{mL}$ . Cell viability was quantified 48 hours post-treatment relative to the untreated control for each cell line (Mean  $\pm$  SEM; n=3). Statistical analysis was performed using one-way ANOVA, Tukey's post-hoc test was conducted to compare treatment groups.

### 3.1.2 Cell morphology analysis

Analysis of cell morphology is essential in drug discovery as it provides important indications of cell activities and their regulations induced by any phenotypic change caused by treatment (136). As shown in Figure 19, *EA* extract notably affects the morphology of both CRC cell lines (HCT-116 and LoVo). In addition, it increases the cell-cell adhesion among cells by alternating the shape to be more flattened epithelial cells, suggesting that *EA* extract inhibits the progression of Epithelial-mesenchymal transition (EMT) in both CRC cells. On the other hand, *EA* extract does not affect the cell morphology of NCE-1 E6/E7 cells as the morphology does not change under the effect of both concentrations used.

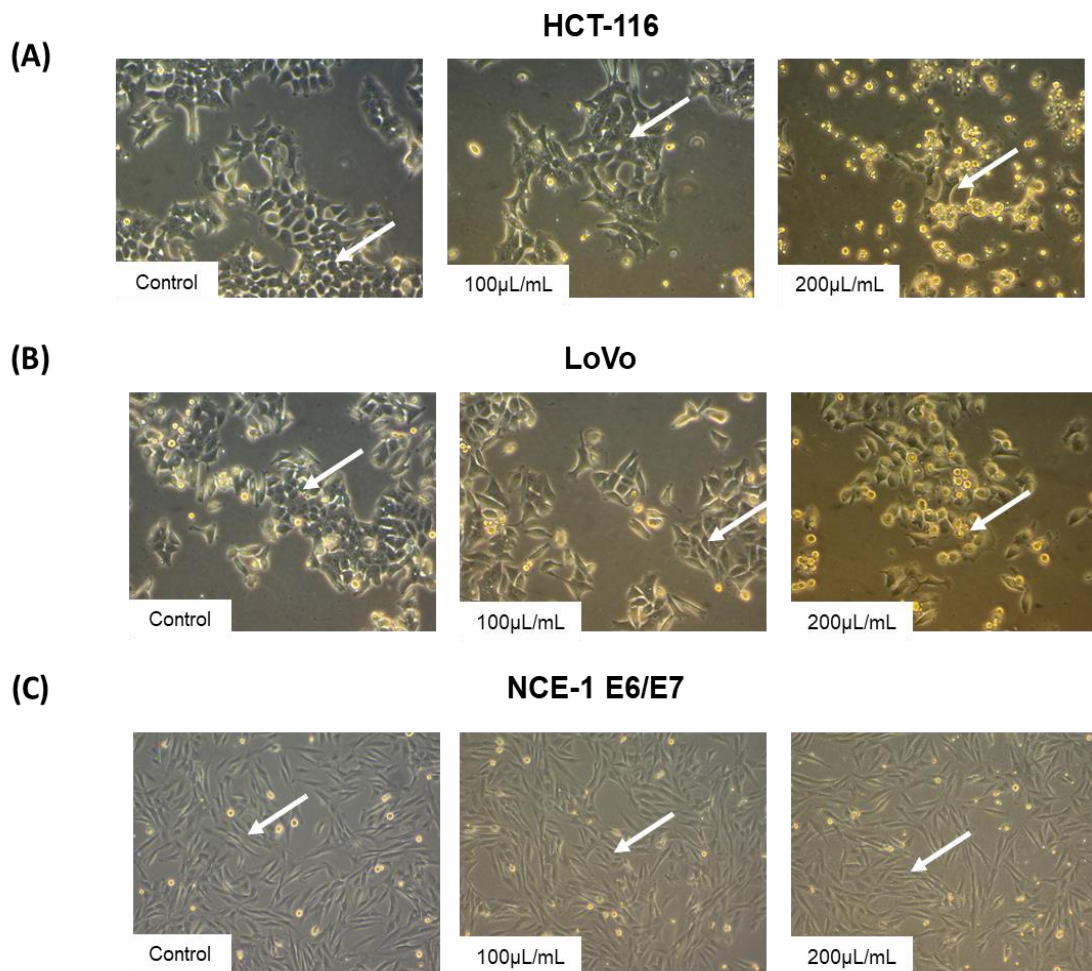


Figure 19. Outcome of *EA* aqueous extract on the morphology of (A) HCT-116, (B) LoVo and (C) NCE-1 E6/E cells after treatment at 100 and 200 $\mu$ L/mL for 48 hours. Images visualized at 10X magnification.

### 3.1.3 Flow cytometric analysis of cell cycle

The cell cycle in mammalian cells is defined as the series of events in a cell to produce duplication of DNA, with cytoplasm and organelles division by mitosis to produce two identical daughter cells. The cell cycle consists of four sequential phases, which are Sub-G<sub>0</sub>, G<sub>0</sub>/G<sub>1</sub>, S, and G<sub>2</sub>/M phase, and specific events are taking place in each phase (154). Cancer is considered a disease of the cell cycle, as the deregulation of the cell cycle is one of the hallmarks of cancer development. In addition, the loss of cell cycle checkpoints is the cause of genetic instability related to cancer (155).

Flow cytometric analysis of cell cycle is a direct analysis to highly measure the DNA content in each cell by quantifying this content after staining the DNA with different dyes such as propidium iodide (PI) (156).

Here, cell cycle analysis is performed to study the effect of our treatment on the cell cycle phases of CRC cell lines (HCT-116 and LoVo). Flow cytometric analysis is used for DNA quantification in each phase of cell cycle of CRC cells under the effect of *EA* extract (100 and 200  $\mu\text{L}/\text{mL}$ ). Peaks in Figures 20 and 21 represent the arrested cells in each phase. The first peak represents arrested cells in G<sub>0</sub>/G<sub>1</sub> phase, the second peak for cells arrested in the S phase, and the third peak for cells arrested in the G<sub>2</sub>/M phase. The results show that *EA* extract significantly disturbs the cell cycle. As shown in figure 20, at 200  $\mu\text{L}/\text{mL}$  concentration, HCT-116 cells are arrested at the G<sub>2</sub>/M phase; however, 100  $\mu\text{L}/\text{mL}$  is not effective. On the other hand, *EA* extract significantly arrests LoVo cells at the S phase at both concentrations (Figure 21).

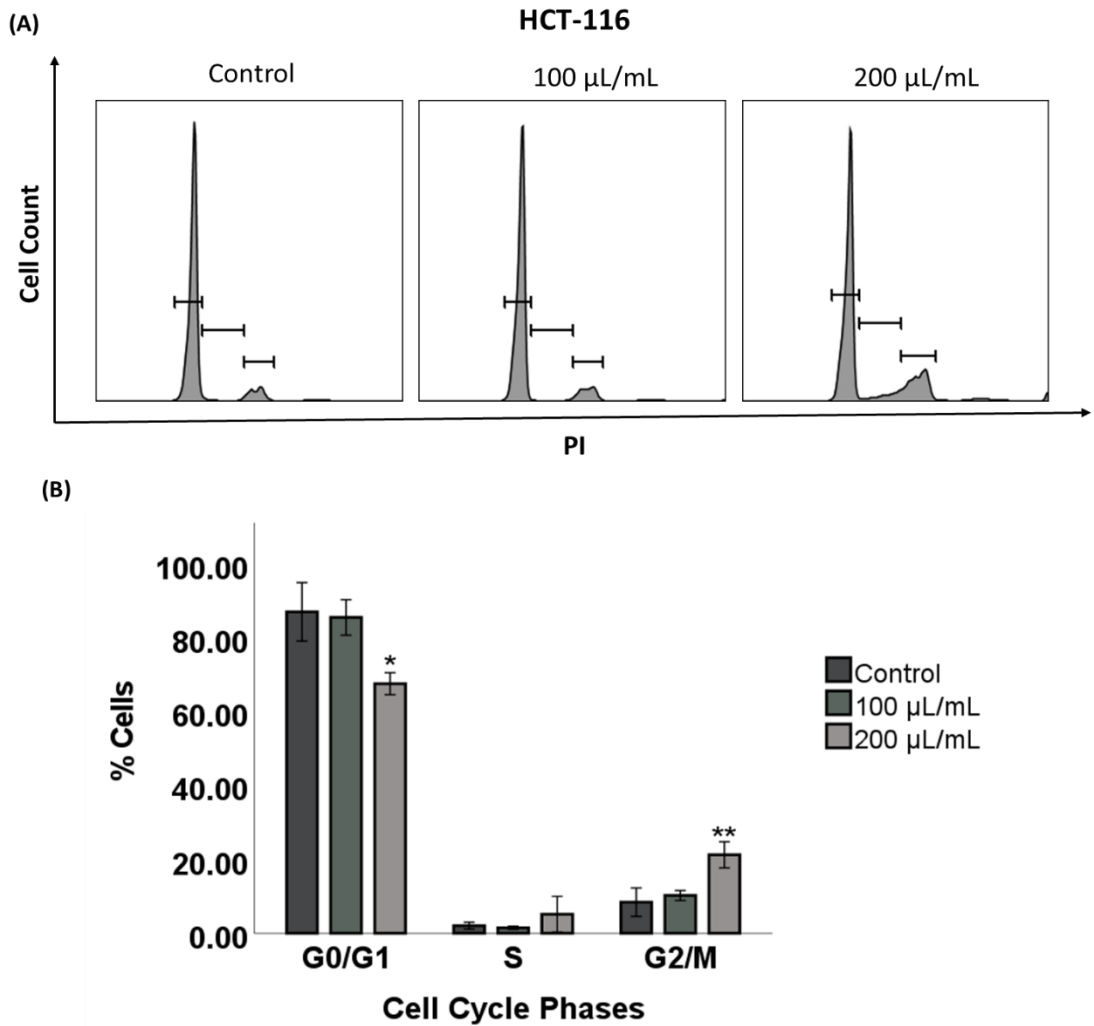


Figure 20. Cell cycle analysis of HCT-116 cells. (A) Peaks are representation of the percentage of cells in G0/G1, S and G2/M phase post-treatment with EA extract for 48 hours. (B) The three phases were quantified and results are presented as the Mean  $\pm$  SEM: (n=3). Statistical analysis was performed using one-way ANOVA, Tukey's post-hoc test was conducted to compare treatment groups and results were stated as Asterisks indicate significant results compared to the untreated control at \* $p < 0.05$  and \*\* $p < 0.01$ .

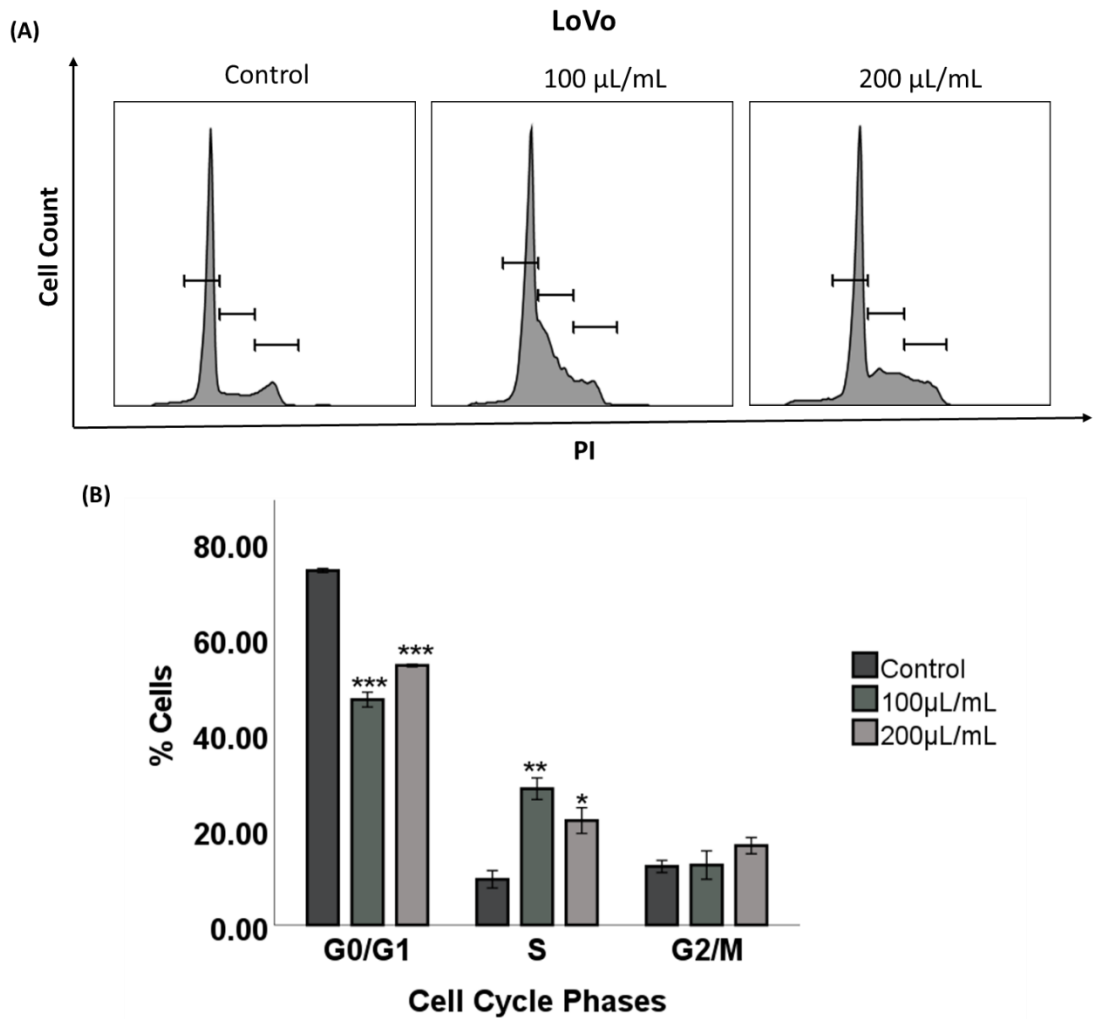


Figure 21. Cell cycle analysis of LoVo cells. (A) Peaks are representation of the percentage of cells in G0/G1, S and G2/M phase post-treatment with EA extract for 48 hours. (B) The three phases were quantified and results are presented as the Mean  $\pm$  SEM: (n=3). Statistical analysis was performed using one-way ANOVA, Tukey's post-hoc test was conducted to compare treatment groups and results were stated as Asterisks indicate significant results compared to the untreated control at \*  $p < 0.05$ , \*\*  $p < 0.01$  and \*\*\*  $p < 0.001$ .

#### 3.1.4 Cell invasion assay

Cancer invasion is the ability of cancer cells to penetrate and the extent to other neighboring tissues, which eventually lead to cancer metastasis (157). As illustrated in Figures 22 and 23, *EA* extract significantly decreases CRC cells invasion by increasing the extract dose. *EA* inhibits the invasion of 38.7 and 97% of HCT-116 cells and 85.2 and 94.5% of LoVo cells at 100 and 200  $\mu\text{L}/\text{mL}$ , respectively. The effect of *EA* is evident as the number of dyed cells is decreasing in crystal violet dye. We modified the staining of this technique by DAPI to confirm the number of invasive cells, as DAPI will only stain the nucleus of the cell. However, crystal violet might stain the pores of the Matrigel®.

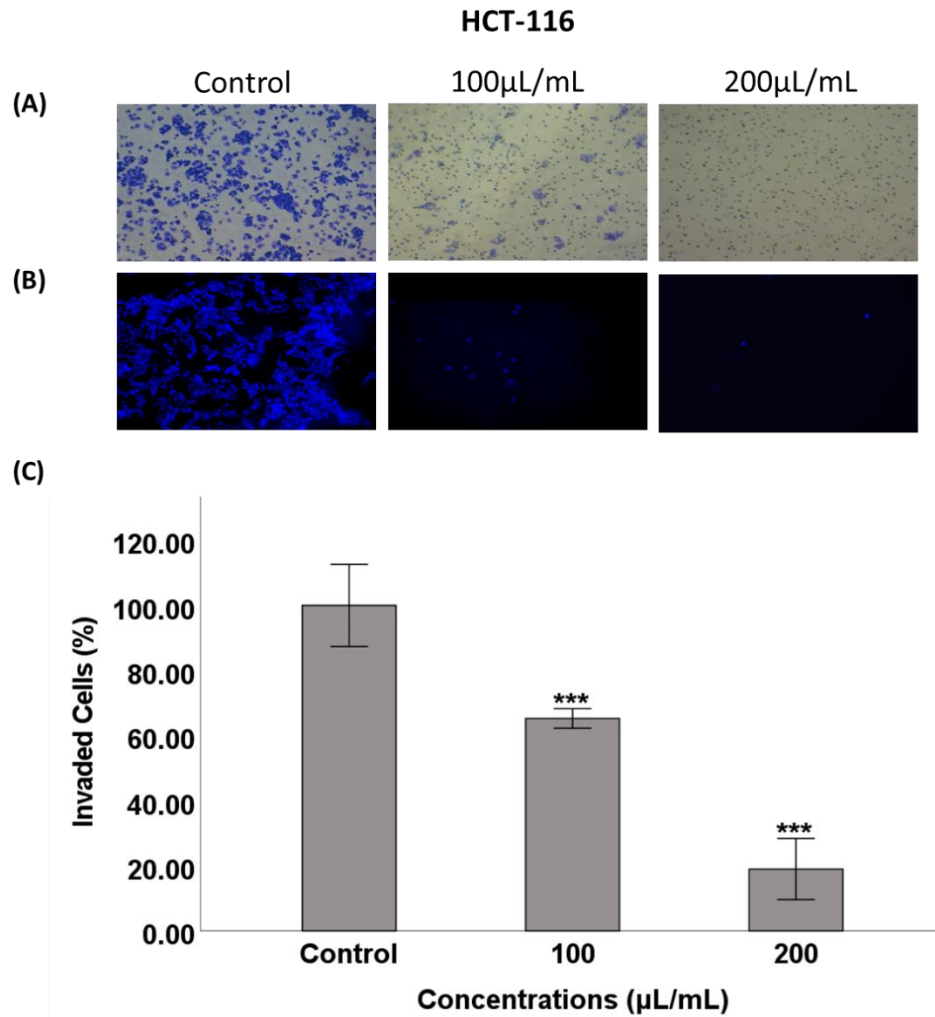


Figure 22. Outcome of *EA* extract on cell invasion of HCT-116 cells. Cells are stained with (A) crystal violet staining (CV) and (B) DAPI. Images were acquired at 10X magnification. (C) Invaded cells quantified by counting the number of invaded cells manually in four different fields and expressed as percentage of treatment relative to the control, and results are presented as the Mean  $\pm$  SEM: (n=3). Statistical analysis was performed using one-way ANOVA, Tukey's post-hoc test was conducted to compare treatment groups. Asterisks indicate significant results compared to the untreated control at \*\*\*  $p < 0.001$ .



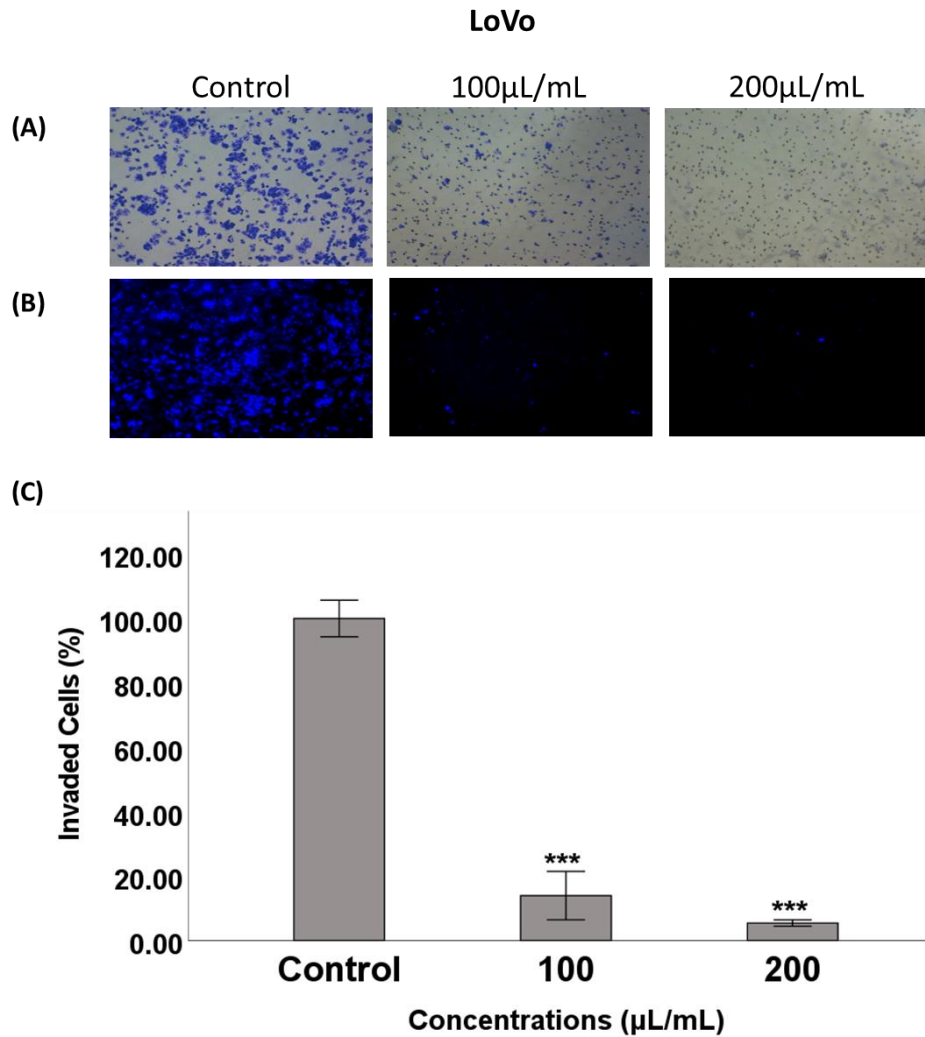


Figure 23. Outcome of *EA* extract on cell invasion of LoVo cells. Cells are stained with (A) crystal violet staining (CV) and (B) DAPI. Images were acquired at 10X magnification. (C) Invaded cells quantified by counting the number of invaded cells manually in four different fields and expressed as percentage of treatment relative to the control, and results are presented as the Mean  $\pm$  SEM: (n=3). Statistical analysis was performed using one-way ANOVA, Tukey's post-hoc test was conducted to compare treatment groups. Asterisks indicate significant results compared to the untreated control at \*\*\*  $p < 0.001$ .

### 3.1.5 Soft agar colony formation assay

Colony formation assay is a technique to evaluate the proliferation rate of cells that can form colonies in soft agar in a certain period. Soft agar indicates a cancer cell's ability to grow in an adhesion-independent manner (158). In this experiment, we found that *EA* inhibits 70.9 and 57.6% of HCT-116 and LoVo cells colonies, respectively, at 100  $\mu\text{L}/\text{mL}$ . In addition, *EA* reduces colony formation of both CRC cell lines compared to untreated control at 200  $\mu\text{L}/\text{mL}$  as shown in Figures 24 and 25.

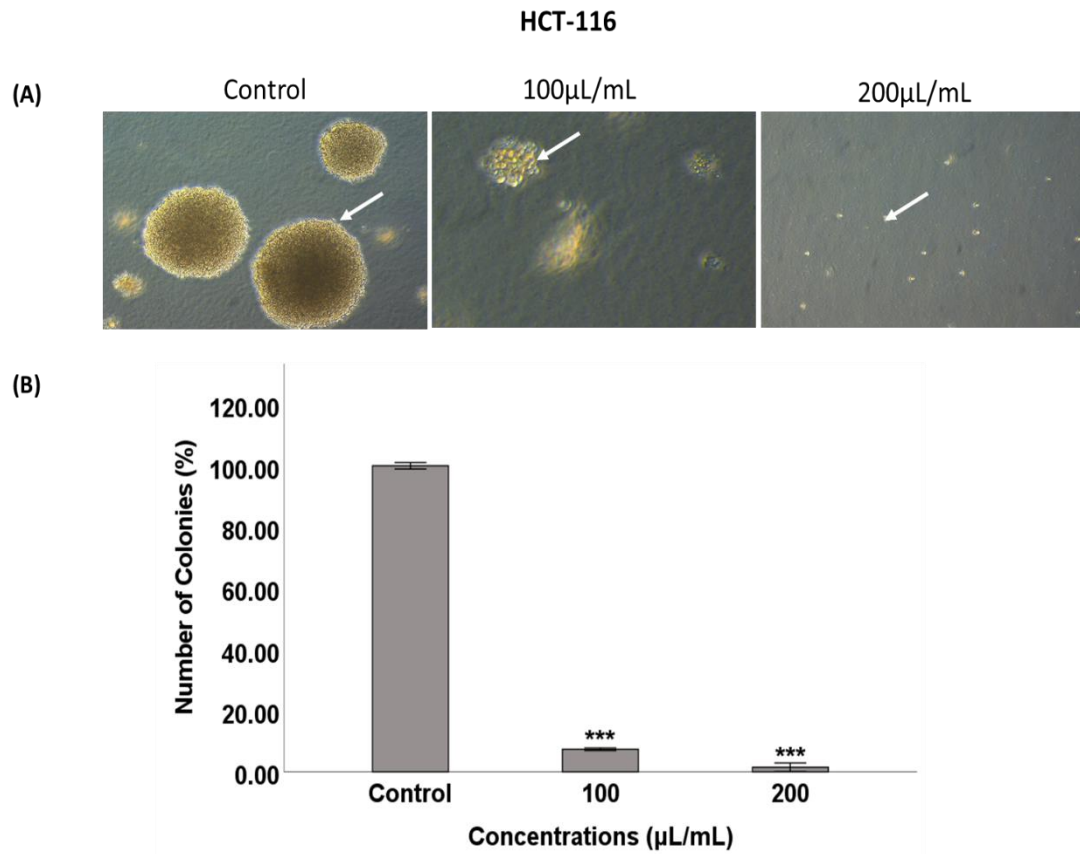


Figure 24. Outcome of *EA* extract on colony formation of HCT-116 cells. (A) Images were acquired at 10X magnification. (B) Formed colonies were quantified by counting the number of colonies manually in four different fields and expressed as percentage of treatment relative to the control. and results are presented as the Mean  $\pm$  SEM: (n=3). Statistical analysis was performed using one-way ANOVA, Tukey's post-hoc test was conducted to compare treatment groups. Asterisks indicate significant results compared to the untreated control at \*\*\*  $p < 0.001$ .

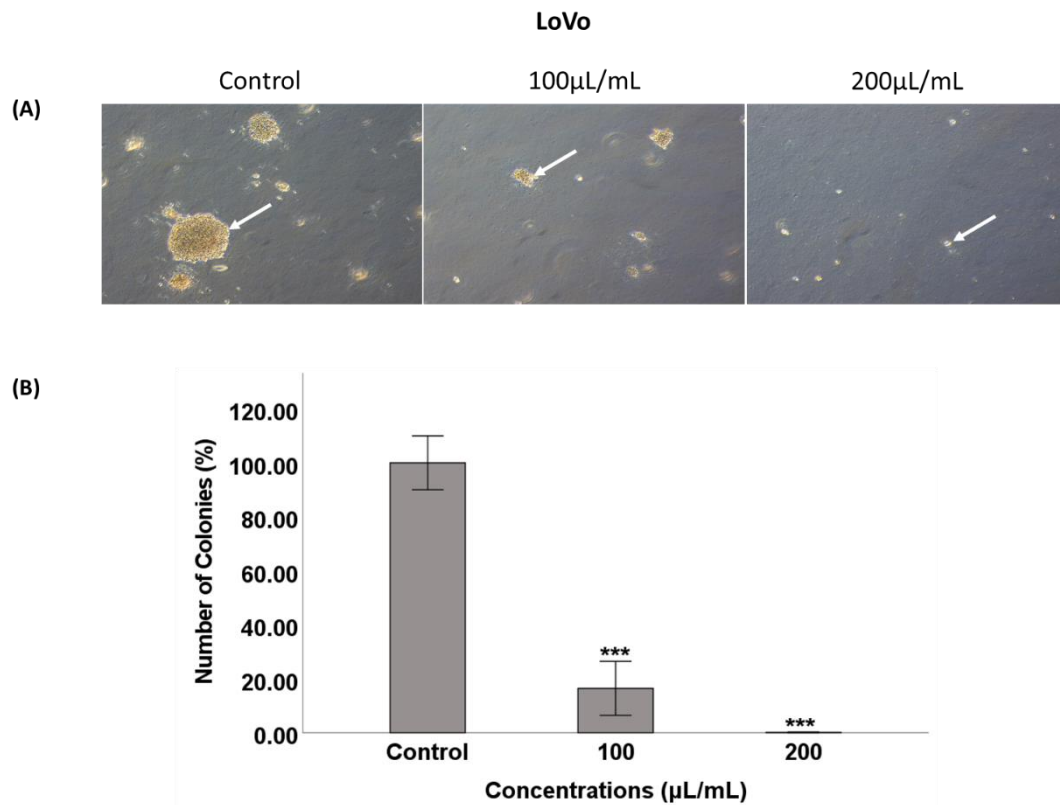


Figure 25. Outcome of *EA* extract on colony formation of LoVo cells. (A) Images were acquired at 10X magnification. (B) Formed colonies were quantified by counting the number of colonies manually in four different fields and expressed as percentage of treatment relative to the control, and results are presented as the Mean  $\pm$  SEM: (n=3). Statistical analysis was performed using one-way ANOVA, Tukey's post-hoc test was conducted to compare treatment groups. Asterisks indicate significant results compared to the untreated control at \*\*\*  $p < 0.001$ .

### 3.1.6 Outcome of *EA* extract on AKT/EGFR and EMT biomarkers in CRC cell lines

Western blot analysis or immunoblotting is an essential technique in drug discovery to identify specific proteins from a complex mixture extracted from tissues or cells (159). According to our results above, *EA* extract has a notable effect on EMT regulator genes. Therefore, we investigated the expression of key biomarkers of EMT in CRC cells (HCT-116 and LoVo) by western blot.

Our data showed that cells treated with *EA* aqueous extract enhanced the expression of calcium-regulated adhesion molecule E-cadherin. Along with a significant downregulation of vimentin, which is a leading protein in the EMT biomarkers. Furthermore, compared to untreated control, *EA* inhibits the expression of phosphorylated  $\beta$ -catenin in both CRC cell lines. Regarding the underlying molecular mechanism, *EA* inhibits the expression of activated AKT that is regulated by EGFR. Accordingly, our flower extract significantly downregulates the expression patterns of EGFR in both HCT-116 and LoVo cells in comparison to the untreated control (Figures 26 and 27).

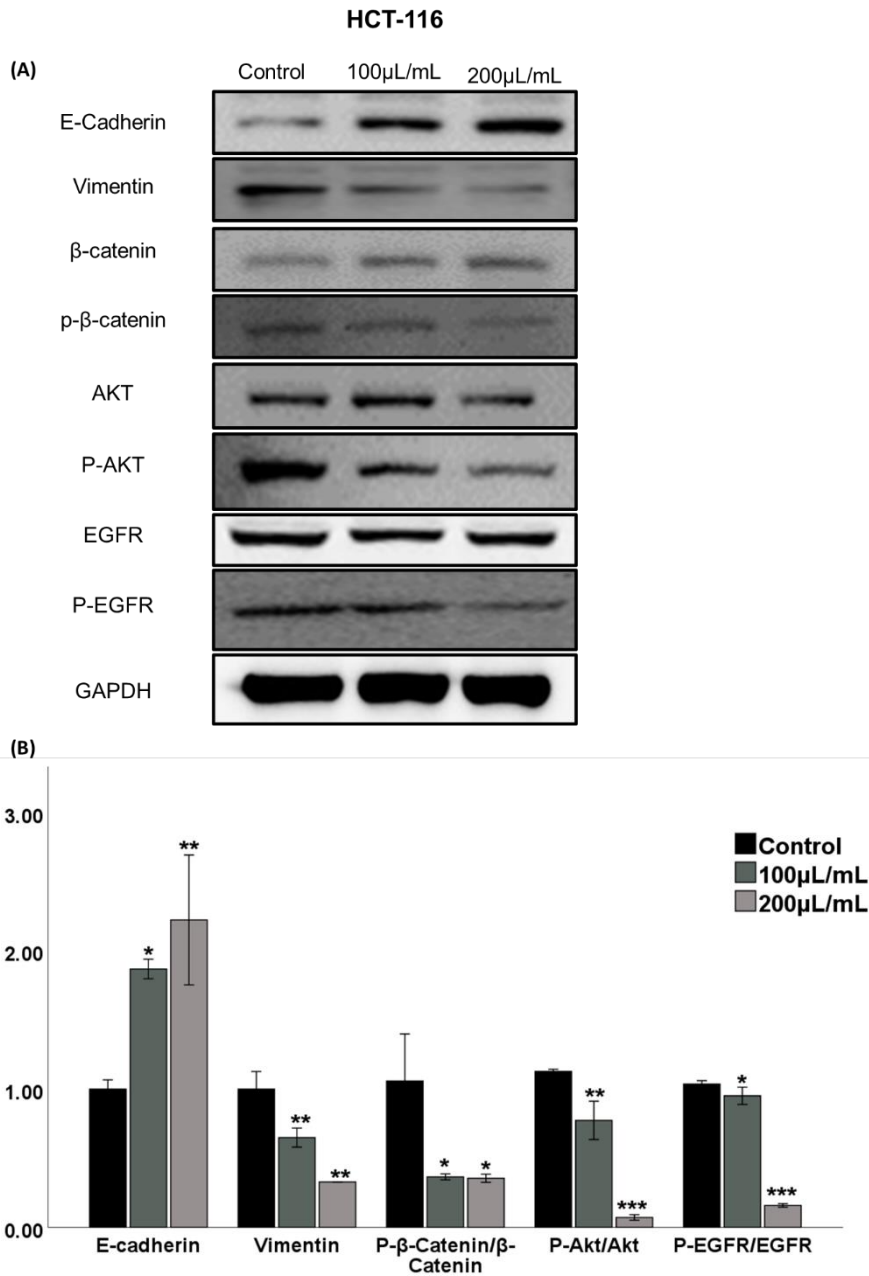


Figure 26. Expression patterns of EMT biomarkers and their molecular pathways provoked by EA extract in HCT-116 cells. GAPDH is used as a housekeeping protein in this assay. Cells were treated with 100 and 200  $\mu$ L/mL of EA extract for 48 hours. Results are presented as the Mean  $\pm$  SEM: (n=3). Statistical analysis was performed using one-way ANOVA, Tukey's post-hoc test was conducted to compare treatment groups. Asterisks indicate significant results compared to the untreated control at \* $p < 0.05$ , \*\* $p < 0.01$ , \*\*\* $p < 0.001$ .

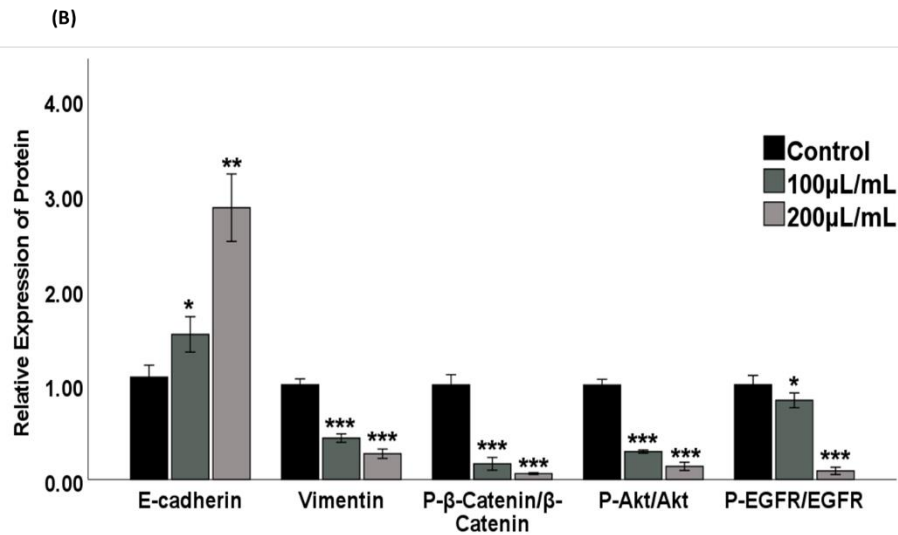
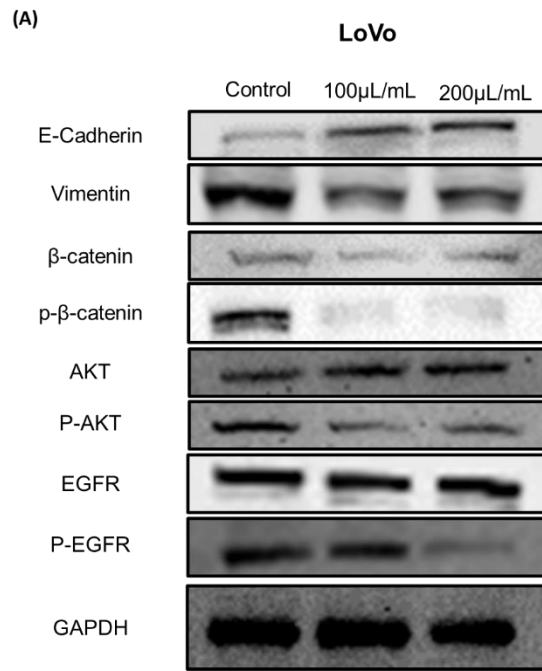


Figure 27. Expression patterns of EMT biomarkers and their molecular pathways provoked by *EA* extract in LoVo cells. GAPDH is used as a housekeeping protein in this assay. Cells were treated with 100 and 200  $\mu$ L/mL of *EA* extract for 48 hours. Results are presented as the Mean  $\pm$  SEM: (n=3). Statistical analysis was performed using one-way ANOVA, Tukey's post-hoc test was conducted to compare treatment groups. Asterisks indicate significant results compared to the untreated control at \*\*  $p < 0.01$ , \*\*\*  $p < 0.001$ .

## 3.2 Effect of DK13 and D14 on CRC cell lines

### 3.2.1 Cell viability assay (AlamarBlue™ assay)

DK13 and DK14 are novel chalcone compounds evaluated for their anti-cancer effect on CRC cell lines HCT-116 and LoVo after 48 hours of treatment. Both compounds, DK13 and DK14, significantly reduce the cell viability of both CRC cell lines (Figures 28 A and B). DK13 at high concentration 60  $\mu$ M inhibits  $71.18\% \pm 2.6$  and  $69.88\% \pm 1.8$  of HCT-116 and LoVo cell lines, respectively. On the other hand, DK14 at 60  $\mu$ M inhibits  $93.06\% \pm 2.05$  and  $84.5\% \pm 1.8$  of HCT-116 and LoVo cell lines, respectively.

Six concentrations (2.5, 5, 10, 20, 40, and 60  $\mu$ M) are used to calculate the  $IC_{50}$  of DK13 and DK14 in HCT-116 and LoVo cell lines. After obtaining the percentage of viable cells upon treatment, a scatter blot is created as a function of concentrations and the  $IC_{50}$  was calculated as shown in Table. 10. Based on the  $IC_{50}$  values of DK13 and DK14 and on our previous studies for the effect of both compounds on breast cancer, 10  $\mu$ M concentration is be used for all experiments (151, 160).

To assess the selectivity of cytotoxic effect of DK13 and DK14 on cancerous cell lines, the effect of 10 and 20  $\mu$ M concentrations were explored on the viability of NCE-1 E6/E7 cell line. As shown in Figure. 29, DK13 significantly inhibited 50.5 and 66.6 % of NCE-1 E6/E7 cells at 10 and 20  $\mu$ M, respectively. On the other hand, DK14 does not show toxicity on NCE-1 E6/E7 cells at 10  $\mu$ M, however it only reduces 13.29% of the cells at 20  $\mu$ M.

According to a recent study, the  $IC_{50}$  of 5-FU is 11.23  $\mu$ M and 12.28  $\mu$ M in HCT-116 and LoVo cells, respectively (161). Thus, a similar concentration is used for the 5-FU for comparison.



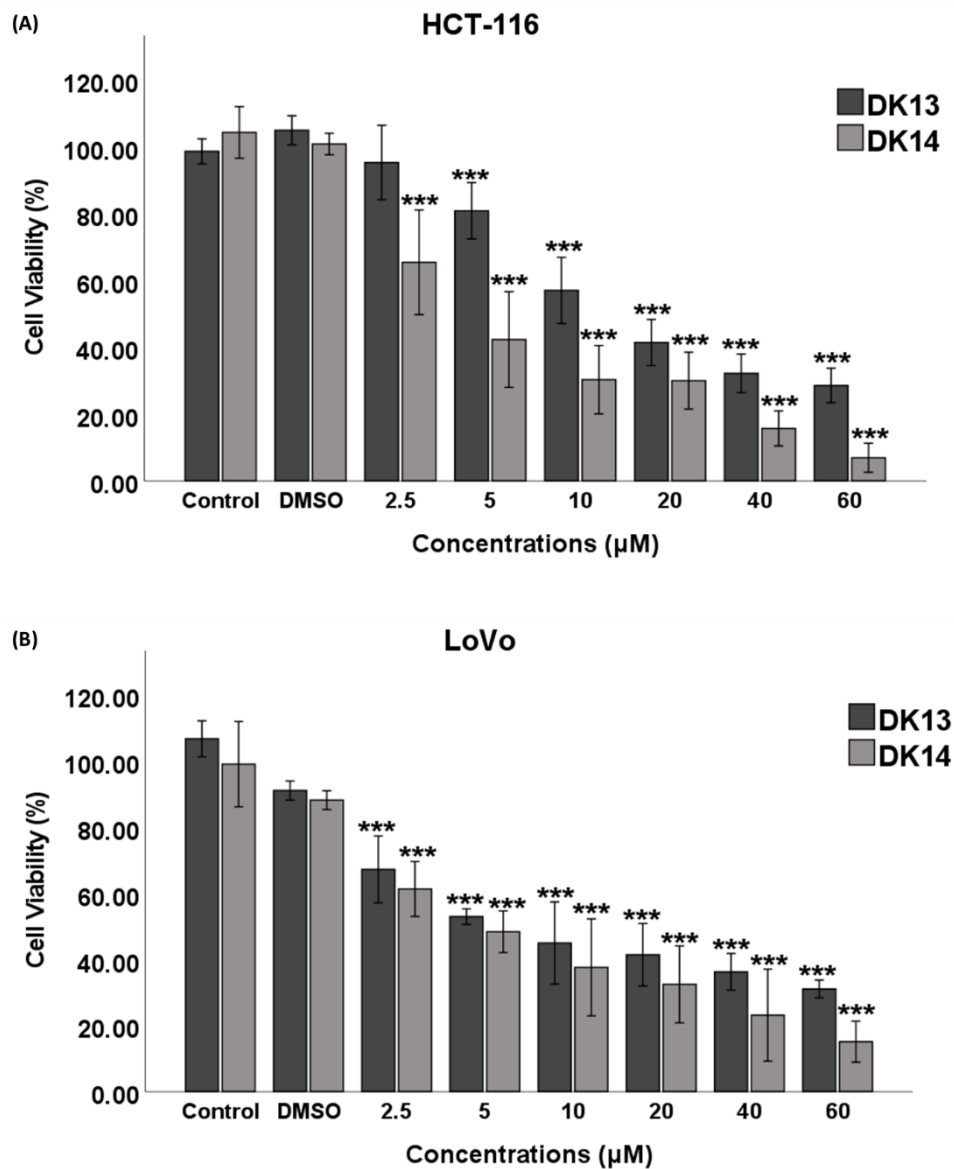


Figure 28. Outcome of different concentrations of DK13 and DK14 on the viability of (A) HCT-116 cells and (B) LoVo. Cells were treated with a range of six different concentrations of both compounds. Percentage of cell viability is calculated 48 hours post-treatment relative to the untreated control for each cell line (Mean  $\pm$  SEM; n=3). Statistical analysis was performed using one-way ANOVA, Tukey's post-hoc test is conducted to compare treatment groups. Asterisks indicate significant results compared to the untreated control at \*\*\*  $p < 0.001$ .

Table 10. IC<sub>50</sub> of DK13 and DK14 in CRC cell lines after 48 hours of treatment.

CRC cell line	IC <sub>50</sub> of DK13	IC <sub>50</sub> of DK14
HCT-116	23.31 μM ± 1.4	7.04 μM ± 1.22
LoVo	17.63 μM ± 4.4	10.08 μM ± 1.4

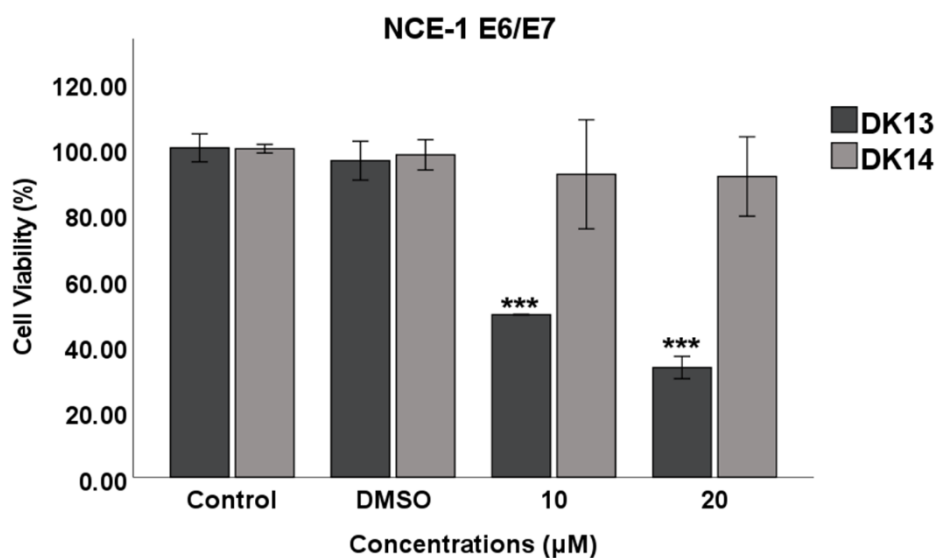


Figure 29: Outcome of DK13 and DK14 on the viability of NCE-1E6/E7. Cells were treated with 10 and 20 μM of both compounds. Percentage of cell viability is calculated 48 hours post-treatment relative to the untreated control for each cell line (Mean ± SEM; n=3). Statistical analysis was performed using one-way ANOVA, Tukey's post-hoc test is conducted to compare treatment groups. Asterisks indicate significant results compared to the untreated control at \*\*\*  $p < 0.001$ .

### 3.2.2 Cell morphology analysis

Afterward, we analyzed the effect of DK13 and DK14 on HCT-116 and LoVo morphological characteristics. Results are compared to the effect of DMSO, and 5-FU treated cells. Notably, DK13 and DK14 at 10 $\mu$ M change the morphology of both cell lines from mesenchymal phenotype to epithelial as the shape of the cells became flat, increasing cell-cell adhesion among treated cells compared to untreated cells, as shown in Figures 30 and 31. However, 5-FU does not show that effect on both cell lines.

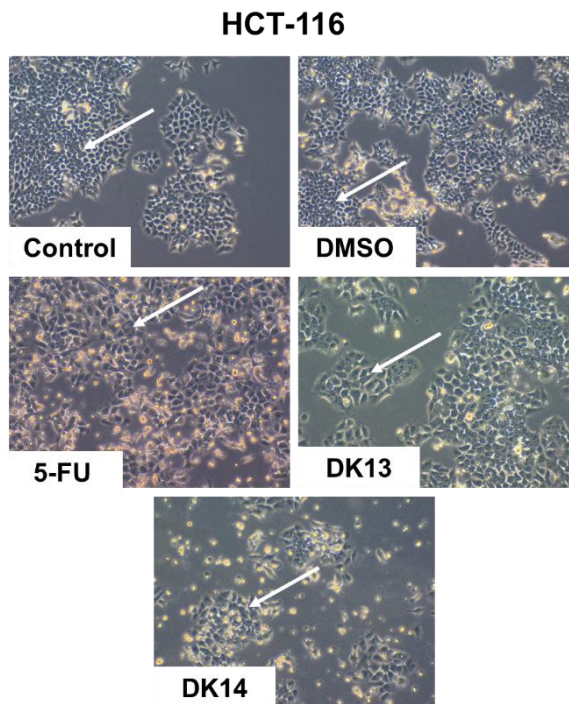


Figure 30. Outcome of DK13 and DK14 on the morphology of HCT-116 cells after treatment at 10 $\mu$ M for 48 hours. Images visualized at 10X magnification.

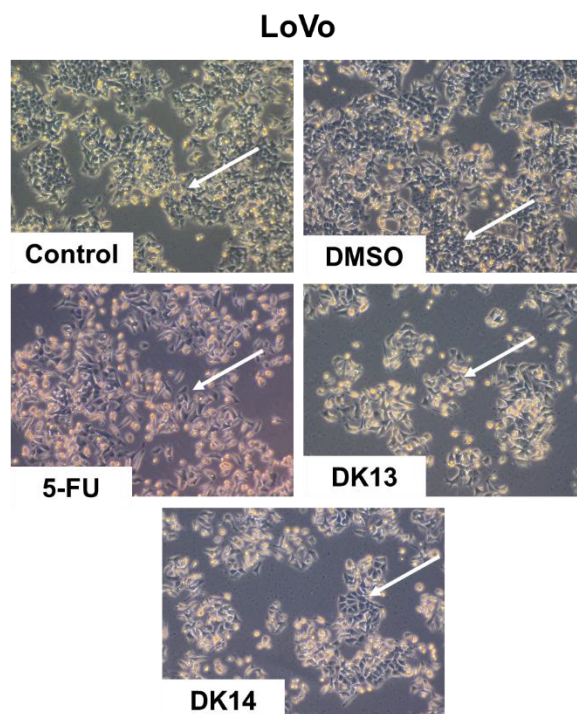


Figure 31: Outcome of DK13 and DK14 on the morphology of LoVo cells after treatment at 10 $\mu$ M for 48 hours. Images visualized at 10X magnification.

### 3.2.3 Flow cytometric analysis of cell cycle

The cell-cycle phase distributions of cells treated with both chalcone compounds are analyzed by flow cytometry to validate the effect of DK13 and DK14 on cell proliferation. DMSO-treated cells display a typical cell-cycle pattern in all phases G0/G1, S-phase, and G2/M. Chalcone analogs DK13 and DK14 arrest HCT-116 and LoVo cells at the G2/M phase. On the other hand, 5-FU arrest the cells of both cell lines at the S phase (Figures 32 and 33).

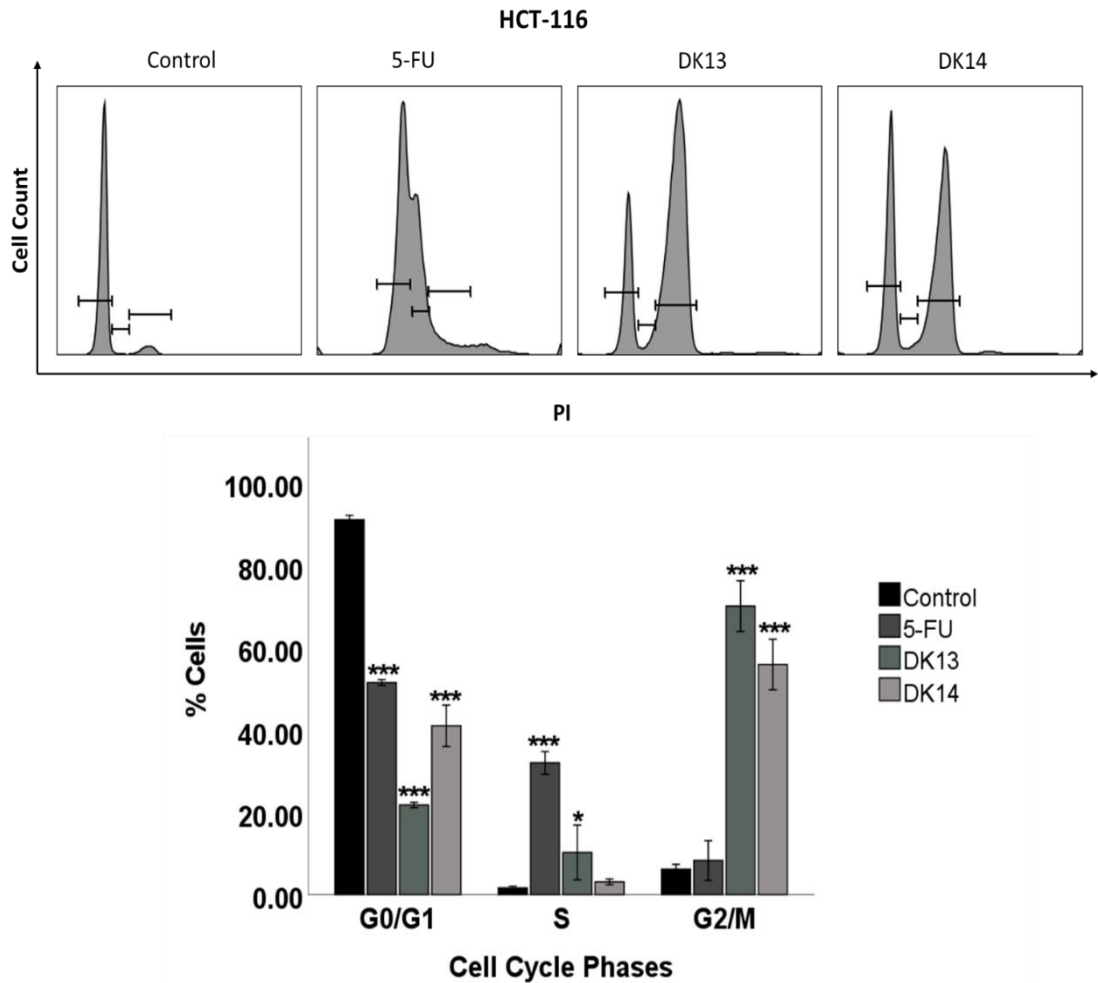


Figure 32. Cell cycle analysis of HCT-116 cells. (A) Peaks are representation of the percentage of cells in G0/G1, S and G2/M phase post-treatment with 10  $\mu$ M of DK13, DK14 and 5-FU for 48 hours. (B) Quantification of cell cycle phases. Results are presented as the Mean  $\pm$  SEM: (n=3). One-way ANOVA, Tukey's post-hoc test was conducted to for comparisons. Asterisks indicate significant results compared to the untreated control at \* $p < 0.05$  and \*\* $p < 0.01$ .

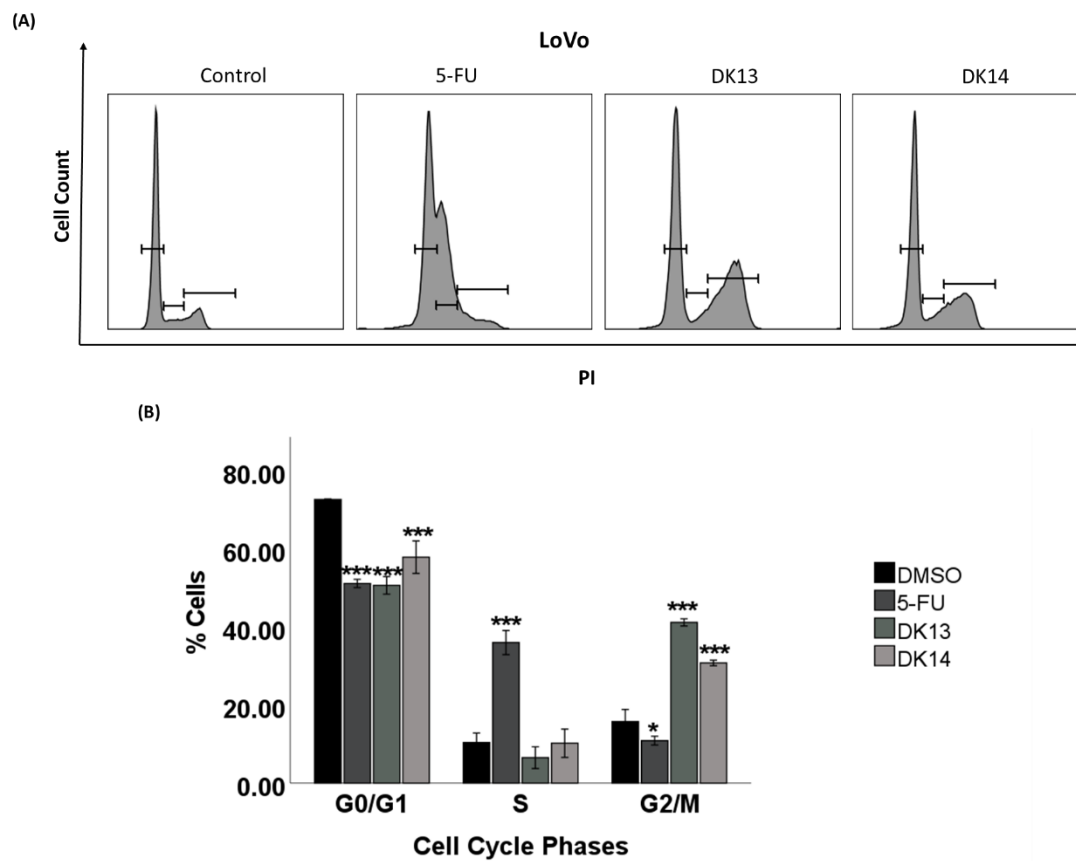


Figure 33. Cell cycle analysis of LoVo cells. (A) Peaks are representation of the percentage of cells in G0/G1, S and G2/M phase post-treatment with 10  $\mu$ M of DK13, DK14 and 5-FU for 48 hours. (B) Quantification of cell cycle phases. Results are presented as the Mean  $\pm$  SEM: (n=3). One-way ANOVA, Tukey's post-hoc test was conducted to for comparisons. Asterisks indicate significant results compared to the untreated control at \*  $p < 0.05$  and \*\*\*  $p < 0.001$ .

#### 3.2.4 Cell invasion assay

Then, the ability of DK13 and DK14 in inhibiting cancer cell invasion is investigated by using Matrigel invasion assay. Our data revealed that DK13 and DK14 significantly inhibit the invasion of HCT-116 cells by 89.2 % and 96.7 %, respectively, and by 86% and 95.8% in the LoVo cell line, respectively. However, 5-FU inhibits 55% and 30% of HCT-116 and LoVo cell invasion. Figures 34 and 35 represent invasive stained cells with crystal violet and DAPI staining, which makes the effect of both DK13 and DK14 on cancer cell invasion clear compared to the DMSO, and 5-FU treated cells.



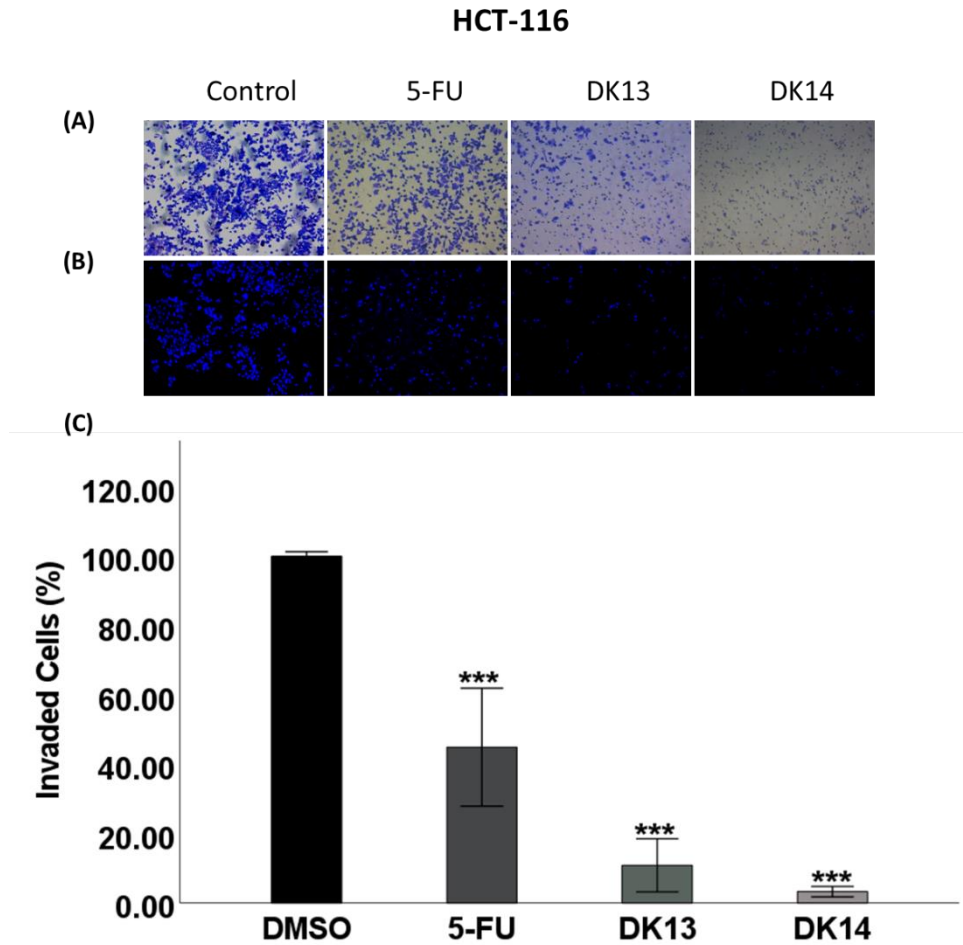


Figure 34. Outcome of DK13, DK14 and 5-FU at 10 $\mu$ M on cell invasion of HCT-116 cells. Cells are stained with (A) crystal violet staining (CV) and (B) DAPI. Images were acquired at 10X magnification. (C) Invaded cells quantified by counting the number of invaded cells manually in four different fields and expressed as percentage of treatment relative to the control, and results are presented as the Mean  $\pm$  SEM: (n=3). One-way ANOVA, Tukey's post-hoc test was conducted to for comparisons. Asterisks indicate significant results compared to the untreated control at \*\*\*  $p < 0.001$ .

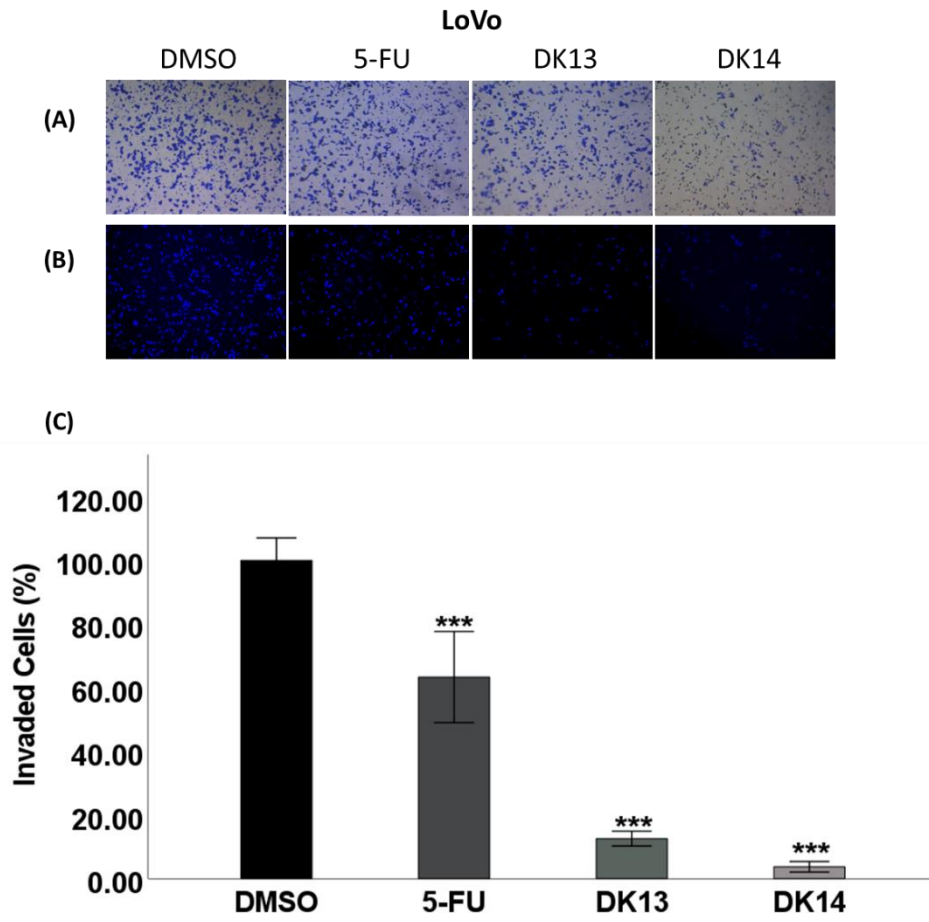


Figure 35. Outcome of DK13, DK14 and 5-FU at 10 $\mu$ M on cell invasion of LoVo cells. Cells are stained with (A) crystal violet staining (CV) and (B) DAPI. Images were acquired at 10X magnification. (C) Invaded cells quantified by counting the number of invaded cells manually in four different fields and expressed as percentage of treatment relative to the control, and results are presented as the Mean  $\pm$  SEM: (n=3). One-way ANOVA, Tukey's post-hoc test was conducted to for comparisons. Asterisks indicate significant results compared to the untreated control at \*\*\*  $p < 0.001$

### 3.2.5 Soft agar colony formation assay

HCT-116 and LoVo cells' ability to form colonies in soft agar is analyzed under the effect of DK13 and DK14. DK13 inhibits 88% and 78.5 of HCT-116 and LoVo cells respectively. And DK14 inhibits 98% of both cell lines compared to the DMSO and 5-FU treated cells (Figures 36 and 37).

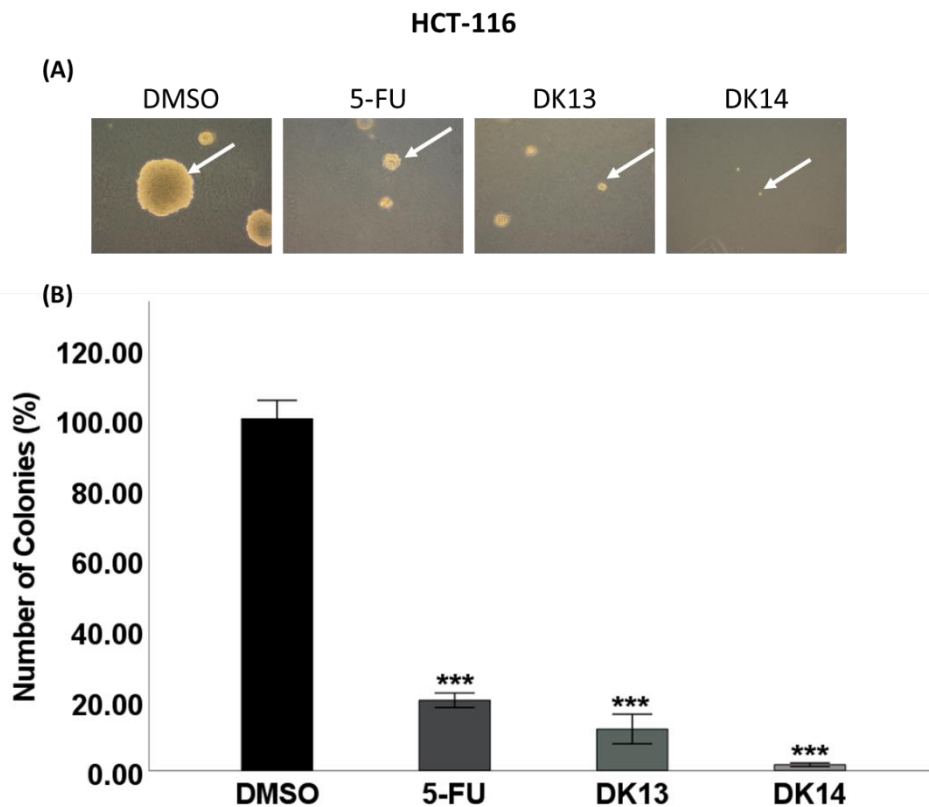


Figure 36. Outcome of DK13, DK14 and 5-FU on colony formation of HCT-116 cells. (A) Images were acquired at 10X magnification. (B) Formed colonies were quantified by counting the number of colonies manually in four different fields and expressed as percentage of treatment relative to the control. and results are presented as the Mean  $\pm$  SEM: (n=3). One-way ANOVA, Tukey's post-hoc test was conducted to for comparisons. Asterisks indicate significant results compared to the untreated control at \*\*\* $p < 0.001$ .

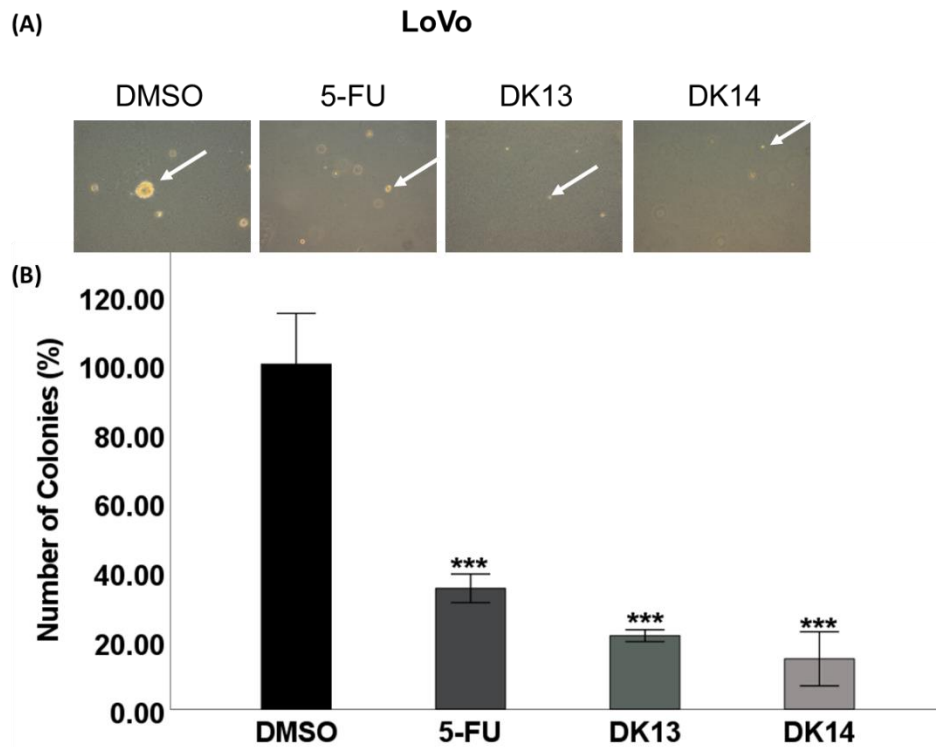


Figure 37. Outcome of DK13, DK14 and 5-FU on colony formation of LoVo cells. (A) Images were acquired at 10X magnification. (B) Formed colonies were quantified by counting the number of colonies manually in four different fields and expressed as percentage of treatment relative to the control, and results are presented as the Mean  $\pm$  SEM: (n=3). One-way ANOVA, Tukey's post-hoc test was conducted for comparisons. Asterisks indicate significant results compared to the untreated control at \*\*\*  $p < 0.001$ .

### 3.2.6 Outcome of DK13 and DK14 on EMT biomarkers and AKT/mTOR in CRC cell lines

According to the results above, DK13 and DK14 are suggested to inhibit the EMT pathway. Thus, we examined the expression patterns of EMT biomarkers in HCT-116 and LoVo cell lines using western blot analysis. The data showed that DK13 and DK14 increases the expression of epithelial protein E-cadherin, while the mesenchymal protein Vimentin is decreased in both cell lines. Furthermore, our results suggested that both chalcone compounds inhibit Wnt/ $\beta$ -Catenin and AKT/mTOR pathways in both CRC cell lines by significantly deregulating the phosphorylated form of  $\beta$ -Catenin, AKT, and mTOR proteins compared to DMSO and 5-FU treated cells (Figures 38 and 39).

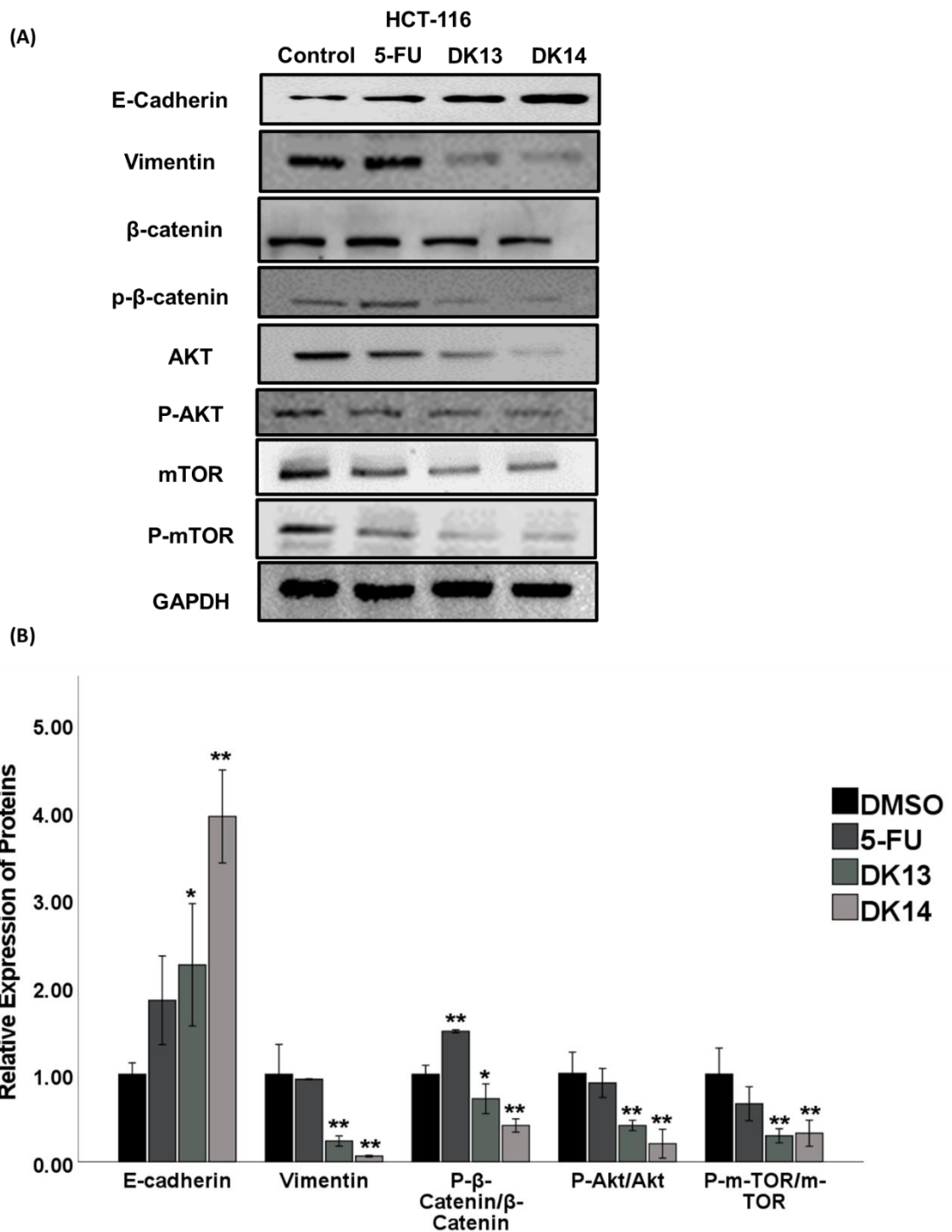


Figure 38. Expression patterns of EMT biomarkers and their molecular pathways induced by DK13 and DK14 in HCT-116 cells. GAPDH was used as housekeeping protein in this assay. Cells were treated with 10  $\mu$ M of DK13, DK14 and 5-FU for 48 hours. Results are presented as the Mean  $\pm$  SEM: (n=3). One-way ANOVA, Tukey's post-hoc test was conducted to for comparisons. Asterisks indicate significant results compared to the untreated control at \* $p < 0.05$  and \*\* $p < 0.01$ .

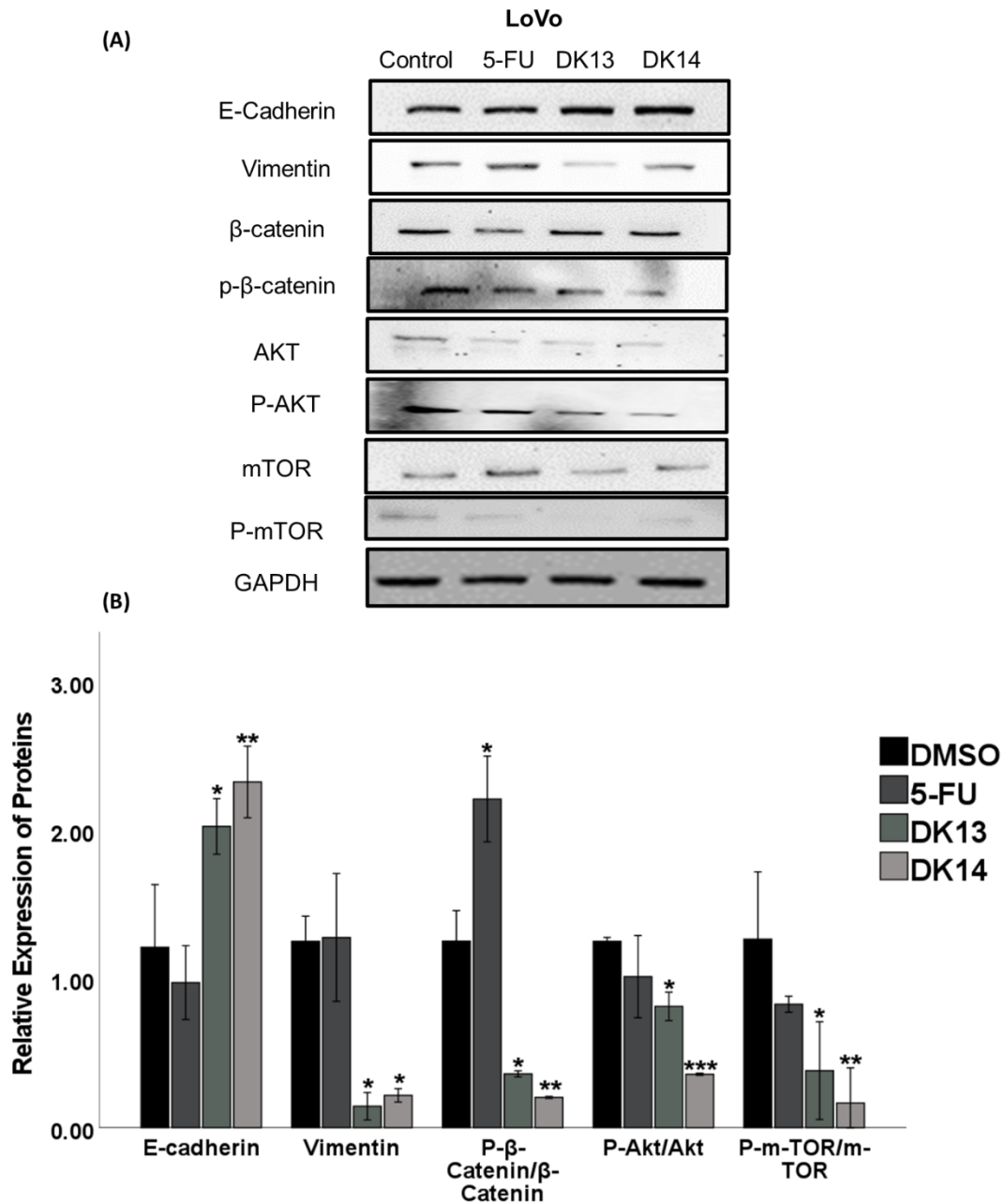


Figure 39. Expression patterns of EMT biomarkers and their molecular pathways induced by DK13 and DK14 in LoVo cells. GAPDH was used as housekeeping protein in this assay. Cells were treated with 10  $\mu$ M of DK13, DK14 and 5-FU for 48 hours. Results are presented as the Mean  $\pm$  SEM: (n=3). One-way ANOVA, Tukey's post-hoc test was conducted for comparisons. Asterisks indicate significant results compared to the untreated control at \*  $p < 0.05$ , \*\*  $p < 0.01$  and \*\*\*  $p < 0.001$ .

#### 4.1 *Drosophila melanogaster* as a model for CRC studies

##### 4.1.1 *Ras* expression in *D. melanogaster* fly lines with *ras* mutation

To confirm the expression of *ras1* (more precisely termed *ras* oncogene at 85D) in fly lines with a constitutively active form of *Ras85D* (the homolog of vertebrate *ras1* in *Drosophila*) under the control of the *sev* enhancer and promoter, controls, real-time PCR is performed. As expected, the expression of *ras1* was significantly upregulated in *Ras85D* as compared to the control group *Yw*. (Figure 40).

##### 4.1.2 ERK1/2 and AKT expression in *D. melanogaster* fly lines with *ras* mutation

To further confirm the oncogenic status of the fly lines used in this study, we scored for the protein expression of (ERK1/2 and AKT), two important biomarkers in the RAS signaling pathway by western blot analysis (162). As expected, the protein expression of both ERK1/2 and phosphorylated AKT/total AKT ratio are significantly upregulated in *Ras85D* fly line as compared to the *Yw* control (Figure 41).



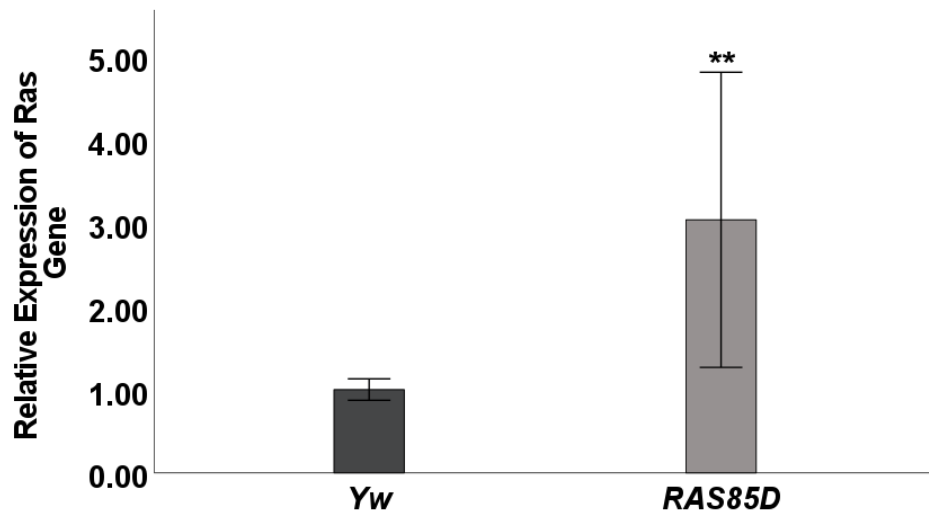


Figure 40. Relative quantification of *ras1* mRNA expression levels in the whole body of *Ras85D* as compared to *Yw* controls. Measurements represent the mean of three independent repeats normalized to the transcript levels of *Yw*. *Rp49* was used as the reference gene. Statistical analysis was performed using one-way analysis of variance (ANOVA), with Tukey's post-hoc test. Asterisks indicate significant results compared to the untreated control at \*\* $p < 0.01$ .

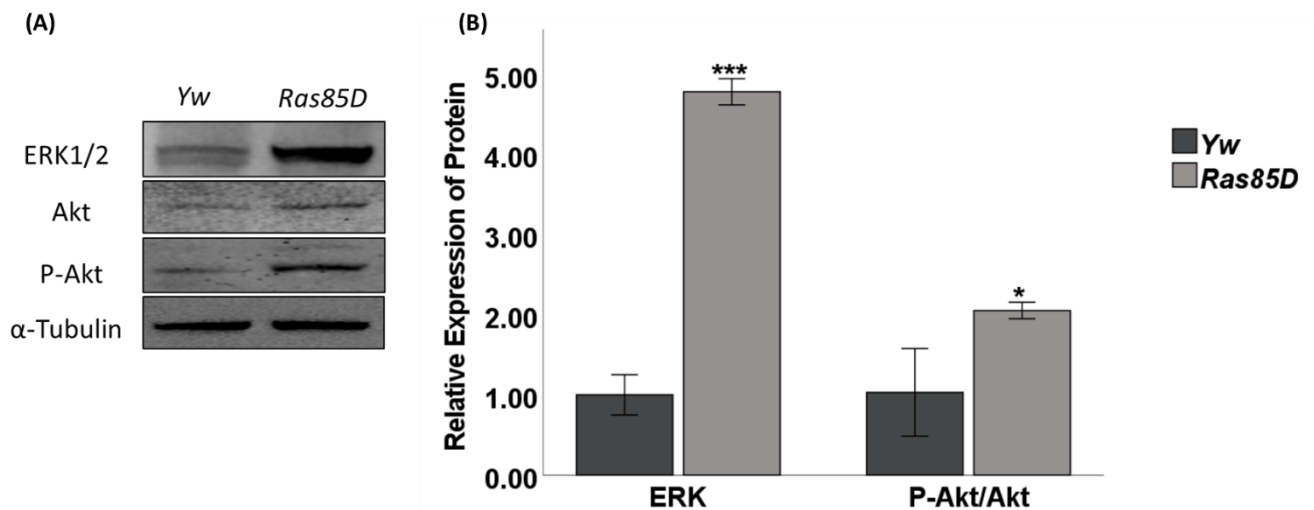


Figure 41. Relative quantification of ERK1/2 and Akt expression patterns in *Ras85D* as compared to *Yw* controls. (A) Representative western blot and (B) quantified expression representing the mean of three independent repeats normalized to the protein levels of the *Yw* control. Alpha-tubulin was used as the reference gene. Statistical analysis was performed using one-way analysis of variance (ANOVA), with Tukey's post-hoc test. Asterisks indicate significant results compared to the untreated control at \* $p < 0.05$  and \*\* $p < 0.01$ .

#### 4.1.3 Effect of *EA* extract on the survival rates of fly lines with *Ras* mutation as compared to wild type flies

To rule out any toxic effect of *EA* on flies, we first scored for the survival rates of orally fed *Y<sub>w</sub>* (wild-type) flies with increasing *EA* aqueous extract concentration ranging from 25 to 500  $\mu\text{L}/\text{mL}$ . As shown in Figure 42, a positive relationship between the lifespan of *Y<sub>w</sub>* flies and the increasing concentration of the *EA* extract is detected. The higher the concentrations of the flower extract (200 and 500  $\mu\text{L}/\text{mL}$ ), the longer the survival span of *EA* treated flies. The hazard ratio (HR) is also calculated by Cox regression and revealed a value equal to 0.605 (95% CI, 0.545-0.672), indicating that *EA* aqueous extract decreases the likelihood of the event, which is the death of *Y<sub>w</sub>* flies.

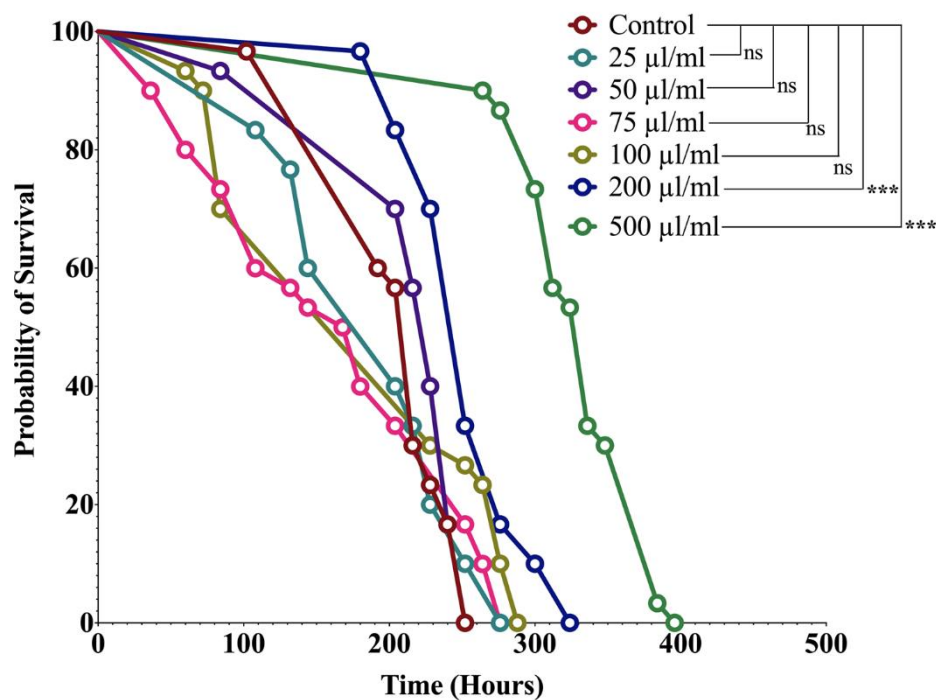


Figure 42. Outcome of *EA* extract on the survival rates of *Y<sub>w</sub>* flies orally with 200 and 500  $\mu\text{L}/\text{mL}$  of *EA* as compared to the untreated control group. The higher the concentration of *EA*, the longer the lifespan of *EA* treated flies. Kaplan-Meier survival test was used to calculate percent survival. The statistical significance of the observed differences was calculated using the log-rank test. Asterisks indicate significant results between compared groups. Asterisks indicate significant results compared to the control at \* $p < 0.05$ , \*\*\* $p < 0.001$  and ns indicating no significant difference.

Accordingly, the 200 and 500  $\mu\text{L}/\text{mL}$  concentration of the *EA* flower extract is adopted and used to explore the effect of *EA* on the lifespan of *ras* mutant fly lines. As expected, both concentrations of *EA* significantly increase the survival rates of *ras* mutant fly line as compared to control groups (Figure 43). Also, the HR of *Ras85D* is 0.377 (95%, CI, 0.377-0.677), indicating that *EA* aqueous extract decreases the likelihood of the event, which is the death of *Ras85D* flies.

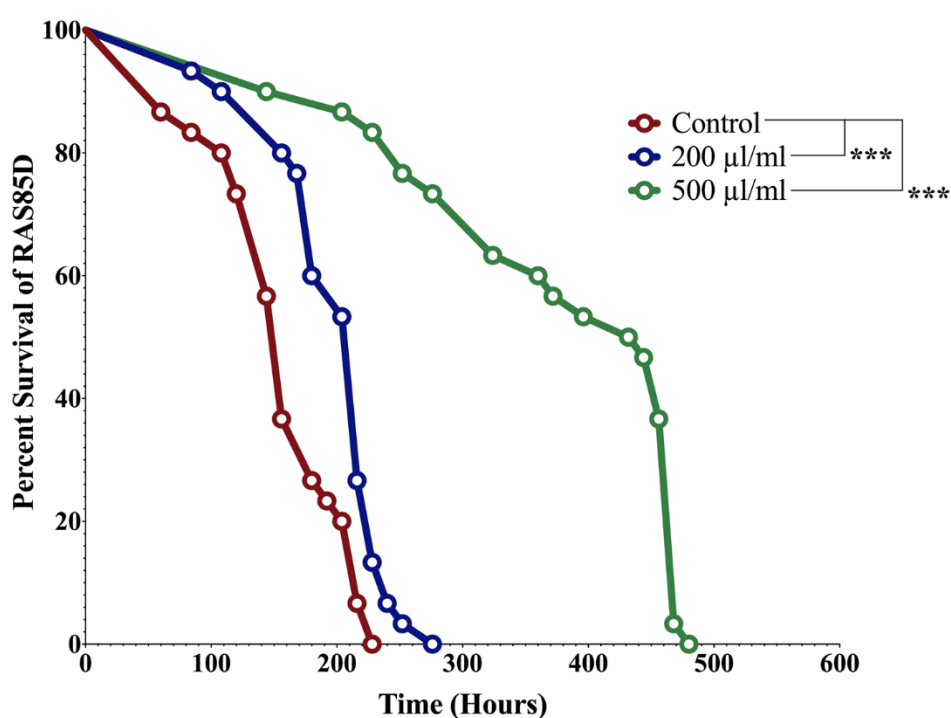


Figure 43. Outcome of *EA* extract on the survival rates of *Ras85D* treated with 200 and 500  $\mu\text{L}/\text{mL}$  of *EA* as compared to the untreated control group. *Ras85D* fly line survive significantly better when treated with the *EA* extract. Also, the higher the concentration of *EA*, the longer the lifespan of *EA* treated flies. Kaplan-Meier survival test was used to calculate percent survival. The statistical significance of the compared groups was calculated using the log-rank test. Asterisks indicate significant difference between the compared groups, with \*\*\* indicates  $p < 0.001$ .

#### 4.1.4 Outcome of DK13 and DK14 on the survival rates of fly lines with *ras* mutation as compared to wild-type flies

To rule out any toxic effect of DK13 and DK14 on flies, we first scored for the survival rates of orally treated *Yw* (wild-type) flies with 10 $\mu$ M of DK13 and DK14. As shown in Figure 44 A, no significant difference is detected in the survival rates of flies treated with DK13 as compared to the control group, with an HR value of 0.946 (95% CI, 0.682- 1.312), eliminating a toxic effect of DK13 on flies. On the contrary, however, flies treated with DK14 exhibit a significant increase in their survival rates as compared to *Yw* control group, with an HR value of 0.606 (95%, CI, 0.451- 0.813), indicating a plausible protective effect of DK14 on flies.

Accordingly, the effect of DK13 and DK14 on the lifespan of *ras* mutant fly lines is investigated and compared to 5-FU (conventional anticancer medication) and to an untreated control. As shown in Figure 42 B, *Ras85D* flies had no significant survival rates as compared to the control group when treated with DK13, with an HR of 0.787 (95%, CI, 0.557- 1.112). On the contrary however, those treated with DK14 exhibit a significantly increased lifespan, with an HR of 0.248 (95%, CI, 0.093- 0.661), as compared to the control group, which indicates the potential effect of DK14 on cancer mutant flies. On the other hand, 5-FU shows toxic effect against *ras* mutant flies as it significantly decreases the survival rate of *Ras85D* flies with an HR=3.429 (95%, CI, 1.477- 7.475) (Figure 44 B) indicating the likelihood of event to happen which is the death of treated flies.

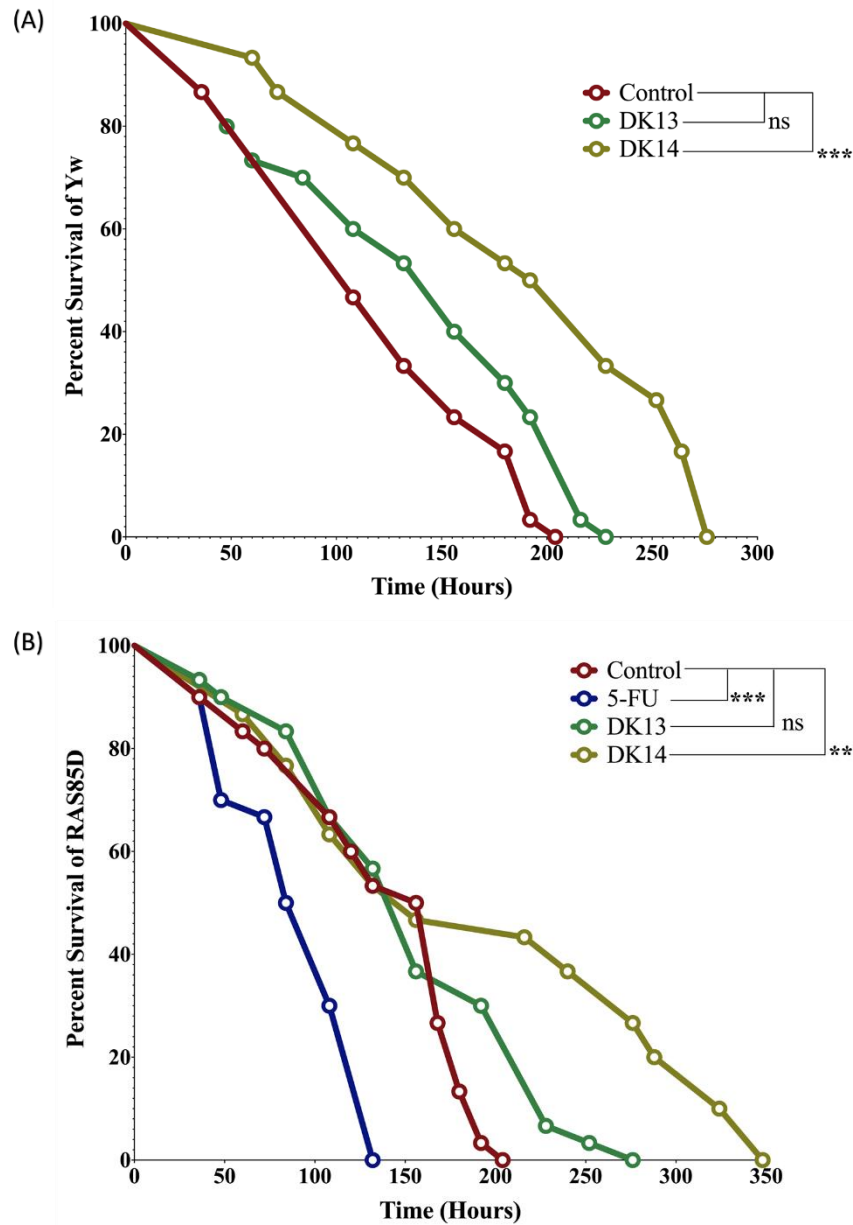


Figure 44. Outcome of DK13 and DK14 on the survival rates of (A) *Yw* flies and (B) *Ras85D* fly line orally treated with 10  $\mu$ M of DK13 and DK14 as compared to the DMSO-treated control groups. Unlike DK13 which did not impact the life span of treated flies of both fly lines, those orally fed with DK14 exhibited a significant increase in their survival rates as compared to the control groups. Kaplan-Meier was used to calculate percent survival, and the statistical significance between compared groups was calculated using the log-rank test. Asterisks indicate significant difference between compared groups, with \*\*\* indicating  $p < 0.001$ , and ns indicating no significant difference.

## CHAPTER 4: DISCUSSION

Cancer has become the leading cause of mortality in recent years, with the highest incidence rate pertaining to CRC (163), despite the current developed approaches used in diagnosing and treating CRC. Traditionally, CRC treatment encloses 5-fluorouracil (5-FU), a therapeutic regimen that is received differently in toxicity and efficacy in CRC patients. Apart from their severe side effects, recently, studies have, for example, reported tumor resistance to some of these systemic chemotherapies such as 5-FU and irinotecan over the treatment course (81). This necessitates the development of alternative, reliable, and targeted therapies against CRC to prevent its progression, control its metastasis, and effectively treat patients with minimal to no side effects. Natural products such as flavonoids have contributed significantly to the field of drug discovery and development, particularly those presented as anti-cancerous agents. Likewise, synthesizing new chemotherapeutic agents like chalcones hold promising potential in establishing novel cancer therapies. Herein, our investigation showed, for the first time, a significant effect of *EA* aqueous extract and nitrogen-based chalcone analogs (DK13 and DK14) against CRC in both *in vitro* (human CRC cell lines [HCT-116 and LoVo]) and *in vivo* (*D. melanogaster* fly lines with *ras* mutation) systems.

#### 4.1 Effect of *EA* aqueous extract on CRC

According to our data, *EA* flower extract reduced the viability of both CRC cell lines (HCT-116 and LoVo). Results of our present work are consistent with our published work regarding the effect of *EA* aqueous extract on HER2-positive cell lines (SK-BR-3 and ZR-751) and TNBC (MDA-MB-231 and MDA-MB-436) cell lines. *EA* had a significant effect against cell viability in both types of cancer. Additionally, *EA* aqueous extract disturbed the cell cycle distribution by arresting HCT-116 cells in the G2/M phase, and LoVo cells are arrested in the S phase. *EA* showed a significant effect on the cell cycle of HER2-positive cancer cell lines by arresting cells in the G0/G1 phase of both SK-BR-3 and ZR-751. In TNBC cell lines, *EA* arrested both TNBC cell lines (MDA-MB-231 and MDA-MB-436) in the S phase (150, 164). According to several phytochemical studies, *EA* contains significant amounts of flavonoids that are suggested to be responsible for its therapeutic effect of (104, 165, 166).

A flavonoid called Baicalin extracted from the *Scutellaria baicalensis* plant showed anti-cancer potency in inhibiting the proliferation of CRC cells (HCT-116 and HT-29). Additionally, this extract deregulated the cell cycle by arresting both CRC cells in S and G2/M phases (167). Supporting our anticipation that *EA*'s anti-cancer effect is due to flavonoids. Moreover, *EA* extract did not affect the viability of human normal immortalized colorectal cell line, NCE-1 E6/E7, as the proliferation rate did not change even at high extract concentrations. The same results were found in normal epithelial cells (HNME-E6/E6 and MCF 10A), which confirms the selectivity of *EA* extract (150, 164). According to a comprehensive review of preclinical and clinical studies, consuming flavonoids decrease the risk of CRC incidence and recurrence (168). Flavonoids were found to be safe on normal human colon fibroblast cell line CCD-18Co and other different normal cell lines like prostate and vein endothelial cells (169,

170). Furthermore, *EA* extracts induced notable morphological alterations of both CRC cell lines by increasing the cell-cell adhesion and changing cells phenotypes into more cuboidal shape, suggesting that *EA* induces the inhibition of the EMT pathway. In normal cases, the EMT event plays a role in developing organisms and wound healing (171, 172). However, the EMT event contributes to many diseases like cancer and is associated with different hallmarks of cancer, such as tissue invasiveness and resistance to chemotherapies (173). Recently, it was found that there is a strong association between EMT and CRC metastasis and tumor invasiveness (174). Our study confirm the effect of *EA* extract on EMT in CRC by affecting its biomarkers such as E-cadherin, Vimentin, and  $\beta$ -catenin. Several studies have demonstrated that CRC is highly related to the loss of E-cadherin expression and associated with its invasiveness (175). According to a clinicopathologic study, Vimentin was identified in 17% of CRC cases; however, the expression was negative in normal samples. The same study found that Vimentin is significantly associated with a short survival rate, distant metastasis, and high tumor grade of CRC patients (176). By increasing the expression of E-cadherin and the junctions between cells, *EA* can be assumed to have potential role in inhibiting the motility of both CRC cell lines (HCT-116 and LoVo). This is illustrated by our findings; *EA*'s extract significantly inhibits the invasive ability of both CRC cell lines. Our present results are consistent with the effect of *EA* on oral cancer by inactivation of the Erk1/2 pathway and EMT inhibition (177). Furthermore, *EA* affect  $\beta$ -catenin expression by inhibiting the regulation of phosphorylated  $\beta$ -catenin in both CRC cell lines. Nucleic  $\beta$ -catenin is mutated in more than 85% of CRC tumors. Further, the accumulation of phosphorylated  $\beta$ -catenin is strongly associated with poor CRC prognosis (178). Flavonoids are reported to have an antitumor effect on CRC by modulating the Wnt/ $\beta$ -catenin pathway. It is promoted by the ligand-receptor



interaction of flavonoids with different parts of the Wnt/ $\beta$ -catenin cascade (128). Further, *EA* extract significantly blocked the colony formation of both CRC cell lines, supported by the significant suppression of AKT and EGFR activities. AKT is responsible for the malignancy of CRC by the activation of the upstream receptor EGFR (179). According to a clinical study, EGFR initiates CRC and plays an essential role in CRC progression; additionally, it is expressed in 90% of CRC tumors (180). As mentioned, flavonoids are suggested to be responsible for the anti-cancer effect of *EA*, an *in silico* study identified flavonoids as effective EGFR inhibitors as they exhibit drug-likeness properties with good docking scores (181). Further, flavonoids inhibit cancer proliferation by suppressing EGFR and AKT due to their pro-oxidant activity (128, 182).

After confirming the potential effect of *EA* extract against CRC *in vitro*, we explored its effect *in vivo* using *ras* mutant *Drosophila melanogaster* fly line expressing a constitutively active form of *Ras85D* under the control of the *sev* enhancer and promoter. Our choice of this model organism was tailored to several factors, one of which is its previously reported suitability for screening studies of anti-cancer agents, in addition to the several conserved physiological and biological pathways it possesses as compared with mammals (183). To confirm *ras* mutation in cancer mutant fly line (*Ras85D*) used, we scored for the expression of *ras* homolog to vertebrate in *Drosophila*, *ras1* (*Ras* oncogene at 85D). We further validated *ras* mutation in those flies by scoring for expression of AKT and ERK1/2, two important biomarkers in the RAS signaling pathway (Figure. 39). In a tumor setting in *Drosophila*, gain of function mutations in *ras* genes promotes the inhibition of the pro-apoptotic protein Head involution defective (*Hid*), a scenario that culminates in, with the appearance of essential cancer hallmarks like impaired autophagy and increased oxidative stress (184,

185). In another *Drosophila* tumor setting, the overexpression of AKT, caused by the inhibition of the *Hippo*, which is a tumor suppressor pathway in *D. melanogaster*, also leads to uncountable cellular division and apoptosis suppression (186). In alliance with this, our findings revealed a significant upregulation in ERK 1/2 and AKT protein levels in *Ras85D* fly line (Figure 39), presenting this line in specific and the fruit fly model system in general as a suitable model for our drug screening project against CRC.

Interestingly, and in concordance with the phenotype observed and reported in the *in vitro* system, *Ras85D* fly line orally treated with *EA* aqueous extract exhibits a significant increase in their life span as compared to their wild-type (*Yw*) control counterpart (Figure. 41) with an HR reported value less than one. This finding presents a potential protective effect of *EA* aqueous extract not only in a tumor setting (Figure 41), but also under normal condition (Figure. 40). Our suggested *EA* protective effect from our findings is congruent with an *in vivo* study that was conducted in rats and reported an increase in wound healing specific markers upon *EA* treatment (187). Along this as well, *EA* was shown to exhibit fast healing ability of colon ulcers (188). Interestingly, the methanolic fruit extract of *EA* was reported to promote a significant gastro-protective effect *in vivo* in an ethanol-induced ulcerogenesis rat model (189). A plausible explanation of this protective *EA* effect could relate to its rich flavonoids content. This anticipation aligns with a recent meta-analysis reporting that high flavonoids intake reduces CRC risk (99), along with other studies reporting an inverse association between flavonoids and different types of cancer, such as gastric and colorectal cancer (190).

#### 4.2 Effect of nitrogen-based chalcone analogs (DK13 and DK14) on CRC

Nitrogen-based chalcone analogs DK13 and DK14 that synthesized through Claisen-Schmidt condensation reaction proved to have a substantial effect on inhibiting cellular proliferation of CRC cell lines HCT-116 and LoVo. Both compounds inhibited cells proliferation of TNBC and HER2 positive cell lines (151, 160). These results support our findings here against CRC cell lines. However, DK14 is shown to be more effective than DK13 on both cell lines, which was explained by Elkhalfa et al. (2020) as DK14 has the methoxy substitution, which makes DK14 more potential than DK13 that, has a 4-methylsulfonyl substitution instead (151). A benzylidenetetralones cyclic chalcone analogs (Q705) had the same effect on HCT-116 as it significantly inhibits HCT-116 cell proliferation, which is comparable with the effect of DK14 on HCT-116 cells (116). In addition, novel polymethoxylated Chalcones showed a similar effect on HCT-116 and LoVo cell lines (191). Moreover, proliferation inhibition of CRC cells (HCT-116 and LoVo) by DK13 and DK14 is confirmed by investigating the effect of both compounds on cell cycle progression. The growth inhibition of HCT-116 and LoVo cells can be explained by G2/M accumulation caused by DK13 and DK14. A similar effect was observed of Q705 on the cell cycle distribution of HCT-116 cells (116). Further, C1 and C2 2'-hydroxyl chalcone derivatives showed the same effect on the cell cycle distribution of CRC cell lines by increasing the percentage cell counts of CRC cells in the G2/M phase compared to normal control (192). Nevertheless, the effect of DK13 and DK14 on cell cycle distribution of TNBC and HER-2 positive cancer was different as both compounds caused S phase blockade in both cancer types (151, 160). The effect of DK13 and DK14 on the cell cycle is related to their chemical structure. The nitrogen mustard group in both compounds acts as an alkylating agent that binds to the DNA and prevents the genetic replication materials (193).

Furthermore, DK13 and DK14 cause morphological changes in HCT-116 and LoVo cells by inducing morphological alternations related to EMT inhibition compared to the DMSO and 5-FU treated cells. DK13 and DK14 significantly increase the expression of E-cadherin protein in both CRC cell lines; the same effect was found in TNBC cells (151). According to a clinical study, E-cadherin is considered a robust biomarker in CRC prognosis and positively associated with CRC patients' survival (194). Vimentin is a mesenchymal marker highly expressed in invasive tumors and CRC cells with invasive potential (195). Clinically, Vimentin is negatively associated with CRC patients' survival (196). Thus, our chalcone compounds significantly decrease Vimentin protein expression compared to their controls. This indicates the potential of DK13 and DK14 as anti-cancer agents against metastatic CRC. Conversely, 5-FU, the first-line therapy for CRC, has no significant effect on Vimentin, and that's similar to the effect of 5-FU (10  $\mu$ M) on gastric cancer cells compared to control (197). Additionally, our results show that DK13 and DK14 could inhibit EMT through the downregulation of  $\beta$ -Catenin phosphorylation in both CRC cell lines as the Wnt/  $\beta$ -Catenin pathway is responsible for regulating the cell migration, invasion, and progression of CRC (198). On the other hand, 5-FU increases the expression of phosphorylated  $\beta$ -Catenin in HCT-116 cells. A study showed that the stemness of CRC by 5-FU is through WNT/ $\beta$ -catenin pathway activation (199). Effect of DK13 and DK14 on EMT biomarkers are supported by the effect of both compounds on CRC cells invasiveness compared to 5-FU. Similarly, KB-34 Chalcone (1,3-diphenyl-2-propen-1-one) derivative inhibited the invasion of CRC cell lines (HT-29 and SW620) (200). In addition, our chalcone compounds have a potential effect against colony formation of CRC cell lines. L2H17, a chalcone derivative, had a similar potential effect on colony formation against CRC *in vitro* and *in vivo* (201). Regarding the molecular pathways

responsible for the anti-cancer activity of DK13 and DK14 on CRC, we investigated the expression patterns of PI3K/AKT/mTOR signaling pathway components upon DK13 and DK14 treatment. PI3K protein is known to have an important role in cancer development, and PI3K/AKT/mTOR pathway activation is shown to be associated with different cellular functions in CRC such as cell survival, tumor progression, and drug resistance (202). Immunohistochemistry found that the biomarkers of PI3K/AKT/mTOR pathway, AKT and mTOR are significantly overexpressed in CRC (203). This correlates with our findings here as DK13 and DK14 significantly downregulate AKT and mTOR in both CRC cell lines.

Next, the effect of both chalcone compounds is tested *in vivo* using *Ras85D* mutant *Drosophila melanogaster* fly line. Previous studies assessing the toxicity of chalcone analogs (3'-hydroxychalcone (compound 1b)) on zebrafish embryos revealed a myotoxic effect of tested chalcones on zebrafish embryos development (204). Likewise, a similar toxicity study on R7, R13, and R15 synthesized chalcones in male Swiss albino mice, revealed a toxic effect of these chalcones denoted by reduction in body weight and oxidative stress-induced liver injuries (205). Captivatingly however, our generated chalcone compounds (DK13 and DK14) show no toxic effect on cancer mutant *D. melanogaster* flies (Figures. 42). Moreover, DK14 exhibits a significant protective effect on the wild-type fly line (*Yw*) and a plausible anti-cancerous effect in one of the *Ras85D* mutant fly line (Figure. 42 A and B) characterized by a significant increase in *ras1* gene expression (Figure 38), as well as an overexpression of ERK1/2 and Akt proteins compared to the *Yw* control group (Figure. 39). It is worth noting here that as compared to the traditionally adopted 5-FU clinical drug, DK13 and DK14 show better results on *Ras85D* mutant fly line, which appeared to be surprisingly toxic in flies, a pattern also reported in 5-FU treated CBA mice (206).

## CHAPTER 5: CONCLUSIONS AND FUTURE DIRECTIONS

CRC is exhibiting heavy burdens on health systems worldwide, with challenges pertinent to the impact of disease progression and treatment costs and side effects on CRC patients and their quality of life. Thus, novel, natural, and safe treatment regimens are required to overcome these challenges. Among various compounds, *EA* and chalcones are recently presented as promising flavonoid resources with potential and safe anti-cancerous effects. *EA* is a traditional plant that has been used by people as diet for centuries. Several studies have evidently shown that *EA* is not only safe to ingest but also plays effective roles as an anti-inflammatory and antimicrobial. Likewise, many *in vivo* and *in vitro* studies have proven the effectivity of nitrogen-based chalcone compounds against many types of cancer. In this study, we provide the first evidence for an effect of both *EA* aqueous extract and chalcone analogs (DK13 and DK14) on CRC *in vivo* and *in vitro*. We show that both *EA* and chalcone compounds effectively suppress the proliferation of CRC cell lines by disturbing cell cycle phases. In addition, we show that both *EA* and chalcone analogs significantly inhibit the invasiveness and tumorigenesis of both CRC cell lines. Moreover, we show that both *EA*, DK13, and DK14) deregulate the EMT progression by promoting an overexpression of E-cadherin and a suppression of Vimentin and  $\beta$ -catenin. Also, we shown an effect of *EA* on inhibiting AKT/EGFR signaling pathways, and effect of DK13 and DK14, on the other hand, in suppressing the AKT/mTOR signaling pathways.

Interestingly, our findings also revealed a promising protective and anti-cancerous effect of *EA* aqueous extract and the DK14 chalcone analog in the *in vivo Drosophila melanogaster* model system, as the lifespan of wild-type and *Ras85D* mutant fly lines increased significantly upon *EA* or DK14 oral treatment. The findings of this study serve as a solid foundation for future studies directed towards unravelling the

potentiality and mechanism of activity of natural resources in treating deadly diseases like CRC.

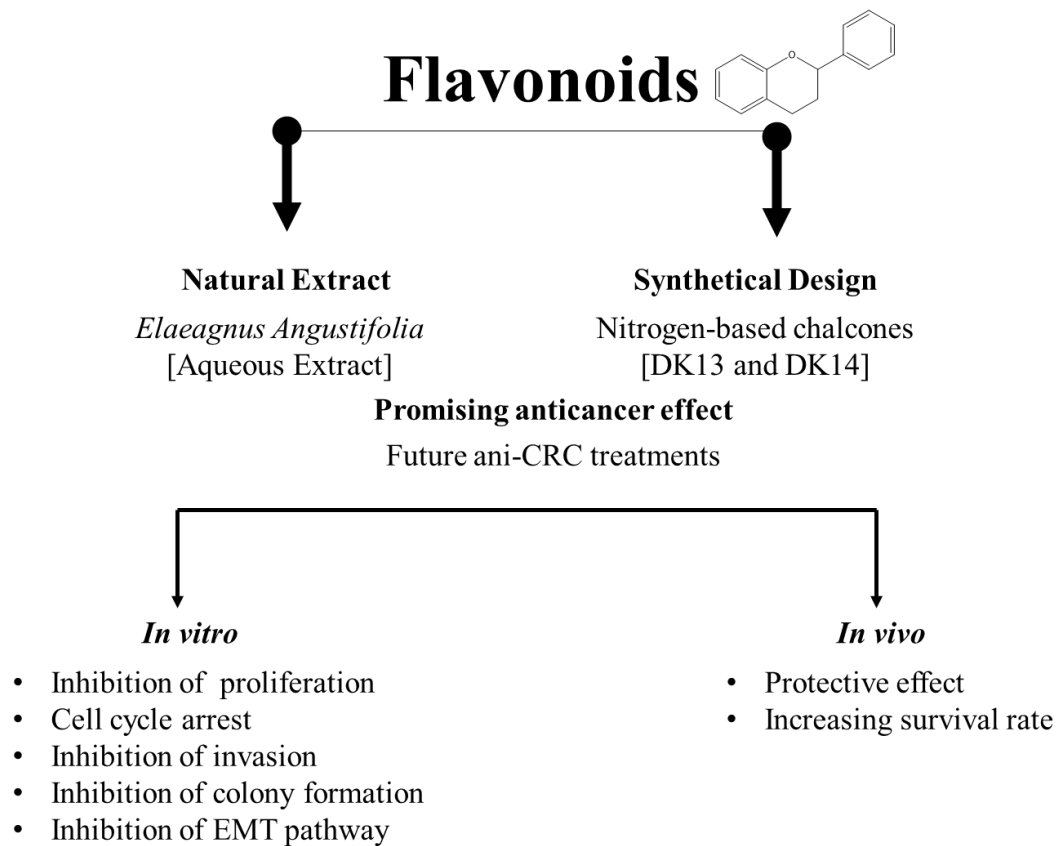


Figure 45: Summary of the main study findings

## 5.1 Limitations

Working with an extract derived from a whole medicinal plant is a challenge on its own. Plants extracts are made of millions chemical compounds, and therefore its therapeutic effect could relate to a sole as well as a to a mixture of these compounds. Further, the stability of the extract, specifically in polar solvents like water, is not easy to maintain. Determining the exact amount of the extract used in our experiments was also another limitation in this research. *EA* extracts were prepared in water, and to get rid of water eventually, high temperature was required, a parameter than could impact the chemical make-up of the extract. This necessitates a better method for water evaporation. Additionally, the use of *in vivo* models like the *D. melanogaster* fruit fly adopted for this study requires proper training and handling, as well as continuous monitoring and delicateness while working with the insect model.



## REFERENCES

1. Saini A, Kumar M, Bhatt S, Saini V, Malik A. CANCER CAUSES AND TREATMENTS. 2020.
2. Chaffer CL, Weinberg RA. A perspective on cancer cell metastasis. *Science*. 2011;331(6024):1559-64.
3. Kuipers EJ, Rosch T, Bretthauer M. Colorectal cancer screening--optimizing current strategies and new directions. *Nat Rev Clin Oncol*. 2013;10(3):130-42.
4. Sung H, Ferlay J, Siegel RL, Laversanne M, Soerjomataram I, Jemal A, et al. Global Cancer Statistics 2020: GLOBOCAN Estimates of Incidence and Mortality Worldwide for 36 Cancers in 185 Countries. *CA Cancer J Clin*. 2021;71(3):209-49.
5. Siegel RL, Miller KD, Fuchs HE, Jemal A. Cancer statistics, 2022. *CA Cancer J Clin*. 2022;72(1):7-33.
6. Xi Y, Xu P. Global colorectal cancer burden in 2020 and projections to 2040. *Translational Oncology*. 2021;14(10):101174.
7. Xie Y-H, Chen Y-X, Fang J-Y. Comprehensive review of targeted therapy for colorectal cancer. *Signal Transduction and Targeted Therapy*. 2020;5(1):22.
8. Granados-Romero J, Valderrama-Treviño A, Contreras Flores E, Barrera-Mera B, Herrera M, Uriarte-Ruiz K, et al. Colorectal cancer: a review. *International Journal of Research in Medical Sciences*. 2017;5:4667.
9. Siegel RL, Miller KD, Goding Sauer A, Fedewa SA, Butterly LF, Anderson JC, et al. Colorectal cancer statistics, 2020. *CA: A Cancer Journal for Clinicians*. 2020;70(3):145-64.
10. Sawicki T, Ruszkowska M, Danielewicz A, Niedzwiedzka E, Arlukowicz T, Przybylowicz KE. A Review of Colorectal Cancer in Terms of Epidemiology, Risk Factors, Development, Symptoms and Diagnosis. *Cancers (Basel)*. 2021;13(9).

11. Bray F, Ferlay J, Soerjomataram I, Siegel RL, Torre LA, Jemal A. Global cancer statistics 2018: GLOBOCAN estimates of incidence and mortality worldwide for 36 cancers in 185 countries. *CA: A Cancer Journal for Clinicians*. 2018;68(6):394-424.
12. Makhlouf NA, Abdel-Gawad M, Mahros AM, Lashen SA, Zaghoul M, Eliwa A, et al. Colorectal cancer in Arab world: A systematic review. *World J Gastrointest Oncol*. 2021;13(11):1791-8.
13. Al-Dahshan A, Chehab M, Bala M, Omer M, AlMohamed O, Al-Kubaisi N, et al. Colorectal cancer awareness and its predictors among adults aged 50-74 years attending primary healthcare in the State of Qatar: a cross-sectional study. *BMJ Open*. 2020;10(7):e035651.
14. Mueller M, Schneider MA, Deplazes B, Cabalzar-Wondberg D, Rickenbacher A, Turina M. Colorectal cancer of the young displays distinct features of aggressive tumor biology: A single-center cohort study. *World J Gastrointest Surg*. 2021;13(2):164-75.
15. Pucciarelli S, Agostini M, Viel A, Bertorelle R, Russo V, Toppan P, et al. Early-age-at-onset colorectal cancer and microsatellite instability as markers of hereditary nonpolyposis colorectal cancer. *Dis Colon Rectum*. 2003;46(3):305-12.
16. Arora R, Malhotra P, Sundriyal S, Yashavanth HS, Pai RJ, Baliga MS. Chapter 19 - Medicinal Plants as Remedies for Gastrointestinal Ailments and Diseases: A Review. In: Watson RR, Preedy VR, editors. *Bioactive Food as Dietary Interventions for Liver and Gastrointestinal Disease*. San Diego: Academic Press; 2013. p. 301-11.
17. Abbott AM, Armstrong L, Jensen EH. Chapter 68 - Small Intestine. In: Yeo CJ, editor. *Shackelford's Surgery of the Alimentary Tract (Seventh Edition)*. Philadelphia: W.B. Saunders; 2013. p. 839-63.
18. Dennis R, Kirberger RM, Barr F, Wrigley RH. Chapter 10 - Gastrointestinal

tract. In: Dennis R, Kirberger RM, Barr F, Wrigley RH, editors. Handbook of Small Animal Radiology and Ultrasound (Second Edition). Edinburgh: W.B. Saunders; 2010. p. 267-95.

19. Rakestraw PC, Hardy J. Chapter 37 - Large Intestine. In: Auer JA, Stick JA, editors. Equine Surgery (Fourth Edition). Saint Louis: W.B. Saunders; 2012. p. 454-94.

20. Azzouz L, Sharma s. Physiology, Large Intestine. 2018.

21. Ponz de Leon M, Percesepe A. Pathogenesis of colorectal cancer. Digestive and Liver Disease. 2000;32(9):807-21.

22. Stracci F, Zorzi M, Grazzini G. Colorectal cancer screening: tests, strategies, and perspectives. Front Public Health [Internet]. 2014 2014; 2:[210 p.]. Available from: <http://europepmc.org/abstract/MED/25386553>.

23. Munteanu I, Mastalier B. Genetics of colorectal cancer. J Med Life. 2014;7(4):507-11.

24. Nagtegaal ID, Odze RD, Klimstra D, Paradis V, Rugge M, Schirmacher P, et al. The 2019 WHO classification of tumours of the digestive system. Histopathology. 2020;76(2):182-8.

25. Sarna S. Colonic Motility: From Bench Side to Bedside. Colloquium Series on Integrated Systems Physiology: From Molecule to Function. 2010;2:1-157.

26. Luo C, Cen S, Ding G, Wu W. Mucinous colorectal adenocarcinoma: clinical pathology and treatment options. Cancer Commun (Lond). 2019;39(1):13.

27. Li Z-H, You D-Y, Gao D-P, Yang G-J, Dong X-X, Zhang D-F, et al. Role of CT scan in differentiating the type of colorectal cancer. Onco Targets Ther [Internet]. 2017 2017; 10:[2297-303 pp.]. Available from: <http://europepmc.org/abstract/MED/28490887>.

28. Numata M, Shiozawa M, Watanabe T, Tamagawa H, Yamamoto N, Morinaga

- S, et al. The clinicopathological features of colorectal mucinous adenocarcinoma and a therapeutic strategy for the disease. *World Journal of Surgical Oncology*. 2012;10(1):109.
29. Yoshida T, Kamimura K, Hosaka K, Doumori K, Oka H, Sato A, et al. Colorectal neuroendocrine carcinoma: A case report and review of the literature. *World J Clin Cases*. 2019;7(14):1865-75.
30. Li C, Zheng H, Jia H, Huang D, Gu W, Cai S, et al. Prognosis of three histological subtypes of colorectal adenocarcinoma: A retrospective analysis of 8005 Chinese patients. *Cancer Med*. 2019;8(7):3411-9.
31. Dekker E, Tanis PJ, Vleugels JLA, Kasi PM, Wallace MB. Colorectal cancer. *The Lancet*. 2019;394(10207):1467-80.
32. Islami F, Goding Sauer A, Miller KD, Siegel RL, Fedewa SA, Jacobs EJ, et al. Proportion and number of cancer cases and deaths attributable to potentially modifiable risk factors in the United States. *CA Cancer J Clin*. 2018;68(1):31-54.
33. Qin Y, Roberts JD, Grimm SA, Lih FB, Deterding LJ, Li R, et al. An obesity-associated gut microbiome reprograms the intestinal epigenome and leads to altered colonic gene expression. *Genome Biology*. 2018;19(1):7.
34. O'Keefe SJD, Li JV, Lahti L, Ou J, Carbonero F, Mohammed K, et al. Fat, fibre and cancer risk in African Americans and rural Africans. *Nature Communications*. 2015;6(1):6342.
35. Queipo-Ortuño MI, Seoane LM, Murri M, Pardo M, Gomez-Zumaquero JM, Cardona F, et al. Gut Microbiota Composition in Male Rat Models under Different Nutritional Status and Physical Activity and Its Association with Serum Leptin and Ghrelin Levels. *PLOS ONE*. 2013;8(5):e65465.
36. Matsumoto M, Inoue R, Tsukahara T, Ushida K, Chiji H, Matsubara N, et al.

Voluntary Running Exercise Alters Microbiota Composition and Increases n-Butyrate Concentration in the Rat Cecum. *Bioscience, Biotechnology, and Biochemistry*. 2008;72(2):572-6.

37. Cai S, Li Y, Ding Y, Chen K, Jin M. Alcohol drinking and the risk of colorectal cancer death: a meta-analysis. *European Journal of Cancer Prevention*. 2014;23(6).

38. Otani T, Iwasaki M, Yamamoto S, Sobue T, Hanaoka T, Inoue M, et al. Alcohol Consumption, Smoking, and Subsequent Risk of Colorectal Cancer in Middle-Aged and Elderly Japanese Men and Women: Japan Public Health Center-based Prospective Study. *Cancer Epidemiology, Biomarkers & Prevention*. 2003;12(12):1492-500.

39. Botteri E, Iodice S, Bagnardi V, Raimondi S, Lowenfels A, Maisonneuve P. Smoking and Colorectal Cancer: A Meta-analysis. *JAMA : the journal of the American Medical Association*. 2009;300:2765-78.

40. Amitay EL, Carr PR, Jansen L, Roth W, Alwers E, Herpel E, et al. Smoking, alcohol consumption and colorectal cancer risk by molecular pathological subtypes and pathways. *British Journal of Cancer*. 2020;122(11):1604-10.

41. Phipps AI, Passarelli MN, Chan AT, Harrison TA, Jeon J, Hutter CM, et al. Common genetic variation and survival after colorectal cancer diagnosis: a genome-wide analysis. *Carcinogenesis*. 2016;37(1):87-95.

42. Blank A, Roberts DE, Dawson H, Zlobec I, Lugli A. Tumor Heterogeneity in Primary Colorectal Cancer and Corresponding Metastases. Does the Apple Fall Far From the Tree? *Frontiers in Medicine*. 2018;5.

43. Shan K, Lu H, Zhang Z, Xie J, Xu L, Wang W, et al. Impact of second forward-view examination on adenoma detection rate during unsedated colonoscopy: a randomized controlled trial. *BMC Gastroenterol*. 2021;21(1):213.

44. Hamada F. [Wnt signaling and cancer]. *Kaibogaku Zasshi*. 2009;84(4):111-2.

45. Foulkes WD. A tale of four syndromes: familial adenomatous polyposis, Gardner syndrome, attenuated APC and Turcot syndrome. *QJM*. 1995;88(12):853-63.
46. Grady WM, Markowitz SD. The molecular pathogenesis of colorectal cancer and its potential application to colorectal cancer screening. *Dig Dis Sci*. 2015;60(3):762-72.
47. Hagland HR, Berg M, Jolma IW, Carlsen A, Søreide K. Molecular Pathways and Cellular Metabolism in Colorectal Cancer. *Digestive Surgery*. 2013;30(1):12-25.
48. Loeb LA, Loeb KR, Anderson JP. Multiple mutations and cancer. *Proceedings of the National Academy of Sciences*. 2003;100(3):776.
49. Saeed O, Lopez-Beltran A, Fisher KW, Scarpelli M, Montironi R, Cimadamore A, et al. RAS genes in colorectal carcinoma: pathogenesis, testing guidelines and treatment implications. *J Clin Pathol*. 2019;72(2):135-9.
50. Albather NK, Saeed WSB, Alsayegh YH, Aldafiri AS, Alkhudhairy MW. Relationship between Headache and Myofascial Pain: Systematic Review. *Journal of Pharmaceutical Research International*. 2021:37-52.
51. Walther A, Houlston R, Tomlinson I. Association between chromosomal instability and prognosis in colorectal cancer: a meta-analysis. *Gut*. 2008;57(7):941.
52. Pouligiannis G, Frayling I, Arends M. DNA mismatch repair deficiency in sporadic colorectal cancer and Lynch Syndrome. *Histopathology*. 2010;56:167-79.
53. Guastadisegni C, Colafranceschi M, Ottini L, Dogliotti E. Microsatellite instability as a marker of prognosis and response to therapy: A meta-analysis of colorectal cancer survival data. *European Journal of Cancer*. 2010;46(15):2788-98.
54. Boland CR, Goel A. Microsatellite Instability in Colorectal Cancer. *Gastroenterology*. 2010;138(6):2073-87.e3.
55. Sleutels F, Barlow D. The origins of genomic imprinting in mammals.

- Advances in genetics. 2002;46:119-63.
56. Røyrvik EC, Ahlquist T, Rognes T, Lothe RA. Slip slidin' away: a duodecennial review of targeted genes in mismatch repair deficient colorectal cancer. *Crit Rev Oncog.* 2007;13(3):229-57.
  57. Kim YS, Deng G. Epigenetic changes (aberrant DNA methylation) in colorectal neoplasia. *Gut Liver.* 2007;1(1):1-11.
  58. Deschoolmeester V, Baay M, Specenier P, Lardon F, Vermorken JB. A review of the most promising biomarkers in colorectal cancer: one step closer to targeted therapy. *Oncologist.* 2010;15(7):699-731.
  59. Du H, Che G. Genetic alterations and epigenetic alterations of cancer-associated fibroblasts (Review). *Oncol Lett.* 2017;13(1):3-12.
  60. Mulyawan I. Role of Ki67 protein in colorectal cancer. *International Journal of Research in Medical Sciences.* 2019;7:647.
  61. Mayer A, Takimoto M, Fritz E, Schellander G, Kofler K, Ludwig H. The prognostic significance of proliferating cell nuclear antigen, epidermal growth factor receptor, and mdr gene expression in colorectal cancer. *Cancer.* 1993;71(8):2454-60.
  62. Liu G, Zhang Y, Huang Y, Yuan X, Cao Z, Zhao Z. PTPN6-EGFR Protein Complex: A Novel Target for Colon Cancer Metastasis. *Journal of Oncology.* 2022;2022:7391069.
  63. An Z, Aksoy O, Zheng T, Fan QW, Weiss WA. Epidermal growth factor receptor and EGFRvIII in glioblastoma: signaling pathways and targeted therapies. *Oncogene.* 2018;37(12):1561-75.
  64. Bolocan A, Ion D, Ciocan D, Paduraru D. Prognostic and Predictive Factors in Colorectal Cancer. *Chirurgia (Bucharest, Romania : 1990).* 2011;107:555-63.
  65. Lech G, Slotwinski R, Slodkowski M, Krasnodebski IW. Colorectal cancer

tumour markers and biomarkers: Recent therapeutic advances. *World J Gastroenterol*. 2016;22(5):1745-55.

66. Russo A, Bazan V, Iacopetta B, Kerr D, Soussi T, Gebbia N. The TP53 Colorectal Cancer International Collaborative Study on the Prognostic and Predictive Significance of p53 Mutation: Influence of Tumor Site, Type of Mutation, and Adjuvant Treatment. *Journal of Clinical Oncology*. 2005;23(30):7518-28.

67. Jauhri M, Bhatnagar A, Gupta S, Bp M, Kumar S, Shokeen Y, et al. Prevalence and coexistence of KRAS, BRAF, PIK3CA, NRAS, TP53, and APC mutations in Indian colorectal cancer patients: Next-generation sequencing-based cohort study. *Tumor Biology*. 2017;39:101042831769226.

68. Zinatizadeh MR, Momeni SA, Zarandi PK, Chalbatani GM, Dana H, Mirzaei HR, et al. The Role and Function of Ras-association domain family in Cancer: A Review. *Genes & Diseases*. 2019;6(4):378-84.

69. Saeed O, Lopez-Beltran A, Fisher KW, Scarpelli M, Montironi R, Cimadamore A, et al. RAS genes in colorectal carcinoma: pathogenesis, testing guidelines and treatment implications. *J Clin Pathol*. 2019;72(2):135-9.

70. Fitzpatrick-Lewis D, Ali MU, Warren R, Kenny M, Sherifali D, Raina P. Screening for Colorectal Cancer: A Systematic Review and Meta-Analysis. *Clinical Colorectal Cancer*. 2016;15(4):298-313.

71. Young PE, Womeldorph CM. Colonoscopy for colorectal cancer screening. *J Cancer*. 2013;4(3):217-26.

72. Hale MF, Sidhu R, McAlindon ME. Capsule endoscopy: current practice and future directions. *World J Gastroenterol*. 2014;20(24):7752-9.

73. Vuik FER, Nieuwenburg SAV, Moen S, Spada C, Senore C, Hassan C, et al. Colon capsule endoscopy in colorectal cancer screening: a systematic review.



Endoscopy. 2021;53(08):815-24.

74. Issa IA, Nouredine M. Colorectal cancer screening: An updated review of the available options. *World J Gastroenterol.* 2017;23(28):5086-96.

75. Hewitson P, Glasziou P, Watson E, Towler B, Irwig L. Cochrane Systematic Review of Colorectal Cancer Screening Using the Fecal Occult Blood Test (Hemoccult): An Update. *Official journal of the American College of Gastroenterology | ACG.* 2008;103(6).

76. Ogunwobi OO, Mahmood F, Akingboye A. Biomarkers in Colorectal Cancer: Current Research and Future Prospects. *Int J Mol Sci.* 2020;21(15).

77. Chen K, Collins G, Wang H, Toh JWT. Pathological Features and Prognostication in Colorectal Cancer. *Curr Oncol.* 2021;28(6):5356-83.

78. Wolpin BM, Mayer RJ. Systemic treatment of colorectal cancer. *Gastroenterology.* 2008;134(5):1296-310.

79. Agrawal D. DIAGNOSIS AND TREATMENT OF COLORECTAL CANCER: A REVIEW. *Journal of Drug Delivery and Therapeutics.* 2012;2.

80. Denlinger CS, Barsevick AM. The challenges of colorectal cancer survivorship. *J Natl Compr Canc Netw.* 2009;7(8):883-94.

81. Van der Jeught K, Xu H-C, Li Y-J, Lu X-B, Ji G. Drug resistance and new therapies in colorectal cancer. *World Journal of Gastroenterology.* 2018;24:3834-48.

82. Holaday J, Berkowitz B. Antiangiogenic Drugs: Insights into Drug Development from Endostatin, Avastin and Thalidomide. *Molecular interventions.* 2009;9:157-66.

83. Moeini R, Mozaffarpur SA, Mojahedi M, Nasrolahpour Shirvani SD, Gorji N, Saghebi R, et al. The prevalence of complementary and alternative medicine use in the general population of Babol, North of Iran, 2018. *BMC Complement Med Ther.*

2021;21(1):113.

84. Azaizeh H, Saad B, Cooper E, Said O. Traditional Arabic and Islamic Medicine, a Re-emerging Health Aid. *Evid Based Complement Alternat Med.* 2010;7(4):419-24.

85. Fjaer EL, Landet ER, McNamara CL, Eikemo TA. The use of complementary and alternative medicine (CAM) in Europe. *BMC Complement Med Ther.* 2020;20(1):108.

86. Greenwell M, Rahman PKSM. Medicinal Plants: Their Use in Anticancer Treatment. *Int J Pharm Sci Res.* 2015;6(10):4103-12.

87. Desai AG, Qazi GN, Ganju RK, El-Tamer M, Singh J, Saxena AK, et al. Medicinal plants and cancer chemoprevention. *Curr Drug Metab.* 2008;9(7):581-91.

88. Al-Menhali A, Jameela S, Latiff A, Elrayess M, Alsayrafi M, Jaganjac M. Cistanche tubulosa induces reactive oxygen species-mediated apoptosis of primary and metastatic human colon cancer cells. *Journal of Applied Pharmaceutical Science.* 2017;7:39-45.

89. Benarba B, Pandiella A. Colorectal cancer and medicinal plants: Principle findings from recent studies. *Biomed Pharmacother.* 2018;107:408-23.

90. Aiello P, Sharghi M, Mansourkhani SM, Ardekan AP, Jouybari L, Daraei N, et al. Medicinal Plants in the Prevention and Treatment of Colon Cancer. *Oxid Med Cell Longev.* 2019;2019:2075614.

91. Babu PVA, Liu D. Chapter 18 - Flavonoids and Cardiovascular Health. In: Watson RR, editor. *Complementary and Alternative Therapies and the Aging Population.* San Diego: Academic Press; 2009. p. 371-92.

92. Dias MC, Pinto D, Silva AMS. Plant Flavonoids: Chemical Characteristics and Biological Activity. *Molecules.* 2021;26(17).

93. Nabavi SM, Šamec D, Tomczyk M, Milella L, Russo D, Habtemariam S, et al.

Flavonoid biosynthetic pathways in plants: Versatile targets for metabolic engineering. *Biotechnol Adv.* 2020;38:107316.

94. Hollman PCH, Katan MB. Dietary Flavonoids: Intake, Health Effects and Bioavailability. *Food and Chemical Toxicology.* 1999;37(9):937-42.

95. Mullie P, Clarys P, Deriemaeker P, Hebbelinck M. Estimation of daily human intake of food flavonoids. *Plant Foods Hum Nutr.* 2007;62(3):93-8.

96. Ballard CR, Maróstica MR. Chapter 10 - Health Benefits of Flavonoids. In: Campos MRS, editor. *Bioactive Compounds: Woodhead Publishing; 2019.* p. 185-201.

97. Landazuri P, Restrepo B, Loango N. Phytotherapy for colorectal cancer: about some phytochemicals and their mechanisms of action]. *Medicinal Plant Communications.* 2020;3:79-84.

98. Gürler SB, Kiraz Y, Baran Y. Chapter 21 - Flavonoids in cancer therapy: current and future trends. In: Ozturk M, Egamberdieva D, Pešić M, editors. *Biodiversity and Biomedicine: Academic Press; 2020.* p. 403-40.

99. Chang H, Lei L, Zhou Y, Ye F, Zhao G. Dietary Flavonoids and the Risk of Colorectal Cancer: An Updated Meta-Analysis of Epidemiological Studies. *Nutrients.* 2018;10(7).

100. Li Y, Zhang T, Chen GY. Flavonoids and Colorectal Cancer Prevention. *Antioxidants (Basel).* 2018;7(12).

101. Farzaei MH, Bahramsoltani R, Abbasabadi Z, Rahimi R. A comprehensive review on phytochemical and pharmacological aspects of *Elaeagnus angustifolia* L. *J Pharm Pharmacol.* 2015;67(11):1467-80.

102. Nazir N, Zahoor M, Nisar M. A Review on Traditional Uses and Pharmacological Importance of Genus *Elaeagnus* Species. *The Botanical Review.* 2020;86(3-4):247-80.

103. Sabouri S, Rad HA, Peighambaroust HS, Fathipour BR, Feshangchi J, Ansari F, et al. The Oleaster (*Elaeagnus angustifolia*): A Comprehensive Review on Its Composition, Ethnobotanical and Prebiotic Values. *Current Pharmaceutical Biotechnology*. 2021;22(3):367-79.
104. Khan SU, Khan AU, Shah AU, Shah SM, Hussain S, Ayaz M, et al. Heavy metals content, phytochemical composition, antimicrobial and insecticidal evaluation of *Elaeagnus angustifolia*. *Toxicol Ind Health*. 2016;32(1):154-61.
105. Saboonchian F, Jamei R, Hosseini Sarghein S. Phenolic and flavonoid content of *Elaeagnus angustifolia* L. (leaf and flower). *Avicenna J Phytomed*. 2014;4(4):231-8.
106. Jawad D, Aljamali N, abd-alameer al Zubaidi T, Obaid N, Salih M, Aljamali N, et al. Review on Chalcone (Preparation ,Reactions, Medical and Bio Applications). 2019;5:16-27.
107. Rammohan A, Reddy JS, Sravya G, Rao CN, Zyryanov GV. Chalcone synthesis, properties and medicinal applications: a review. *Environmental Chemistry Letters*. 2020;18(2):433-58.
108. Ye H, Wan L, Han X, Wang G, hu J, Tang M, et al. Millepachine (MIL), a novel chalcone, induces G2/M arrest by inhibiting CDK1 activity and causing apoptosis via ROS-mitochondrial apoptotic pathway in human hepatocarcinoma cells in vitro and in vivo. *Carcinogenesis*. 2013;34.
109. Koosha S, Alshawsh MA, Looi CY, Seyedan A, Mohamed Z. An Association Map on the Effect of Flavonoids on the Signaling Pathways in Colorectal Cancer. *Int J Med Sci*. 2016;13(5):374-85.
110. Kim WK, Bang MH, Kim ES, Kang NE, Jung KC, Cho HJ, et al. Quercetin decreases the expression of ErbB2 and ErbB3 proteins in HT-29 human colon cancer cells. *The Journal of Nutritional Biochemistry*. 2005;16(3):155-62.

111. Lim DY, Park JHY. Induction of p53 contributes to apoptosis of HCT-116 human colon cancer cells induced by the dietary compound fisetin. *American Journal of Physiology-Gastrointestinal and Liver Physiology*. 2009;296(5):G1060-G8.
112. Leonardi T, Vanamala J, Taddeo SS, Davidson LA, Murphy ME, Patil BS, et al. Apigenin and naringenin suppress colon carcinogenesis through the aberrant crypt stage in azoxymethane-treated rats. *Exp Biol Med (Maywood)*. 2010;235(6):710-7.
113. Totta P, Acconcia F, Leone S, Cardillo I, Marino M. Mechanisms of naringenin-induced apoptotic cascade in cancer cells: involvement of estrogen receptor alpha and beta signalling. *IUBMB Life*. 2004;56(8):491-9.
114. Agarwal C, Singh RP, Dhanalakshmi S, Tyagi AK, Tecklenburg M, Sclafani RA, et al. Silibinin upregulates the expression of cyclin-dependent kinase inhibitors and causes cell cycle arrest and apoptosis in human colon carcinoma HT-29 cells. *Oncogene*. 2003;22(51):8271-82.
115. Wang W, Heideman L, Chung CS, Pelling JC, Koehler KJ, Birt DF. Cell-cycle arrest at G2/M and growth inhibition by apigenin in human colon carcinoma cell lines. *Mol Carcinog*. 2000;28(2):102-10.
116. Drutovic D, Chripkova M, Pilatova M, Kruzliak P, Perjesi P, Sarissky M, et al. Benzylidenetetralones, cyclic chalcone analogues, induce cell cycle arrest and apoptosis in HCT116 colorectal cancer cells. *Tumour Biol*. 2014;35(10):9967-75.
117. Mahmoud A, Elkhalfa D, Alali F, Al Moustafa A-E, Khalil A. Novel Polymethoxylated Chalcones as Potential Compounds Against KRAS-Mutant Colorectal Cancers. *Current Pharmaceutical Design*. 2020;26(14):1622-33.
118. Ocasio-Malave C, Donate MJ, Sanchez MM, Sosa-Rivera JM, Mooney JW, Pereles-De Leon TA, et al. Synthesis of novel 4-Boc-piperidone chalcones and evaluation of their cytotoxic activity against highly-metastatic cancer cells. *Bioorg Med*

Chem Lett. 2020;30(1):126760.

119. Colozza G, Koo B-K. Wnt/ $\beta$ -catenin signaling: Structure, assembly and endocytosis of the signalosome. *Development, Growth & Differentiation*. 2021;63(3):199-218.

120. Ghosh N, Chatterjee S, Sil PC. Wnt Signaling. In: Offermanns S, Rosenthal W, editors. *Encyclopedia of Molecular Pharmacology*. Cham: Springer International Publishing; 2020. p. 1-13.

121. Bugter JM, Fenderico N, Maurice MM. Mutations and mechanisms of WNT pathway tumour suppressors in cancer. *Nature Reviews Cancer*. 2021;21(1):5-21.

122. Komiya Y, Habas R. Wnt signal transduction pathways. *Organogenesis*. 2008;4(2):68-75.

123. Valkenburg KC, Graveel CR, Zylstra-Diegel CR, Zhong Z, Williams BO. Wnt/ $\beta$ -catenin Signaling in Normal and Cancer Stem Cells. *Cancers (Basel)*. 2011;3(2).

124. MacDonald BT, Tamai K, He X. Wnt/beta-catenin signaling: components, mechanisms, and diseases. *Dev Cell*. 2009;17(1):9-26.

125. Zhu W, Wang H, Zhu D. Wnt/ $\beta$ -catenin signaling pathway in lung cancer. *Medicine in Drug Discovery*. 2022;13:100113.

126. Dong S, Liang S, Cheng Z, Zhang X, Luo L, Li L, et al. ROS/PI3K/Akt and Wnt/beta-catenin signalings activate HIF-1alpha-induced metabolic reprogramming to impart 5-fluorouracil resistance in colorectal cancer. *J Exp Clin Cancer Res*. 2022;41(1):15.

127. Emons G, Spitzner M, Reineke S, Moller J, Auslander N, Kramer F, et al. Chemoradiotherapy Resistance in Colorectal Cancer Cells is Mediated by Wnt/beta-catenin Signaling. *Mol Cancer Res*. 2017;15(11):1481-90.

128. Amado NG, Predes D, Moreno MM, Carvalho IO, Mendes FA, Abreu JG.

Flavonoids and Wnt/beta-catenin signaling: potential role in colorectal cancer therapies. *Int J Mol Sci.* 2014;15(7):12094-106.

129. Previs RA, Mills GB, Westin SN. Chapter 34 - Novel Therapeutic Approaches and Targets for Ovarian Cancer. In: Leung PCK, Adashi EY, editors. *The Ovary (Third Edition)*: Academic Press; 2019. p. 547-74.

130. Fattahi S, Amjadi-Moheb F, Tabaripour R, Ashrafi GH, Akhavan-Niaki H. PI3K/AKT/mTOR signaling in gastric cancer: Epigenetics and beyond. *Life Sci.* 2020;262:118513.

131. Kotelevets L, Scott MGH, Chastre E. Targeting PTEN in Colorectal Cancers. In: Jordan P, editor. *Targeted Therapy of Colorectal Cancer Subtypes*. Cham: Springer International Publishing; 2018. p. 55-73.

132. Stefani C, Miricescu D, Stanescu S, II, Nica RI, Greabu M, Totan AR, et al. Growth Factors, PI3K/AKT/mTOR and MAPK Signaling Pathways in Colorectal Cancer Pathogenesis: Where Are We Now? *Int J Mol Sci.* 2021;22(19).

133. Tsubaki M, Takeda T, Noguchi M, Jinushi M, Seki S, Morii Y, et al. Overactivation of Akt Contributes to MEK Inhibitor Primary and Acquired Resistance in Colorectal Cancer Cells. *Cancers (Basel).* 2019;11(12).

134. Hua H, Kong Q, Zhang H, Wang J, Luo T, Jiang Y. Targeting mTOR for cancer therapy. *J Hematol Oncol.* 2019;12(1):71.

135. ul Islam B, Suhail M, Khan SM, Ahmad A, Zughairi AT, Husain MF, et al. Flavonoids and PI3K/Akt/mTOR Signaling Cascade: A Potential Crosstalk in Anticancer Treatment. *Current Medicinal Chemistry.* 2021;28(39):8083-97.

136. 10 - EFFECT OF PLASTICIZERS ON PROPERTIES OF PLASTICIZED MATERIALS. In: Wypych G, editor. *Handbook of Plasticizers (Second Edition)*. Boston: William Andrew Publishing; 2012. p. 209-306.

137. Kalluri R, Weinberg RA. The basics of epithelial-mesenchymal transition. *J Clin Invest.* 2009;119(6):1420-8.
138. Kim DH, Xing T, Yang Z, Dudek R, Lu Q, Chen YH. Epithelial Mesenchymal Transition in Embryonic Development, Tissue Repair and Cancer: A Comprehensive Overview. *J Clin Med.* 2017;7(1).
139. Gonzalez DM, Medici D. Signaling mechanisms of the epithelial-mesenchymal transition. *Sci Signal.* 2014;7(344):re8.
140. Niknami Z, Muhammadnejad A, Ebrahimi A, Harsani Z, Shirkoohi R. Significance of E-cadherin and Vimentin as epithelial-mesenchymal transition markers in colorectal carcinoma prognosis. *EXCLI J.* 2020;19:917-26.
141. Ribatti D, Tamma R, Annese T. Epithelial-Mesenchymal Transition in Cancer: A Historical Overview. *Transl Oncol.* 2020;13(6):100773.
142. Cao H, Xu E, Liu H, Wan L, Lai M. Epithelial-mesenchymal transition in colorectal cancer metastasis: A system review. *Pathol Res Pract.* 2015;211(8):557-69.
143. Lotha R, Sivasubramanian A. FLAVONOIDS NUTRACEUTICALS IN PREVENTION AND TREATMENT OF CANCER: A REVIEW. *Asian Journal of Pharmaceutical and Clinical Research.* 2018;11:42.
144. Jennings BH. *Drosophila* – a versatile model in biology & medicine. *Materials Today.* 2011;14(5):190-5.
145. Potter CJ, Turenchalk GS, Xu T. *Drosophila* in cancer research: an expanding role. *Trends in Genetics.* 2000;16(1):33-9.
146. Duffy JB. GAL4 system in *Drosophila*: a fly geneticist's Swiss army knife. *Genesis.* 2002;34(1-2):1-15.
147. Hales K, Korey C, Larracuente A, Roberts D. Genetics on the Fly: A Primer on the *Drosophila* Model System. *Genetics.* 2015;201:815-42.



148. Sadaqat Z, Kaushik S, Kain P. Gut Feeding the Brain: *Drosophila* Gut an Animal Model for Medicine to Understand Mechanisms Mediating Food Preferences. 2021.
149. Wang C, Zhao R, Huang P, Yang F, Quan Z, Xu N, et al. APC loss-induced intestinal tumorigenesis in *Drosophila*: Roles of Ras in Wnt signaling activation and tumor progression. *Developmental Biology*. 2013;378(2):122-40.
150. Jabeen A, Sharma A, Gupta I, Kheraldine H, Vranic S, Al Moustafa AE, et al. *Elaeagnus angustifolia* Plant Extract Inhibits Epithelial-Mesenchymal Transition and Induces Apoptosis via HER2 Inactivation and JNK Pathway in HER2-Positive Breast Cancer Cells. *Molecules*. 2020;25(18).
151. Elkhalfa D, Siddique AB, Qusa M, Cyprian FS, El Sayed K, Alali F, et al. Design, synthesis, and validation of novel nitrogen-based chalcone analogs against triple negative breast cancer. *Eur J Med Chem*. 2020;187:111954.
152. Ricciardi R, Ghabreau L, Yasmeeen A, Darnel AD, Akil N, Al Moustafa AE. Role of E6/E7 onco-proteins of high-risk human papillomaviruses in human colorectal carcinogenesis. *Cell Cycle*. 2009;8(12):1964-5.
153. Rampersad SN. Multiple applications of Alamar Blue as an indicator of metabolic function and cellular health in cell viability bioassays. *Sensors (Basel)*. 2012;12(9):12347-60.
154. Kench T, Vilar R. Chapter Fourteen - Metal complexes as G-quadruplex binders. In: Neidle S, editor. *Annual Reports in Medicinal Chemistry*. 54: Academic Press; 2020. p. 485-515.
155. Vermeulen K, Van Bockstaele DR, Berneman ZN. The cell cycle: a review of regulation, deregulation and therapeutic targets in cancer. *Cell Prolif*. 2003;36(3):131-49.

156. Pozarowski P, Darzynkiewicz Z. Analysis of Cell Cycle by Flow Cytometry. In: Schönthal AH, editor. Checkpoint Controls and Cancer: Volume 2: Activation and Regulation Protocols. Totowa, NJ: Humana Press; 2004. p. 301-11.
157. Purushothaman P, Chandra Verma S. Chapter 7 - Human DNA Tumor Viruses and Oncogenesis. In: Verma AS, Singh A, editors. Animal Biotechnology. San Diego: Academic Press; 2014. p. 121-37.
158. Bao X, Fukuda M. Chapter Twenty-Two - A Tumor Suppressor Function of Laminin-Binding  $\alpha$ -Dystroglycan. In: Fukuda M, editor. Methods in Enzymology. 479: Academic Press; 2010. p. 387-96.
159. Mahmood T, Yang PC. Western blot: technique, theory, and trouble shooting. N Am J Med Sci. 2012;4(9):429-34.
160. Rizeq B, Gupta I, Kheraldine H, Elkhalfa D, Al-Farsi HF, Moustafa AA, et al. Novel Nitrogen-Based Chalcone Analogs Provoke Substantial Apoptosis in HER2-Positive Human Breast Cancer Cells via JNK and ERK1/ERK2 Signaling Pathways. Int J Mol Sci. 2021;22(17).
161. Wang Y, Liu X, Liu J, Zhang T. Knockdown of REG Ialpha Enhances the Sensitivity to 5-Fluorouracil of Colorectal Cancer Cells via Cyclin D1/CDK4 Pathway and BAX/BCL-2 Pathways. Cancer Biother Radiopharm. 2019;34(6):362-70.
162. Zenonos K, Kyprianou K. RAS signaling pathways, mutations and their role in colorectal cancer. World J Gastrointest Oncol. 2013;5(5):97-101.
163. Van der Jeught K, Xu HC, Li YJ, Lu XB, Ji G. Drug resistance and new therapies in colorectal cancer. World J Gastroenterol. 2018;24(34):3834-48.
164. Fouzat A, Hussein OJ, Gupta I, Al-Farsi HF, Khalil A, Al Moustafa A-E. *Elaeagnus angustifolia* Plant Extract Induces Apoptosis via P53 and Signal Transducer and Activator of Transcription 3 Signaling Pathways in Triple-Negative Breast Cancer

Cells. *Frontiers in Nutrition*. 2022;9.

165. Zhao P, Zhou S, Li J, Guo T, Wang Y. Four flavonoid glycosides from the pulps of *Elaeagnus angustifolia* and their antioxidant activities. *Proceedings of the 2012 2nd International Conference on Computer and Information Applications (ICCIA 2012)*2012.

166. Amiri Tehranizadeh Z, Baratian A, Hosseinzadeh H. Russian olive (*Elaeagnus angustifolia*) as a herbal healer. *Bioimpacts*. 2016;6(3):155-67.

167. Wang CZ, Calway TD, Wen XD, Smith J, Yu C, Wang Y, et al. Hydrophobic flavonoids from *Scutellaria baicalensis* induce colorectal cancer cell apoptosis through a mitochondrial-mediated pathway. *Int J Oncol*. 2013;42(3):1018-26.

168. Afshari K, Haddadi NS, Haj-Mirzaian A, Farzaei MH, Rohani MM, Akramian F, et al. Natural flavonoids for the prevention of colon cancer: A comprehensive review of preclinical and clinical studies. *J Cell Physiol*. 2019;234(12):21519-46.

169. Kawaii S, Tomono Y, Katase E, Ogawa K, Yano M. Antiproliferative Activity of Flavonoids on Several Cancer Cell Lines. *Bioscience, Biotechnology, and Biochemistry*. 1999;63(5):896-9.

170. Fernández J, Silván B, Entrialgo-Cadierno R, Villar CJ, Capasso R, Uranga JA, et al. Antiproliferative and palliative activity of flavonoids in colorectal cancer. *Biomedicine & Pharmacotherapy*. 2021;143:112241.

171. Georgakopoulos-Soares I, Chartoumpakis DV, Kyriazopoulou V, Zaravinos A. EMT Factors and Metabolic Pathways in Cancer. *Front Oncol*. 2020;10:499.

172. Lamouille S, Xu J, Derynck R. Molecular mechanisms of epithelial-mesenchymal transition. *Nat Rev Mol Cell Biol*. 2014;15(3):178-96.

173. Zhou P, Li B, Liu F, Zhang M, Wang Q, Liu Y, et al. The epithelial to mesenchymal transition (EMT) and cancer stem cells: implication for treatment

resistance in pancreatic cancer. *Mol Cancer*. 2017;16(1):52.

174. Huang K, Gao N, Bian D, Zhai Q, Yang P, Li M, et al. Correlation between FAK and EGF-Induced EMT in Colorectal Cancer Cells. *J Oncol*. 2020;2020:5428920.

175. Christou N, Perraud A, Blondy S, Jauberteau MO, Battu S, Mathonnet M. E-cadherin: A potential biomarker of colorectal cancer prognosis. *Oncol Lett*. 2017;13(6):4571-6.

176. Al-Maghrabi J. Vimentin immunoeexpression is associated with higher tumor grade, metastasis, and shorter survival in colorectal cancer. *Int J Clin Exp Pathol* [Internet]. 2020 2020; 13(3):[493-500 pp.]. Available from: <http://europepmc.org/abstract/MED/32269687>.

177. Saleh AI, Mohamed I, Mohamed AA, Abdelkader M, Yalcin HC, Aboukassim T, et al. *Elaeagnus angustifolia* Plant Extract Inhibits Angiogenesis and Downgrades Cell Invasion of Human Oral Cancer Cells via Erk1/Erk2 Inactivation. *Nutr Cancer*. 2018;70(2):297-305.

178. Sebio A, Kahn M, Lenz HJ. The potential of targeting Wnt/beta-catenin in colon cancer. *Expert Opin Ther Targets*. 2014;18(6):611-5.

179. Zhang S, Deng Z, Yao C, Huang P, Zhang Y, Cao S, et al. AT7867 Inhibits Human Colorectal Cancer Cells via AKT-Dependent and AKT-Independent Mechanisms. *PLoS One*. 2017;12(1):e0169585.

180. Li JL, Lin SH, Chen HQ, Liang LS, Mo XW, Lai H, et al. Clinical significance of HER2 and EGFR expression in colorectal cancer patients with ovarian metastasis. *BMC Clin Pathol*. 2019;19:3.

181. Shah A, Seth KA. *In Silico* Identification of Novel Flavonoids Targeting Epidermal Growth Factor Receptor. *Current Drug Discovery Technologies*. 2021;18(1):75-82.

182. Subbaraj GK, Kumar YS, Kulanthaivel L. Antiangiogenic role of natural flavonoids and their molecular mechanism: an update. *The Egyptian Journal of Internal Medicine*. 2021;33(1).
183. Yadav AK, Srikrishna S, Gupta SC. Cancer Drug Development Using *Drosophila* as an in vivo Tool: From Bedside to Bench and Back. *Trends Pharmacol Sci*. 2016;37(9):789-806.
184. Bilak A, Su TT. Regulation of *Drosophila melanogaster* pro-apoptotic gene hid. *Apoptosis*. 2009;14(8):943-9.
185. Zoranovic T, Manent J, Willoughby L, Matos de Simoes R, La Marca JE, Golenkina S, et al. A genome-wide *Drosophila* epithelial tumorigenesis screen identifies Tetraspanin 29Fb as an evolutionarily conserved suppressor of Ras-driven cancer. *PLoS Genet*. 2018;14(10):e1007688.
186. Ye X, Deng Y, Lai ZC. Akt is negatively regulated by Hippo signaling for growth inhibition in *Drosophila*. *Dev Biol*. 2012;369(1):115-23.
187. Natanzi M, Pasalar P, Kamalinejad M, Dehpour A, Tavangar SM, Sharifi R, et al. Effect of Aqueous Extract of *Elaeagnus angustifolia* Fruit on Experimental Cutaneous Wound Healing in Rats. *Acta medica Iranica*. 2012;50:589-96.
188. Khodakarm A, Mehrabani D, Homafar L, Farjanikis G. Healing Effects of *Elaeagnus angustifolia* Extract in Experimentally Induced Ulcerative Colitis in Rats. *Journal of Pharmacology and Toxicology*. 2014;10(1):29-35.
189. Gürbüz İ, Üstün O, Yesilada E, Sezik E, Kutsal O. Anti-ulcerogenic activity of some plants used as folk remedy in Turkey. *Journal of Ethnopharmacology*. 2003;88(1):93-7.
190. Rodriguez-Garcia C, Sanchez-Quesada C, J JG. Dietary Flavonoids as Cancer Chemopreventive Agents: An Updated Review of Human Studies. *Antioxidants*

(Basel). 2019;8(5).

191. Mahmoud A, Elkhalfa D, Alali F, Al Moustafa AE, Khalil A. Novel Polymethoxylated Chalcones as Potential Compounds Against KRAS-Mutant Colorectal Cancers. *Curr Pharm Des.* 2020;26(14):1622-33.

192. Pande AN, Biswas S, Reddy ND, Jayashree BS, Kumar N, Rao CM. In vitro and in vivo anticancer studies of 2'-hydroxy chalcone derivatives exhibit apoptosis in colon cancer cells by HDAC inhibition and cell cycle arrest. *EXCLI J.* 2017;16:448-63.

193. Singh RK, Kumar S, Prasad DN, Bhardwaj TR. Therapeutic journey of nitrogen mustard as alkylating anticancer agents: Historic to future perspectives. *Eur J Med Chem.* 2018;151:401-33.

194. Bruun J, Eide PW, Bergsland CH, Bruck O, Svindland A, Arjama M, et al. E-cadherin is a robust prognostic biomarker in colorectal cancer and low expression is associated with sensitivity to inhibitors of topoisomerase, aurora, and HSP90 in preclinical models. *Mol Oncol.* 2021.

195. Wang Q, Zhu G, Lin C, Lin P, Chen H, He R, et al. Vimentin affects colorectal cancer proliferation, invasion, and migration via regulated by activator protein 1. *J Cell Physiol.* 2021;236(11):7591-604.

196. Ngan CY, Yamamoto H, Seshimo I, Tsujino T, Man-i M, Ikeda JI, et al. Quantitative evaluation of vimentin expression in tumour stroma of colorectal cancer. *Br J Cancer.* 2007;96(6):986-92.

197. Kurata T, Fushida S, Kinoshita J, Oyama K, Yamaguchi T, Okazaki M, et al. Low-dose eribulin mesylate exerts antitumor effects in gastric cancer by inhibiting fibrosis via the suppression of epithelial-mesenchymal transition and acts synergistically with 5-fluorouracil. *Cancer Manag Res.* 2018;10:2729-42.

198. Cheng X, Xu X, Chen D, Zhao F, Wang W. Therapeutic potential of targeting the Wnt/beta-catenin signaling pathway in colorectal cancer. *Biomed Pharmacother.* 2019;110:473-81.
199. Cho YH, Ro EJ, Yoon JS, Mizutani T, Kang DW, Park JC, et al. 5-FU promotes stemness of colorectal cancer via p53-mediated WNT/beta-catenin pathway activation. *Nat Commun.* 2020;11(1):5321.
200. Jin H, Kim HS, Seo GS, Lee SH. A new chalcone derivative, 3-phenyl-1-(2,4,6-tris(methoxymethoxy)phenyl)prop-2-yn-1-one), inhibits phorbol ester-induced metastatic activity of colorectal cancer cells through upregulation of heme oxygenase-1. *Eur J Pharmacol.* 2018;841:1-9.
201. Xu S, Chen M, Chen W, Hui J, Ji J, Hu S, et al. Chemopreventive effect of chalcone derivative, L2H17, in colon cancer development. *BMC Cancer.* 2015;15:870.
202. Bahrami A, Khazaei M, Hasanzadeh M, ShahidSales S, Joudi Mashhad M, Farazestanian M, et al. Therapeutic Potential of Targeting PI3K/AKT Pathway in Treatment of Colorectal Cancer: Rational and Progress. *J Cell Biochem.* 2018;119(3):2460-9.
203. Johnson SM, Gulhati P, Rampy BA, Han Y, Rychahou PG, Doan HQ, et al. Novel expression patterns of PI3K/Akt/mTOR signaling pathway components in colorectal cancer. *J Am Coll Surg.* 2010;210(5):767-76, 76-8.
204. Lee YT, Fong TH, Chen HM, Chang CY, Wang YH, Chern CY, et al. Toxicity assessments of chalcone and some synthetic chalcone analogues in a zebrafish model. *Molecules.* 2014;19(1):641-50.
205. Winter E, Pizzol CD, Locatelli C, Silva AH, Conte A, Chiaradia-Delatorre LD, et al. In vitro and in vivo effects of free and chalcones-loaded nanoemulsions: insights and challenges in targeted cancer chemotherapies. *Int J Environ Res Public Health.*

2014;11(10):10016-35.

206. Han R, Yang YM, Dietrich J, Luebke A, Mayer-Proschel M, Noble M. Systemic 5-fluorouracil treatment causes a syndrome of delayed myelin destruction in the central nervous system. *J Biol.* 2008;7(4):12.